Extraction of carotenoids from natural products and nanoparticle formation using supercritical fluid

NEROME Hazuki

Extraction of carotenoids from natural products and nanoparticle formation using supercritical fluid

March 2015

NEROME Hazuki

Graduate School of Engineering

Nagoya University

Contents

Chapter 1

Introduction

1-1. Introduction

Recently, the demand of functional food is increasing with raising of an interest in consumer's health. In the food industry, safety and instantaneous potency are demand in the functional food. However, as conventional method, organic solvent is used for extraction of functional substances. Furthermore, there are concerned about toxic solvent, residual solvent, low level absorption of the extracts, and degradation in the extraction process.

In this study, we focused on carotenoid as functional substance. Carotenoid is fat-soluble pigment such as β-carotene and lycopene which are contained abundantly in brightly colored vegetables. These carotenoids has antioxidantive effect, anti-inflammatory action, and anticancer activity. Therefore, those is paid attention as high-quality natural pigment and dietary supplement. However, the almost carotenoid is extracted from a plant by organic solvent. Furthermore, those are poorly absorbed to the human body, because of hydrophobic property. Therefore, the extraction by safety method and the micronization for improvement of absorption efficiency, which are important.

In our research, we suggested that extraction and micronization of carotenoid by high-pressure fluid. In addition, the improvements of extraction and concentration, dispersibility, transportability, and storability of target substance, absorption, which can be achieved by one step of the process. Purpose of this work was to determine the optimum conditions for extraction and micronization of carotenoid from natural products. Supercritical CO_2 was used as high pressure fluid solvent.

1-2. Supercritical fluids

Supercritical-fluid (SCF) research has been worldwide investigated since the late

1970s to early 1980s. A lot of researchers have studied the fundamentals, applications, and commercialization of SCF processes. SCF has a state of which gases and liquids are co-existed at a critical temperature and pressure, and shows unique properties differing from those of conventional gases and liquids under standard conditions (high-density, low-viscosity). In a supercritical region, a state of liquid-like density can be transformed into a vapor-like density at a given pressure and temperature. The properties of SCF could be utilized as an alternative solvent for separation and reaction processes, thus been applied to various processes that are attractive from academic and engineering points of views.

Carbon dioxide (CO_2) and water are well known to be used as SCF. Supercritical CO_2 (SC-CO_2) has been extensively used at a mild temperature of 31 ℃ in extraction processes. SC-CO_2 is non-toxic, non-flammable, and easily separated from extraction by depressurization, and thus may be a cure of the problems caused by industrial processes that rely on noxious solvent such as acetone, methanol or hexane. When CO_2 gas reaches its supercritical point at modest temperature (31 ℃) and pressure (7.4 MPa), it has a liquid-like dense and maintains its ability to flow with almost no viscosity or surface tension **(Figure 1-1)**. In addition, SC-CO_2 can be obtained using conventional industrial processes, without further contribution to the greenhouse effects. Once the pressure is released, SC-CO_2 evaporates instantaneously with no trace. SC-CO_2 is a small linear molecule, which can diffuse more quickly than conventional bulk liquid solvents, especially in condensed phases such as polymers. These features make it an excellent solvent for food processing. Decaffeination of coffee and an extraction of hops are typical examples for the commercial plants. Furthermore, SC-CO_2 is found to be an intriguing

medium in which new materials can be synthesized [1].

Water has a critical point at a high temperature of 374 ℃ and a pressure of 22.1 MPa, because of its polarity **(Figure 1-1)**. Water near the critical point is quite different from ambient liquid water. For example, the dielectric constant (ε) is much lower, and the number and persistence of hydrogen bonds are both diminished. As a result, Supercritical water (SCW) behaves like many organic solvents in that organic compounds enjoy high solubilities in near-critical water and complete miscibility with supercritical water. Moreover, gases are also miscible in SCW so employing a SCW reaction environment provides an opportunity to conduct chemistry in a fluid single phase that would otherwise occur in a multiphase system under more conventional conditions. The advantages of a single supercritical phase reaction medium are that higher concentration of reactants can often be attained and that there are no inter-phases mass transport processes to hinder reaction rates [1,2]. Some examples of commercial plants that use the SCF technology in East Asia and Japan are summarized in **Table1-1** and **Table1-2** for SC-CO_2 and SCW extraction processes, respectively [3]. An increasing industrial activity is appearing due to regulations that restrict the use of the organic solvent for food processing. Specially, various kinds of seasoning produced by SC-CO_2 extraction are now significant market. Furthermore, the next market for flavors appears to be moving towards soft drinks. And the application of SC-CO_2 extraction to the several kinds of supplements is also growing up depending on the life style and the aging society. Therefore, the factories are operating at full capacity to satisfy the current demand and some companies plan to expand their facilities or construct the new plants. The application of SCW technology in industrial activity is mainly for treatment of manufacturing wastes. Some companies listed in **Table**

1-2 have succeeded in the recycling high purity water to the factory.

In this way, a SCF technology contributes greatly to the development of food and health and the environment.

SCF characteristics has been described in detail in the **chapter 2**.

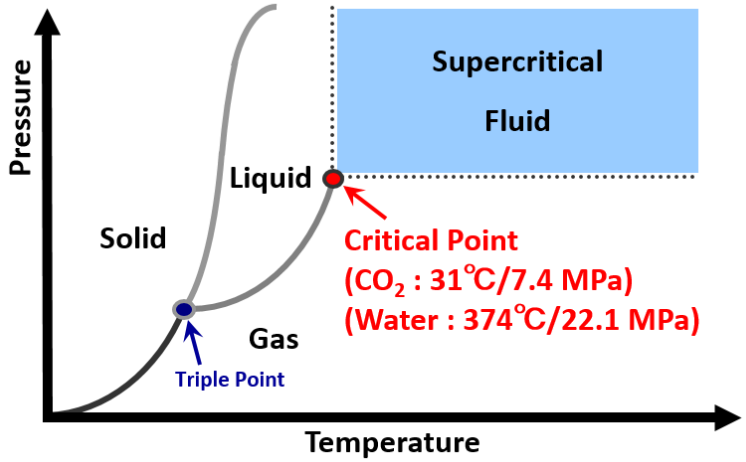

Figure 1-1. Pressure-temperature phase diagram of CO_2 and water [1]

Table 1-1. Commercial operation plant for SC-CO_2 extraction in the East Asia [3]

Year's	Company	Country	Extraction objects	Capacity[L]	Vessel
1984	Fuji flavor	Japan	Pigment, Flavor	200	1
1986	Fuji flavor	Japan	Pigment, Flavor	300	1
1986	Sumitomo Seika	Japan	-	50	1
1987	Yasuma	Japan	Paprika oleoresin	100	1
1988	Takeda Pharmaceuticals	Japan	Organic solvent from medicine	1200	1
1988	Japan Tabaco	Japan	-	200	1
1989	T. Hasagawa	Japan	-	300	2
1989	Mori Oil and Fat	Japan	-	500	1
1989	Takasago International	Japan	Essential oil	420	1
1991	Fuji Flavor	Japan	-	300	1
1992	Japan Tabacco	Japan	-	390	5
1993	T. Hasegawa	Japan	-	500	2
1994	Nan Fang	China	Aroma	350	2
1995	Ilhwa	Korea	Ginseng	170	1
1995	Green Tek 21	Korea	-	100	1
1995	-	China	Hop	500	1
1997	-	China	-	200	2
1998	Mori Oil and Fat	Japan	Esseitial oil	500	2
1998	Guangxia	China	Hop	500	3
1999	Shaanxi	China	Hop	500	2
1999	-	Taiwan	Rice	500	2
1999	-	China	-	500	2
2001	Mori Oil and Fat	Japan	Essential oil	500	1
2001	Guangxia	China	Hop	3500	3
2001	Guangxia	China	Hop	1500	3
2001	Guangxia	China	Hop	1500	3
2001	-	China	Ginseng	360	1
2001	-	China	-	1000	2
2001	-	China	-	600	2
2001	-	China	-	1000	2
2001	-	China	-	1000	2

Table 1-2. Commercial operation plant for SCW extraction in Japan [3]

Company	Development Stage	Objectives
Organo corporation	Commercial stage	Technical tie-up with MODAR, Inc. Treatment of semiconductor manufacturing wastes Technical tie-up with General Atomics (GA) and MODEC, Inc.
	Pilot scale	Decomposition of PCBs, Treatment of sewage sludge
Komatsu and Kurita group	Pilot scale	Technical tie-up with GA Objectives are unknown
Shinko Pantec Co., Ltd	Pilot scale	Technical with eco-waste (Chemature) Treatment sewage sludge
Mitsubishi Heavy Industries	Pilot scale	Technical tie-up with SRJ Decomposition of PCBs
Ishikawajima-Harima Heavy Industries	Pilot scale	Waste from food processing Contaminated water by pesticide
Hitachi plant and construction	Bench scale	Technical tie-up with MODEC, Inc. Treatment sewage sludge
NGK insulator, Ltd.	Unknown	Technical Tie-up with MODEC, Inc. Objectives are unknown
Toshiba corporation	Bench scale (Batch operation)	Treatment solid waste (ion exchenge resin, etc)
Japan steel works	-	Manufacturing of high pressure equipment
Nippon Sanso	-	Manufacturing of oxygen supply equipment

1-3. Extraction of functional substance

In the extraction of active ingredients from the natural product, organic solvents extraction have been used generally because it have merit such as high yield of extract and low cost of process. Currently, ethanol, ethyl acetate and *n*-hexane are mainly used

as extraction solvent to obtain the active ingredients. However, the use of organic solvent becomes problem such as harmful influence by residual solvent in extracts, oxidation and thermal denaturation of the target component, the environmental impact [4].

Solvent extraction of solid samples, which is commonly known as solid–liquid extraction, but which should be referred to, in a more correct use of the physicochemical terminology, as leaching or lixiviation, is one of the oldest ways of solid sample pretreatment. Among the techniques used for implementation of this step, Soxhlet has been the leaching technique mostly used for a long time. This assertion is supported by the fact that Soxhlet has been a standard technique during more than one century and, at present, it is the main reference to which the performance of other leaching methods is compared. In conventional Soxhlet, originally used for the determination of fat in milk, the sample is placed in a thimble-holder, and during operation gradually filled with condensated fresh solvent from a distillation flask. When the liquid reaches the overflow level, a siphon aspirates the solute of the thimble-holder and unloads it back into the distillation flask, carrying the extracted analytes into the bulk liquid. This operation is repeated until complete extraction is achieved. The most significant drawbacks of Soxhlet extraction, as compared to the other conventional techniques for solid sample preparation are, the long time required for the extraction and the large amount of solvent wasted, which is not only expensive to dispose of but which can itself cause additional environmental problems. Samples are usually extracted at the boiling point of the solvent for a long period of time and the possibility of thermal decomposition of the target compounds cannot be ignored, when thermolabile analytes are involved. The conventional Soxhlet device is unable to provide agitation, which would accelerate the process. Due to the large amount of solvent used, an evaporation/concentration step after

the extraction is mandatory. The technique is restricted to solvent selectivity and is not easily automated [5]. Soxhlet extraction have been used for comparison often as a conventional method. In this work, this method was also used as comparison.

1-4. A brief review of supercritical fluids extraction

Application of SCF extraction of natural product have been used and studied by many researcher and there are several hundred reports. The extraction method using SCF has the following advantages. First, the diffusion of SCF in substances is faster than the liquid, it is possible to extract in a short time compared with the conventional extraction method. Moreover, the solvent density of the SCF can be easily controlled by operating temperature and pressure. Thus, even in a single solvent, it is possible to fraction of the target substance by operating conditions. Even though several compounds, such as pentane, butane, nitrous oxide, sulfur hexafluoride and fluorinated hydrocarbon, have been studied as SCF extraction, SC-CO_2 is widely used as the common extraction solvent. It doesn't need solvent separation process from extract because SC-CO_2 become a gas at atmospheric pressure. Therefore, there is no concern of the residual solvent, and easy recovery the solvent, doesn't need waste liquid processing after extraction. Further, in the case of extraction with CO_2, the online analysis with high performance liquid chromatography (HPLC) or gas chromatography (GC) are readily possible. On the other hand, there is also disadvantages of high cost for high pressure resistance extraction vessel and the requirement of flow path. SC-CO_2 extraction techniques was used for extraction of natural product such as flavor material or remove dispensable component like caffeine in food industry. That is the start point of industrialization of the SCF extraction process. In recent years, it has attracted attention as a safe extraction method of functional

substance from natural products [6].

In this section, previous works in the SCF extraction field will be briefly reviewed. The works including extraction of essential oil and natural pigment.

1-4-1. Extraction of essential oil [6-16]

In the essential oil extraction process, it can be used mild temperature and pressure as 40-50 ℃ and 8-10 MPa, because components of essential oil are easily soluble in SC-CO_2 [7-15]. Generally, solubility to the SC-CO_2 depend on the molecular structure of target compounds as follows,

- solubility increase with polarity of target compound
- solubility decrease with increasing molecular weight
- solubility increase by side chain
- solubility decrease by aromatic series
- low polarity and low molecular weight compound is completely soluble

Because of these characteristics, SC-CO_2 extraction are suited to the extraction of essential oils from natural products. **Figure 1-2** Shows solubility of essential oil component to the SC-CO_2.

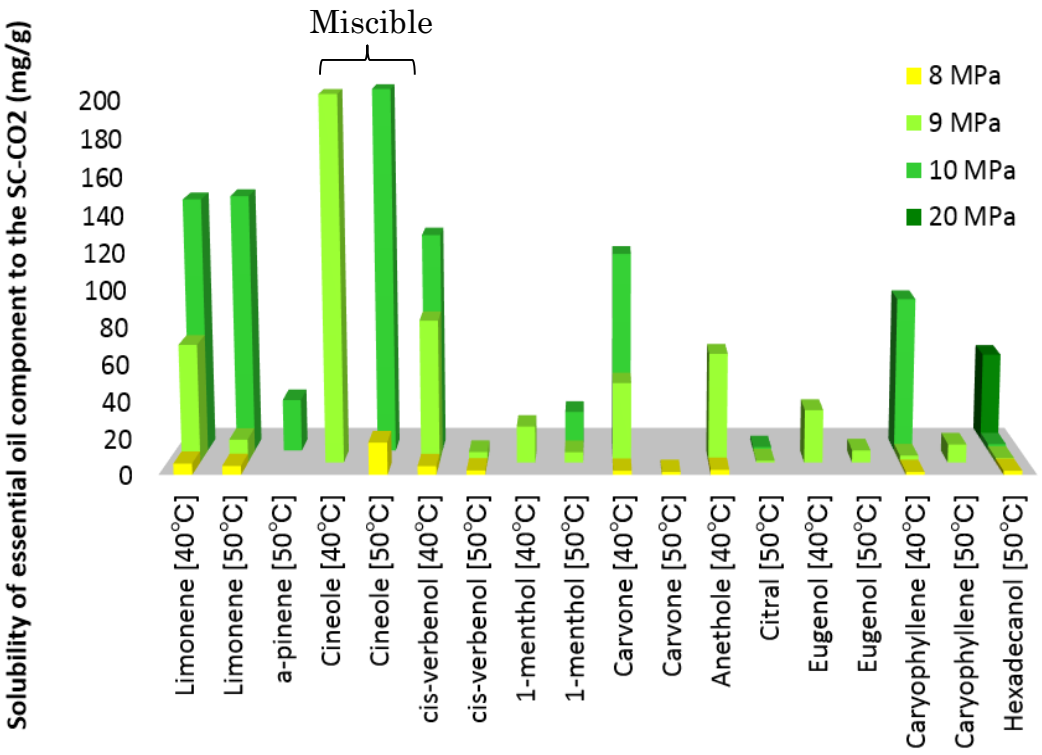

Figure 1-2. Solubility of essential oil component to the SC-CO_2 (mg/g) [16]

1-4-2.Extraction of natural pigment [6, 17-21]

Plants pigment has been attracting attention because of its functionality, such as antioxidant. The most components are fat-soluble substances, and it can be dissolved in SC-CO_2. However, the molecular weight is larger than the essential oil components. Therefore extraction conditions are set to higher, 40-100 ℃ and 30-50 MPa.

Chandra et al. reported α-carotene and β-carotene which are one of the carotenoid pigment are successfully collected by SC-CO_2 from carrot. And SC-CO_2 enabled high selectivity for carotenoid extraction. 96.7 % and 83.8 % of α-carotene and β-carotene were recovered at 40℃ / 50 MPa comparing with organic solvent extraction using chloroform.

1-5. Micro to nano particle formation of functional substance [22]

Recently, the development of the fine particles and ultra-fine particles have been attracting attention call as nanotechnology. Generally, methods for producing particles are as follows. Particle formation by physical milling method, micronization by cooling or removing the solvent method, micronization by reaction method, and a micronization by anti-solvent method.

In the process according to the cooling and solvent removal, the mixture in the container stable state (non-saturated), to obtain a crystal by the supersaturated by cooling or removal of solvent.

Curcumin fine particles which is the active component of turmeric was development as not precipitated in the liquid in the bottle with higher absorption into the body by emulsion solvent removal method.

Spray-drying method is applied to the solvent removal method. Spraying a solution which is prepared dissolving the target substance into the hot air, to obtain particles by evaporating the solvent. This method has been widely used for food processing such as non-fat dry milk and instant coffee production.

In the micronization process by the reaction, the reaction creates a large supersaturation by creating the low solubility of the compound, to produce a crystallized components. The method which including the calcium carbonate, is an essential operation in the field of pharmaceuticals and fine chemicals. In the case of anti-solvent method, to precipitate crystals by adding anti-solvent which is lower solubility into the solution. This method has been widely used for industrially. The method of pH controlling which is used for protein and amino acid crystallization is also a kind of anti-solvent method.

Normally, the method for obtaining crystal by cooling is used under constant

pressure. On the other hand, crystallization by applying a pressure under a constant temperature has been developed. This method has been applied to the separating isomers of cresol on an industrial scale. **Table 1-3** shows the principle and operation of the crystallization.

Table 1-3. Principle and operation of the crystallization [22]

Operation	The principle of supersaturation creation	example
Cooling	Solubility decreases	Crystallization of many aqueous systems, Purification of organic substance, single crystal growth
Solvent evaporation	Concentration	Crystallization of many aqueous systems, single crystal growth
Two-phase mixture	Reaction, precipitation operation	Manufacturing of pharmaceuticals, high-performance ultra-fine particles
Addition of anti-solvent	Solubility decrease	Organic substance, separation and purification of amino acids
Pressurization	Change of phase equilibrium	Purification of organic substance

1-6. A brief review of particles formation by supercritical fluids (RESS, SAS, SEDS) [6, 22-27]

In recent years, crystallization method using a SCF has been attracting attention because this method is able to produce particles with relatively uniform particle size. Previous particle production method is primarily to use phase separation by heat operation

or solvents operation. However, in the case of using SCF, basic is phase separation by pressure operation. Therefore the method is expected that, thermal denaturation and residual solvent faced by conventional methods, as well as solving the problem of secondary aggregation, as a method that enables ultra-fine particles production.

Particle production method using a SCF, basically is divided into "rapid expansion method RESS" and "anti-solvent Method GAS, SAS".

1-6-1. Rapid Expansion of Supercritical Solution (RESS) method [6]

Rapid Expansion of Supercritical Solution (RESS) method have been used for micronization of solid which is able to dissolve into a SCF. Raw material which was dissolved in a SCF is sprayed into a precipitator through a nozzle, and the solubility of the material in the SCF is reduced immediately by returning to ambient pressure and temperature. Therefore, nucleation and crystal growth is caused by supersaturation. Particles of target material is able to collect from precipitator. This micronization method can be utilizing the principle of exhaust pressure in the recovery section of the SC-CO_2 extraction, it is expected that can be carried out simultaneously with the extraction. However, the process is limited to raw material which are reasonably soluble to SCF. Furthermore this technique has disadvantage that it is difficult to obtain nanoparticles.

1-6-2. Anti-solvent process

Anti-solvent method is to precipitate the objective solute dissolving in the organic solvent by reducing the solubility with adding SC-CO_2. The process uses SC-CO_2 as anti-

solvent unlike RESS process to use the SC-CO_2 as good-solvent.

Gas Anti-Solvent (GAS) process is one of the anti-solvent methods. In this process, nucleation is occurred by the solubility decrease because of gas dissolution to the liquid. This process has been developed for micronization of explosives which is difficult to mechanical pulverization by Krukonis et al. [24].

1-6-3. Supercritical anti-solvent (SAS) process

Supercritical anti-solvent (SAS) process is one of the micronization methods which is modified GAS process that is applied to make fine particles from various materials such as medicine, pigment and cosmetic materials [36-41]. In a typical SAS process, solution which contains object compounds and organic solvent is fed to a nozzle into a precipitator for produced particles filled with SC-CO_2. Supersaturation was caused by mixing with solution and SC-CO_2 in the precipitator. After that, crystal nucleation and growth occurs. There are several factors on the particle size and morphology such as operating temperature, pressure, CO_2 and solution flow rate, kind of organic solvent and nozzle type and its inner diameter [42-49].

Commercialization which is utilizing SCF is already progressing as an application and development in the field of dye, pharmaceutical and cosmetic industries. Specific examples are described below. Gao et al. reviewed the preparation of fine pigment particles using the SAS techniques. Obtained pigment particles were 600 nm. It is expected to use as a high value-added pigment with excellent color properties such as color density and definition [25]. Cocero et al. have succeeded in formation of lycopene micro particles size

of 10 μm by SAS technique. In addition, they were also carried out research to create the complex of biopolymer and carotenoids using SAS method. [1-3]. Although in the SAS method known as available for particle production of micro to nano-size, the nanoparticles of carotenoids has not been produced yet.

1-6-4. Solution enhanced dispersion by supercritical fluids (SEDS) process

The solution enhanced dispersion by supercritical fluids (SEDS) process is one of modified SAS process. The solution and SC-CO_2 are sprayed into a precipitator by a coaxial nozzle. [50-54]. Lee et al. have obtained fine particles of cetirizine dihydrochloride β-cyclodextrin complex using the SEDS method. They have succeeded in reducing the bitterness of medicine by inclusion with cyclodextrin [26]. Currently, SEDS method is becoming the mainstream of fine particle formation method that targets to pharmaceuticals. In this work, SEDS method was used for nano particle formation of carotenoid.

Table 1-4 Particle production method using SC-CO_2 [28, 30-35]

Years	Process	Target	Result Particle size[μm]	Author	Ref.
1989	GAS	Nitroguanidine	A few μm	Gallagher	[28]
1992	GAS	Cyclotrimethylene trinitramine(RDX)	1-200	Gallagher	[30]
1992	RESS	Insline	-	Debenedetti	[31]
1993	GAS	Insline	2-4	Yeo	[32]
1993	SAS	Insline	4	Yeo	[32]
1996	SAS	Insline	1-5	Winters	[33]
1996	SAS	Tryosin	1-5	Winters	[33]
1997	GAS	Pigment	0.6	Gao	[34]
1999	SAS	Antibiotics	0.64	Reverchon	[35]

1-7. The purpose of this work

Continuous process of the extraction of functional compounds from natural products and fine particle formation of extracts has been desired for target component concentration process of the extract and storage. Additionally, previous work in this laboratory, continuous process of β-glucan hydrothermal extraction and micronization from *Ganoderma lucidum* and *Hordeum vulgare* using subcritical water have been successful [50-52]

However, a continuous process of carotenoid extraction and micronized using SC-CO_2 has not yet been studied. Therefore we want to suggest a concept of the continuous process of SC-CO_2 extraction and micronization as final goal as shown in **Figure 1-3** and **Figure 1-4**.

Figure 1-3 shows scheme of concept of the continuous process of SC-CO_2 extraction and RESS process. If the target substance is dissolved in the SC-CO_2, this method can be applied. It aimed particle formation of extract by using a rapid solubility decrease when depressurizing the SC-CO_2 after extracting target substances from a raw material.

On the other hand, **Figure 1-4** shows scheme of concept of the continuous process of SC-CO_2 extraction and SEDS process. If the target substances cannot dissolve in the SC-CO_2, this method can be applied.

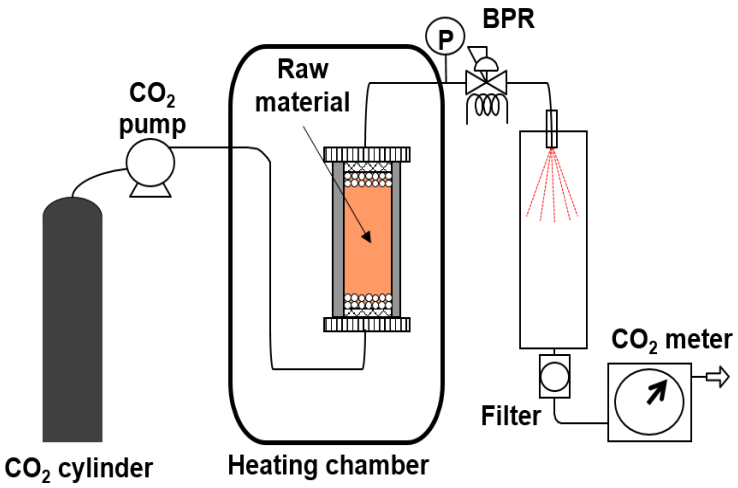

Figure 1-3 Scheme of concept of the continuous process of SC-CO_2 extraction and RESS process

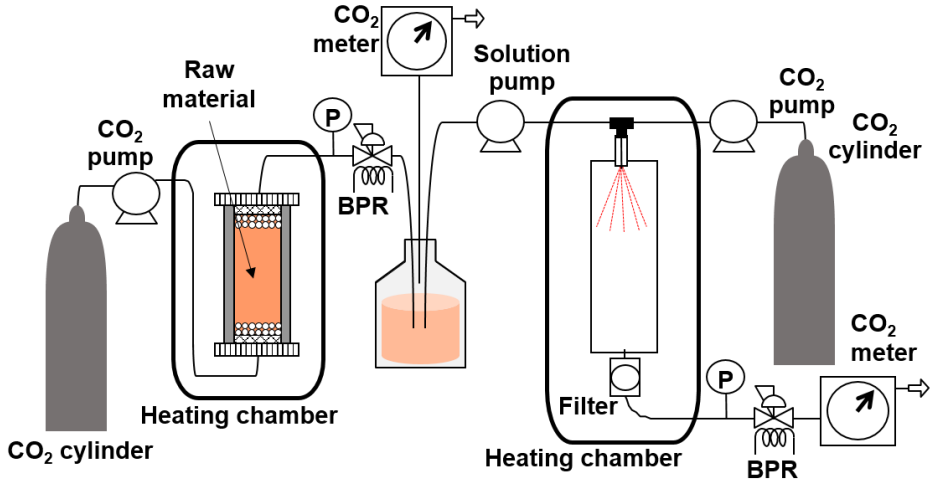

Figure 1-4 Scheme of concept of the continuous process of SC-CO_2 extraction and SEDS process

In this study, in order to construct the continuous process as shown in Fig, determination of optimal conditions of the extraction and micronization has been performed. Carotenoid extraction from natural products is grasped in the extraction

section, the section of fine particles formation, particles of the model substance of pure carotenoids were studied. Main purpose is to grasp the respective behavior and determination of optimum condition of the process.

1-8. Contents of this thesis

In **Chapter 1**, background of this work, previous research and purpose were described.

In **Chapter 2**, the characteristics of the supercritical fluid which was used as a solvent was described as the basis of this study.

In **Chapter 3**, extraction of functional ingredients from natural products such as gac fruit and spices saffron have been described.

Extraction behavior of functional ingredients were grasped and the optimum conditions were determined.

In **Chapter 4**, micronization of lycopene and β-carotene as a model substance were conducted. Optimum operating conditions for obtaining the nanoparticles was determined.

In **Chapter 5**, summary and future prospects of this study were described.

References

[1] Y. Arai, T. Sako, Y. Takebayashi, Supercritical fluids molecular interactions, physical properties, and new applications, *Springer-Verlag* Berlin Hidelberg, Germany (2002)

[2] P.G. Jessop, W. Leitner, Chemical Synthesis Using Supercritical Fluids, *Wiley-VCH Verlag GmbH, D-69469 Weinheim,* Germany (1999)

[3] R. Fukuzato, Current status of supercritical fluid technology in the East Asia, *Procieding of 2nd Int. Symp. On Supercritical fluid tech for energy and env. App.*, Nagoya, Japan, 40-46 (2003)

[4] Edited by the Chemical Society of Japan, Fifth Edition Experimental Chemistry Fundamentals I basis of experiments and information, *Maruzen Publishing* (2003)

[5] M.D. Luque de Castro, L.E. Garcia-Ayuso, Soxhlet extraction of solid materials: an outdated technique with a promising innovative future, *Analytica Chimica Acta*., 369,1-10 (1998)

[6] R. Fukusato, M. Goto, separation technology series 24 practical supercritical fluid technology, *Separation technology Association, Japan* (2012)

[7] E. Reverchon, G. Della Porta, Supercritical COS Extraction and Fractionation of Lavender Essential Oil and Waxes, *J. Agric. Food Chem.*, 43, 1654-1658 (1995)

[8] E. Reverchon, C. Marrone, Supercritical extraction of clove bud essential oil: isolation and mathematical modeling, *Chem. Eng. Sci.*, 52, 3421-3428 (1997)

[9] E. Reverchon, F. Senatore, Supercritical Carbon Dioxide Extraction of Chamomile Essential Oil and Its Analysis by Gas Chromatography-Mass Spectrometry, *J. Agric. food Chem.*, 42, 154-158 (1994)

[10] G. Wenqiang, L. Shufen, Y. Ruixiang, T. Shaokun, Q. Can, Comparison of essential oils of clove buds extracted with supercritical carbon dioxide and other three traditional extraction methods, *Food Chemistry*, 101, 1558–1564 (2007)

[11] E. Reverchon, F. Senatore, Isolation of Rosemary Oil: Comparison between Hydrodistillation and Supercritical CO_2 Extraction, *Flavour and fragrance journal*, 7, 227-230 (1992)

[12] H. Sovova, R. Komers, J. Kucera, J. Jez, Supercritical carbon dioxide extraction of caraway essential oil, *Chemical Engineering Science*, 49, 2499-2505 (1994)

[13] V.M. Rodrigues, P.T.V. Rosa, M.O.M. Marques, A.J. Petenate, M.A.A. Meireles: Supercritical Extraction of Essential Oil from Aniseed (Pimpinella anisum L) Using CO_2: Solubility, Kinetics, and Composition Data, *J. Agric. Food Chem.*, 51, 1518-1523 (2003)

[14] B.C. Roy, M. Goto, T. Hirose, Extraction of Ginger Oil with Supercritical Carbon Dioxide: Experiments and Modeling, *Ind. Eng. Chem. Res*., 35, 607-612 (1996)

[15] M. Akgun, N.A. Akgun, S. Dincer, Extraction and Modeling of Lavender Flower Essential Oil Using Supercritical Carbon Dioxide, *Ind. Eng. Chem. Res.*, 39, 473-477 (2000)

[16] E. Reverchon, Supercritical fluid extraction and fractionation of essential oils and related products, *J. Supercritical Fluids*, 10, 1-37 (1997)

[17] M. Skerget, Z. Knez, Solubility of Binary Solid Mixture α-Carotene-Capsaicin in Dense CO_2, *J. Agric. Food Chem*., 45, 2066-2069 (1997)

[18] A. Chandra, M.G. Nairw, Supercritical Fluid Carbon Dioxide Extraction of a-and b-Carotene from Carrot (Daucus carota L.), *Phytochemical Analysis*, 8, 244–246 (1997)

[19] P. Manninen, J. Pakarinen, H. Kallio, Large-Scale Supercritical Carbon Dioxide Extraction and Supercritical Carbon Dioxide Countercurrent Extraction of Cloudberry Seed Oil, *J. Agric. Food Chem.*, 45, 2533-2538 (1997)

[20] K. Kitada, S. Machmudah, M. Sasaki, M. Goto, Y. Nakashima, S. Kumamoto, T. Hasegawa, Supercritical CO_2 extraction of pigment components with pharmaceutical importance from Chlorella vulgaris, *J. Chem Technol Biotechnol*., 84, 657–661 (2009).

[21] U. Topal, M. Sasaki, M. Goto, K. Hayakawa, Extraction of Lycopene from Tomato Skin with Supercritical Carbon Dioxide: Effect of Operating Conditions and Solubility Analysis, *J. Agric. Food Chem.*, 54, 5604-5610 (2006)

[22] M. Matsuoka, Society of Chemical Engineers, Japan, ed., Crystallization engineering, *Baifukan* (2002)

[23] M. Adschiri, supercritical fluid technology and nanotechnology development, *CMC Publishing* (2004)

[24] V.J. Krukonis, P.M. Gallagher, M.P. Coffey, Gas anti-solvent recrystallization process, US Patent

[25] Y. Gao, T. K. Mulenda, Y. F. Shi, W. K. Yuan, Fine particles preparation of Red Lake C pigment by supercritical fluid, *J. Supercritical Fluids*, 13, 369-374 (1998)

[26] C.W. Lee, S. J. Kim, Y.S. Youn, E. Widjojokusumo, Y.H. Lee, J. Kim, Y.W. Lee, R.R. Tjandrawinat, Preparation of bitter taste masked cetirizine dihydrochloride / cyclodextrin inclusion complex by supercritical antisolvent (SAS) process, *J. Supercritical Fluids*, 55, 1, 348-357 (2010).

[27] A.D. Shine, J. Gelb Jr. Microencapsulation process using supercritical fluids, WO Patent

[28] P.M. Gallagher, M.P. Coffey, V.J. Krukonis, N. Klasutis, Gas Antisolvent Recrystallization: New Process To Recrystallize Compounds Insoluble in Supercritical Fluids, *Supercritical Fluid Science and Technology*, 406, 334-354 (1989)

[29] E. Weidner, R. Steiner, Z. Knez, Powder generation from polyethyleneglycols with compressible fluids, *Process Technology Proceedings*, 12, 223-228 (1996)

[30] P.M. Gallagher, M.P. Coffey, V.J. Krukonis, Gas Anti-Solvent Recrystallization of RDX: Formation of Ultra-fine Particles of a Difficult-to-Cornminute Explosive, *J. Supercriticnl Fluids*, 130-142 (1992)

[31] P.G. Debenedetti, J.W. Tom, S.D.Yeo, G.B. Lim, Application of supercritical fluids for the production of sustained delivery devices, *J. Controlled Release*, 24, 21-44 (1993)

[32] S.D. Yeo, G.B. Lim, P.G. Debendetti, H. Bernstein, Formation of microparticulate protein powder using a supercritical fluid antisolvent, *Biotechnology and Bioengineering*, 41, 341–346 (1993)

[33] M.A. Winters, B.A. Knutson, P.G. Debenedetti, H.G. Sparks, T.M. Przybycien, C.L. Stevenson, S.J.J. Prestrelski, Precipitation of proteins in supercritical carbon dioxide, *J. Pharmaceutical Sciences*, 85, 586–594 (1996)

[34] Y. Gao, T.K. Mulenda, Y.F. Shi, W.K. Yuan, Fine particles preparation of Red Lake C Pigment by supercritical fluid, *J. Supercritical Fluids*, 13, 369-374 (1998)

[35] E. Reverchon, G.D. Porta, Production of antibiotic micro- and nano-particles by supercritical antisolvent precipitation, *Powder Technol.*, 106, 23–29 (1999)

[36] P. Boonnoun, H. Nerome, S. Machmudah, M. Goto, A. Shotipruk, Supercritical anti-solvent micronization of chromatography purified marigold lutein using hexane and ethyl acetate solvent mixture, *J. Supercritical Fluids*, 80, 15-22 (2013)

[37] Y.C. Cho, J.H. Cheng, S.L. Hsu, S.E. Hong, T.M. Lee, C.M.J. Chang, Supercriticalcarbon dioxide anti-solvent precipitation of anti-oxidative zeaxanthin highlyrecovered by elution chromatography from Nannochloropsis oculata, *Sep. Purif. Technol*., 78, 274-280 (2011)

[38] E. Reverchon, I. D. Marco, Supercritical antisolvent precipitation ofcephalosporins, *Powder Technol.*, 164, 139–146 (2006)

[39] Y. Wang, Y. Wang, J. Yang, R. Pfeffer, R. Dave, B. Michniak, The application of asupercritical antisolvent process for sustained drug delivery, *Powder Technol.*, 164, 94–102 (2006)

[40] E. Reverchon, I. D. Marco, Supercritical antisolvent micronization of cefoni-cid: thermodynamic interpretation of results, *J. Supercritical Fluids.*, 31, 207–215 (2004)

[41] I. D. Marco, E. Reverchon, Supercritical antisolvent micronization of cyclodex-trins, *Powder Technol*., 183, 239–246 (2008)

[42] P. Boonnoun, H. Nerome, S. Machmudah, M. Goto, A. Shotipruk, Supercritical anti-solvent micronization of marigold-derived lutein dissolved in dichloromethane and ethanol, *J. Supercritical Fluids*, 77, 103-109 (2013)

[43] S. D. Yeo, M.S. Kim, J. C. Lee, Recrystallization of sulfathiazole and chlorpropamide using the supercritical fluid antisolvent process, *J. Supercritical Fluids*, 25, 143–154 (2003)

[44] M. S. Kim, S. Lee, J. S. Park, J. S. Woo, S. J. Hwang, Micronization of cilostazol using supercritical antisolvent (SAS) process: effect of process parameters, *Powder Technol*., 177, 64–70 (2007)

[45] M. Bahrami, S. Ranjbarian, Production of micro- and nano-composite particles by supercritical carbon dioxide, *J. Supercritical Fluids*, 40, 263–283 (2007)

[46] G. Caputo, E. Reverchon, Use of urea as habit modifier in the supercritical antisolvent micronization of sulfathiazole, *Ind. Eng. Chem. Res*., 46(12), 4265–4272 (2007)

[47] E. Reverchon, R. Adami, G. Caputo, I. D. Marco, Spherical microparticles production by supercritical antisolvent precipitation: Interpretation of results, *J. Supercritical Fluids*, 47, 70–84 (2008)

[48] K. Byrappa, S. Ohara, T. Adschiri, Nanoparticles synthesis using supercritical fluid technology-towards biomedical applications, *Adv. Drug. Deliver. Rev.*, 60, 299–327 (2008)

[49] E. Badens, O. Boutin, G. Charbit, Laminar jet dispersion and jet atomization in pressurized carbon dioxide, *J. Supercritical Fluids*, 36(1), 81–90 (2005)

Chapter 2

Fundamentals

2-1. Introduction [1]

Knowledge of thermodynamic principles and transport properties of supercritical fluid (SCF) are required to understand the super critical fluid techniques and interdependence of relevant process parameters. In the development of technology for extraction and micronization processes, solvent selection is great importance, but as solvents generally chosen from those that are liquid at atmospheric pressure, the selection of solvent has been very limited. Of particular with SCFs, since the physical properties of these solvents can be broadly controlled with temperature and pressure. The unique of solvent properties of SCF, i.e., substances above their critical temperature and critical pressure, were first observed more than a century ago (Hannay and Hogarth). However supercritical technology require an expensive high-pressure equipment and preparation has been difficult. Therefore the commercialization has been slowly developed.

2-2. Supercritical fluids [1,2]

Substance changes to the three states of the gas and liquid and solid by changes in environmental conditions such as temperature and pressure. This is determined by the balance of the intermolecular forces and kinetic energy. Transition of the gas-liquid-solid tri-state is shown in **Figure 2-1.** The horizontal axis is temperature, and the vertical axis represents the pressure. This is called a state diagram (phase diagram). Triple point is a state in which the three-phase gas liquid solid coexist. The lower temperature than the triple point in the solid and the vapor equilibrium, the vapor pressure is given by sublimation curve. The temperature above the triple point, the liquid and vapor are parallel. Pressure at this time is a saturated vapor pressure, is given by the evaporation curve (vapor pressure curve).

Evaporation curves have endpoints in high temperature and high pressure side, which is called the critical point. Gas-liquid interface also disappears. In the vicinity of the critical point, evaporation and condensation are repeated, the density fluctuation also increases. A fluid in a state of higher than the critical temperature and critical pressure is called a supercritical fluid. The supercritical fluid is a dense fluid having a high kinetic energy, the liquid behavior in terms of dissolving the solute and it shows as on behavior in torus of variability in terms of variability of the density shows a gas behavior.

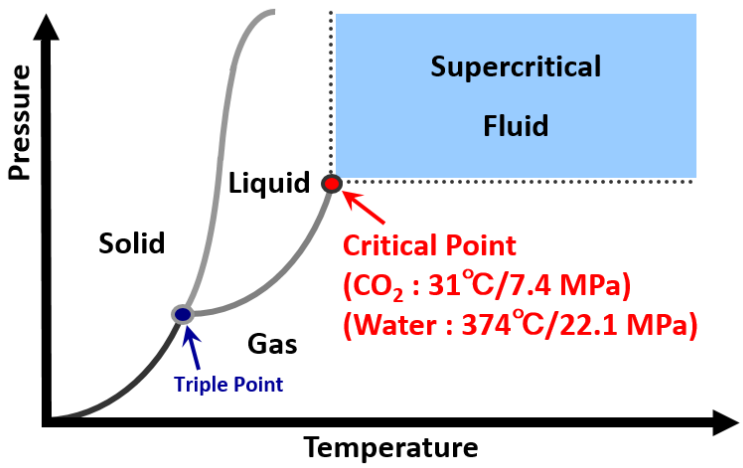

Figure2-1. A schematic representation of the phase diagram of a single substance, showing the supercritical fluid region as a hatched area

Table 2-1 shows CO_2 properties in gas, supercritical and liquid phase. Supercritical fluid is the region where the maximum solvent capacity and the largest variation in solvent properties can be achieved with small changes in temperature and pressure. It offers very attractive extraction characteristics, owing to its favorable diffusivity, viscosity, surface

tension and other physical properties. Its diffusivity is one to two orders of magnitude higher than those of other liquids, which facilitates rapid mass transfer and faster completion of extraction than conventional liquid solvents. Its low viscosity and surface tension enable itself to easily penetrate the botanical material from which the active component is to be extracted. The gas-like characteristics of SCF provide ideal conditions for extraction of solutes giving a high degree of recovery in a short period of time. However, it also has superior dissolving properties of a liquid solvent, it can also selectively extract target compounds from a complex mixture. Strong density depend on pressure and temperature dependence of solubility of certain solutes in an SCF solvent it the most crucial phenomenon that is exploited in SCF extraction. Many of the same qualities which make SCF ideal for extraction also make them good candidates for use as a superior medium for chemical reactions offering enhanced reaction rates and preferred selectivity of conversion. One such a reaction is completed, the solvent fluids is vented to precipitate the reaction product.

Table 2-1. Physical properties of CO_2 at individual phases[3]

	Gas phase	SCF phase	Liquid phase
Density (g/cm^3)	0.0006 – 0.002 0.002 – 0.006	0.2 – 0.9	0.6 – 1.6
Viscosity ($\times 10^{-3}$ Pa·s)	10 – 30	10 – 90	200 – 300
Diffusivity (cm^2/s)	0.1 – 0.4	$(0.2 – 0.7) \times 10^3$	$(0.2 – 2.0) \times 10^5$

Table2-2. Critical data for pure components [4]

Solvent	T_c [℃]	P_c [MPa]	Solvent	T_c [℃]	P_c [MPa]
Helium	-268	0.23	Propane	96.65	4.25
Hydrogen	-240.2	1.29	Hydrogen sulfide	100.15	4.25
Neon	-228.8	2.76	Ethyl fluoride	102.16	5.02
Nitrogen	-147	3.39	Radon	104.5	6.28
Carbon monoxide	-140.3	3.5	Carbonyl sulfide	105.65	6.35
Argon	-122.4	4.87	Dichlorodifluoromethane	111.85	4.14
Oxygen	-118.6	5.04	Perfluorobutane	113.2	2.32
Nitric oxide	-93	6.48	Propadiene	120	5.47
Methane	-82.75	4.6	Cycloperopane	124.7	5.49
Krypton	-63.7	5.5	Dimethil ether	126.85	5.24
Carbon tetrafluoride	-45.55	3.74	Ammmonia	132.4	11.35
Silicon tctrafluoride	-14.05	3.72	Isobutene	135.05	3.65
Siliane	-3.46	4.84	Methyl chloride	143.1	6.7
Ethylene	9.25	5.04	Chlorine	143.75	7.98
Xenon	16.55	5.84	Hydrogen jodide	150.85	8.31
Hexafluormethane	19.85	3.06	n-Butane	152.05	3.8
Trifluoromethane	26.15	4.86	Methil amine	156.85	7.43
Chlorotrifluiromethane	28.8	3.87	Sulfur dioxide	157.65	7.88
1,1 Difluoroethene	29.7	4.46	Diethilether	193.55	3.64
Carbon dioxide	31	7.38	n-Pentane	196.55	3.37
Ethane	32.25	4.88	Diethylamine	223.35	3.71
Chlorotrifluorosilane	34.5	3.47	n-Hexane	234.35	3.01
Acetylene	35.15	6.14	Acetone	234.95	4.7
Nitrous Oxide	36.5	7.24	Isopropanol	235.15	4.76
Monofluoromethane	41.85	5.6	Methanol	239.45	8.09
Sulfurhexafluoride	45.6	3.76	Ethanol	240.75	6.14
Hydrogen chloride	51.55	8.31	Ethyl acetane	250.1	3.83
Trifluorobromomethane	67.05	3.97	n-Heptane	267.15	2.74
1,1,1 Trifluoroethane	73.1	3.76	Acetonitrile	272.35	4.83
Chloropentafluoroethane	80	3.23	Cyclohexane	280.35	4.07
Hydrogen bromide	90	8.55	Benzene	289.05	4.89
Propylene	91.8	4.6	Toluene	318.65	4.1
Chlorodifluoromethane	96.15	4.97	Water	374.15	22.12

A list of other SCFs and their critical properties are given in **Table 2-2.** All of the substance have critical points. However, significant supercritical fluids which have been used industrially are water, carbon dioxide and methanol. Methanol have the intermediate properties between water and CO_2. Especially water and CO_2 exist on the nature. Therefore these substance are well known as environment friendly solvent.

2-3. Properties of SCF

2-3-1. Density [1,5]

Thermodynamically, SCF is a state where the pressure and temperature are beyond the critical point clause. In practice, an SCF solvent is mostly used as an extractant in the approximate range of temperature up to 1.2 times the critical temperature and pressure up to 2.5 times the critical pressure. This range of operating conditions provides liquid-like densities as can be seen from **Figure 2-2**. Further, as indicated in **Figure 2-3**, the carination of density, ρ, and static dielectric constant, ε, with pressure show similar trends. For example, for CO_2, both ρ and ε rise sharply between 7 to 20 MPa. It is important to note that at around 20 MPa and beyond, both parameters attain values similar to those for liquids. This provides an explanation as to why SC-CO_2 exhibits high solvent power above a certain pressure, depending on that needs to be dissolved, and thus can be used as good solvent in moment, i.e., it is nonpolar and hence in the SCF state, it serves as a good solvent for natural molecules that are nonpolar. However, it has a quadruple moment for which it can also dissolve slightly polar and some polar substances at relatively high pressures (>25 MPa).

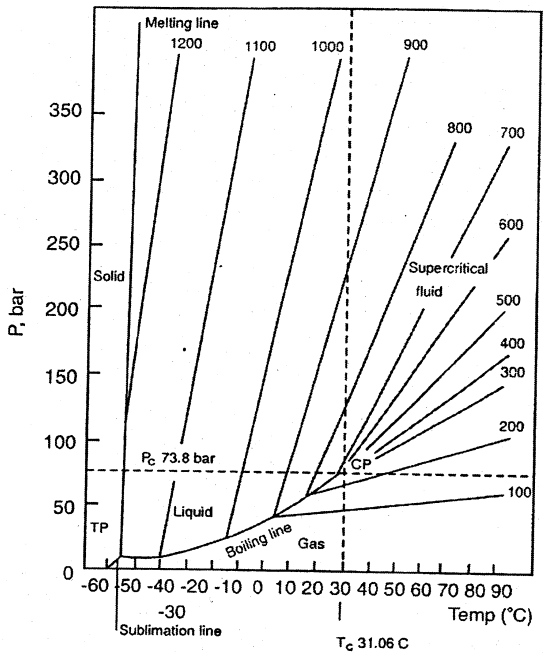

Figure 2-2. P-T diagram of CO_2 at densities from 100 to 1200 g/L, (100 bar=10 MPa) [6]

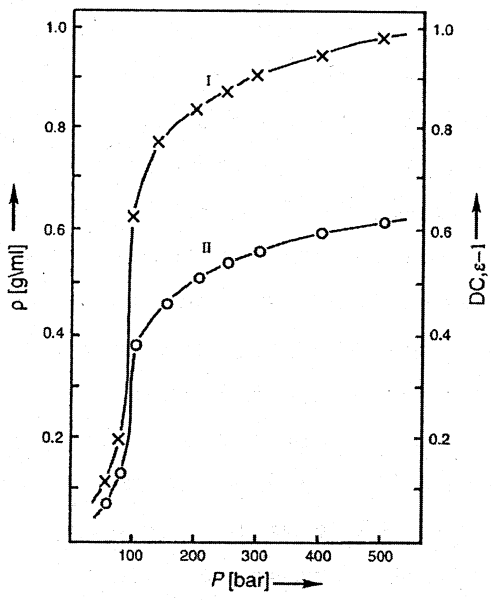

Figure 2-3. Variations with pressure of density, ρ(I), and the dielectric constant ε(II), of CO_2 at 40 ℃(100 bar=10 MPa) [6]

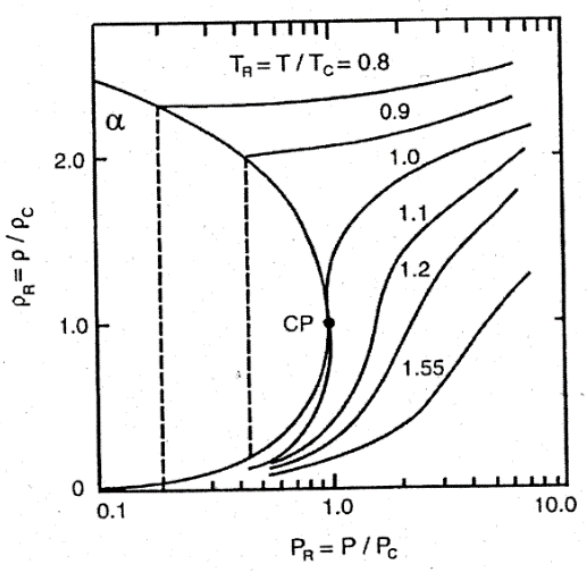

Figure 2-4. Variation of the reduced density (ρ_r) of a pure component near its critical point [1]

Density is varied with pressure and temperature. The solvent capacity at the SCF state is density dependent and it is the sharp variability of density with pressure and temperature in this state that provides uniqueness to an SCF solvent, **Figure 2-4** illustrates such variation of density with pressure at different temperature in terms of the reduced parameters of T_r (= T/T_c) and P_r (P/P_c). At $P > P_c$, the variation of density with an increase in temperature from subcritical to supercritical condition is monatomic. For example, at a reduced temperature, T_r in the range of 0.9 to 1.2, the reduced solvent density, ρ_r (or ρ/ρ_c), can increase from 0.1 to 2.0, as the reduced pressure, P_r, increases in the range from 1 to 2. However, the density of the SCF solvent reduces as T_r is increased to 1.55 and reduced pressures greater than 10 are needed to attain liquid-like densities. By regulating the pressure and temperature. It is thus possible to alter density, which in turn regulates the solvent power of the SCF solvent. In the view of compressibility, as can be seen from **Figure2-4**, the compressibility of any fluid is very high in the vicinity of its critical point

and diverges to infinity at its critical point. In other words, an SCF solvent is highly compressible and essentially gas-like, in contrast to liquid solvents. This high compressibility of the SCF solvent facilitates the alteration of density and hence the solvent power. It also allows fine tuning of the solvent power for selective separation of one or more active constituents out of the total extractable from a raw materials. In short, as the density of the SCF solvent can be carried continuously between gas-like and liquid-like values with moderate changes of pressure, it is possible to make avail of a wide spectrum of solvent properties in a single SCF solvent by simply changing temperature and pressure and also density. Therefore, it is possible to form multiple products in the same SCF extraction plant, taking advantage of the possible variability of solvent properties that one may achieve with SC-CO_2 [5].

2-3-2. Thermodynamic properties [6]

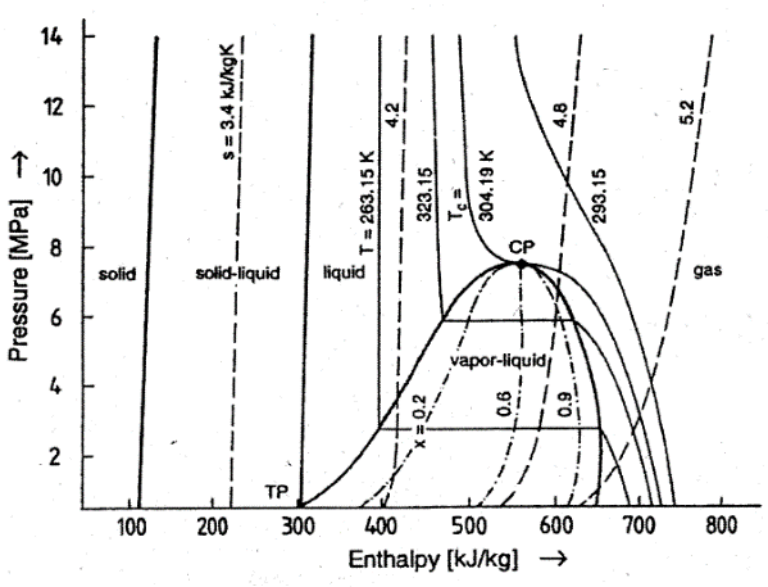

Figure 2-5. Enthalpy dependence on pressure for CO_2 [6]

Enthalpy, internal energy, entropy and others are important thermodynamic properties, which can be related to operating variables of processing equipment, e.g., enthalpy to a temperature increase in a heat exchanger or increasing pressure in an autoclave. Variation of these properties can be calculated in dependence of pressure, temperature and composition of the mixture using equation of state.

Figure 2-5 shows enthalpy of CO_2 in dependence of pressure. As shown in the figure, enthalpy of gas decreases with pressure at constant temperature. Enthalpy of the liquid phase at constant temperature remains constant for moderate pressures. Only at high pressures in the range of more than 100 bar (=10 MPa) dose influence of pressure on the thermodynamic properties of the most liquids become substantial.

Interdependence of thermodynamic properties is often represented in a *T*,*S*-diagram, as presented for CO_2 in **Figure 2-6.** Thermodynamic work needed for a reversible cyclic process can be determined by the area in a *T*,*S*-diagram included by the process cycle. At constant temperature, the entropy of CO_2 decreases with increasing pressure.

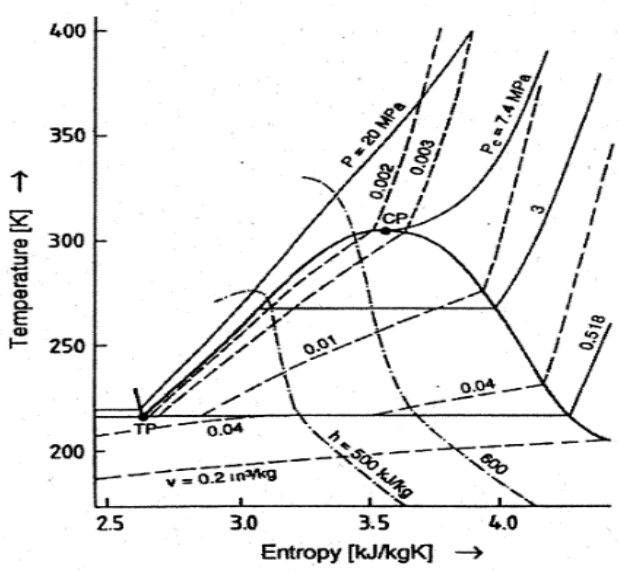

Figure 2-6. *T*,*S* diagram for CO_2 [6]

Heat capacity, C_p, of CO_2 in the region up to 220 bar (=22 MPa) is plotted in **Figure 2-7**. At higher pressure, variation of C_p, with pressure is low. In grass, heat capacity C_p decreases with temperature and increases with pressure. Since supercritical solvents are applied while undergoing major changes of pressure and temperature, behavior of C_p is better related to density, **Figure 2-8.** On the other hand, since P and T are adjustable parameters in a process, dependence on P and T must be familiar.

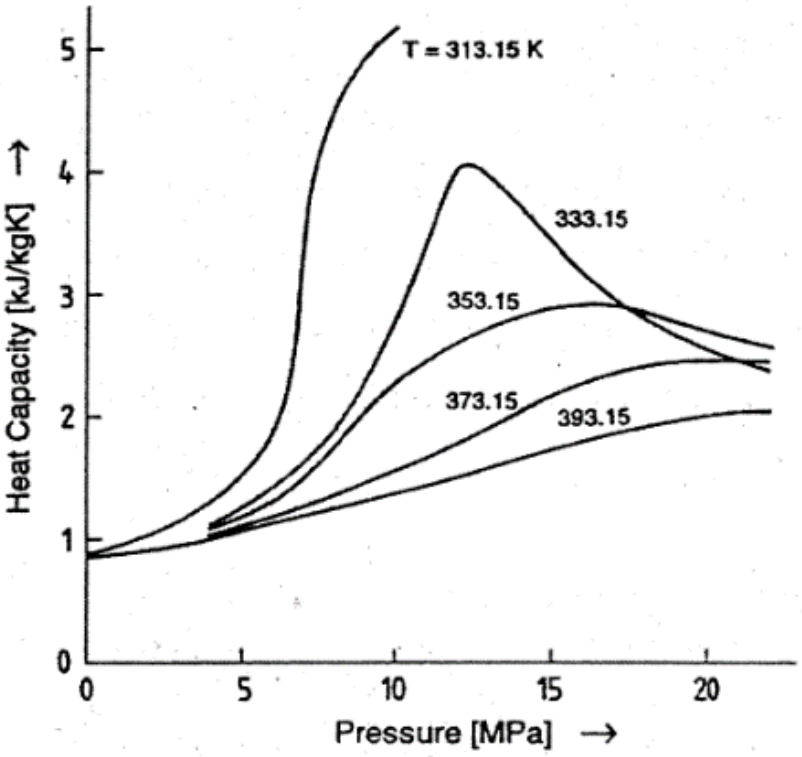

Figure 2-7. Heat capacity C_p of gaseous CO_2 [6]

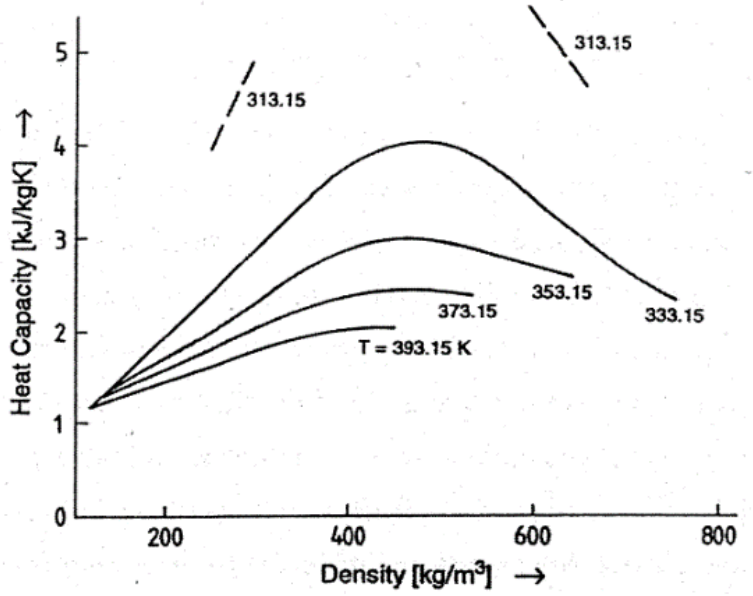

Figure 2-8. Heat capacity C_p of CO_2 as function of density [6]

2-3-3. Transport properties [1]

In SCF extraction, as in other technical processes, fluids and solids are transported, their temperature is changed by heat transfer and composition of mixtures is altered by mass transport via phase boundaries. Bulk transport of matter is determined by viscosity, transport of thermal energy by thermal conductivity and molecular transport is characterized by the diffusion coefficient. Enhanced pressure, as necessary for SCF extraction process, strongly influences these transport properties. Contrary to equilibrium properties, the influence of pressure on nonequilibrium properties like viscosity, thermal conductivity and diffusion coefficient cannot be calculated with thermodynamic relations.

2-3-3-1. Viscosity [2]

The addition of stress on one point of the internal fluid, the fluid velocity gradient is generated internally by moving. CO_2 viscosity of a wide range of temperature and

pressure including the gas and liquid regions was shown in **Figure 2-9** [Vesovic et al. 1990]. Viscosity of the saturated gas and the saturated liquid is indicated by the saturation line in this figure. They coincide at the critical point. Left vertical line than the saturation line (4.6 MPa) is a counter line. When the pressure below the critical pressure, isobars of gas and liquid viscosity is a curve that starts from a point corresponding to the saturated vapor pressure of the saturation line. In the case of behavior of isobars of 0.1 MPa, in the low-pressure gas, viscosity is increasing with increasing temperature. In addition, viscosity increases with increasing pressure. Its influence is greater than in the low pressure. On the other hand, as can be seen from the isobar of high pressure liquid of viscosity and the saturated liquid, the value of the viscosity with the temperature rise in the liquid state is reduced. This is because the movement of the molecules is facilitated by increasing temperature, the increase of the free volume of the molecule in the liquid or increasing the number of vacancies. However, if the pressure is further increased, the viscosity increases with temperature decreases in the range of 8 MPa of 20 MPa of the medium density fluid. However, the viscosity is increased by increasing temperature to a certain point. Furthermore, when the pressure increases, viscosity decreases monotonically with temperature.

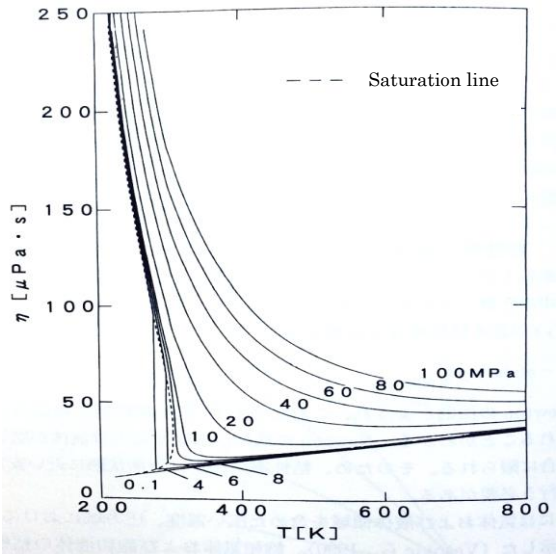

Figure 2-9 Viscosity behavior of CO_2 [7]

2-3-3-2. Diffusivity [1]

Diffusion is transport of matter without convection or mechanically induced mixing. Although the diffusion process is a transient phenomenon in the system, their effects are usually very small and an average value is considered for the thermodynamic state of the system at which the diffusivity is measured. **Figure 2-10** shows the self-diffusion of CO_2 as function of temperature over a wide pressure range, which is approximately the same as the diffusivity of a molecule having a similar size diffusing thorough CO_2. It can be seen that diffusivities of solutes in organic liquids are of the order of 10^{-5} cm^2/sec, which are much lower (by one or two orders of magnitude) than the self –diffusivity of CO_2. The diffusivity in SC-CO_2, in general, increases with temperature and decreases with pressure. At a low pressure, the diffusivity is nearly independent of composition, whereas at higher densities, the composition dependence becomes more significant.

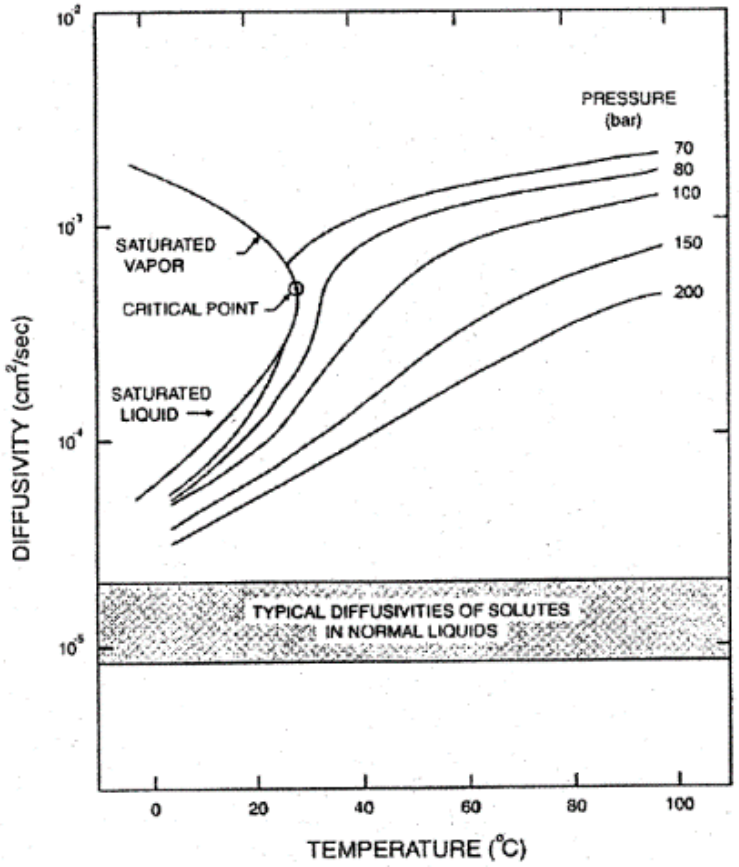

Figure 2-10. Diffusivity behavior of CO_2 (100 bar=10 MPa)[1]

2-3-3-3. Thermal conductivity [6]

Thermal conductivity is defined as the proportionality constant of the linear relationship of heat flux with respect to temperature gradient. Thermal conductivity, λ, depends on temperature, pressure, or density of the fluid. In general, thermal conductivity decreases with increasing temperature at the supercritical condition, passes through a minimum value at any pressure, and then increases with increasing temperature and increasing density for most SCF, as represented in **Figure 2-11**. The influence of pressure is less after a minimum value of λ is observed at each pressure when temperature is increased as shown in **Figure 2-12**.

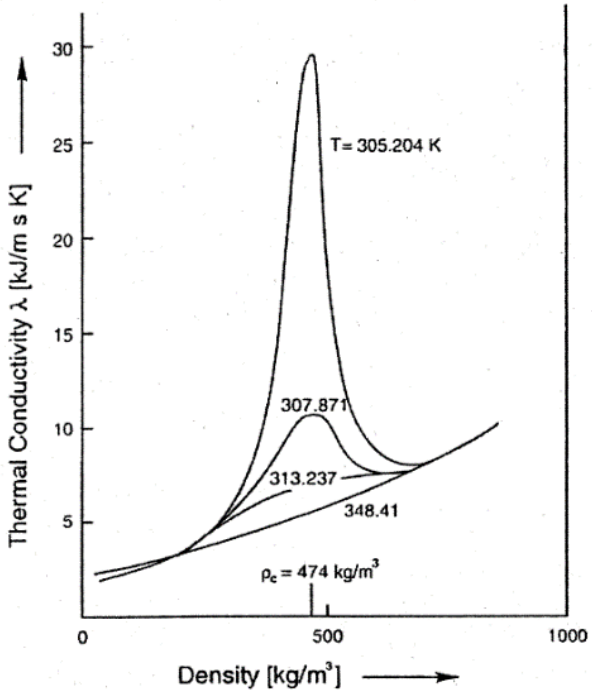

Figure 2-11. Thermal conductivity of CO_2 in the vicinity of the critical point [6]

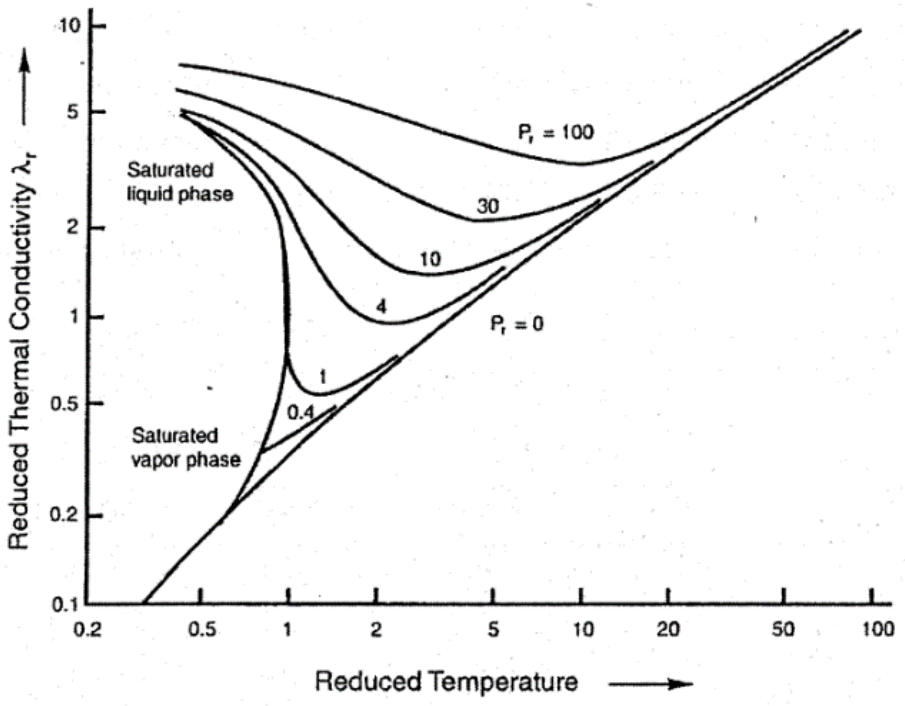

Figure 2-12. Reduced thermal conductivity for bi-atomic gases [6]

2-3-3-4. Surface tension [6]

Surface tension between two phases decides the stability of the phase boundary and may even break a continuous liquid film into spherical droplets depending on the relative magnitudes of strong attraction on the liquid side over the weak attraction on the gaseous phase. The surface tension, σ of a pure liquid caries between 20 and 40 dynes/cm. Surface tension of a liquid decreases with pressure and increases with temperature, as can be seen in **Figure 2-13**. Surface tension of a gas, however, increases with pressure. Surface tension approaches zero at the critical point, as the density difference between the phases is zero, as can be seen in **Figure 2-14.**

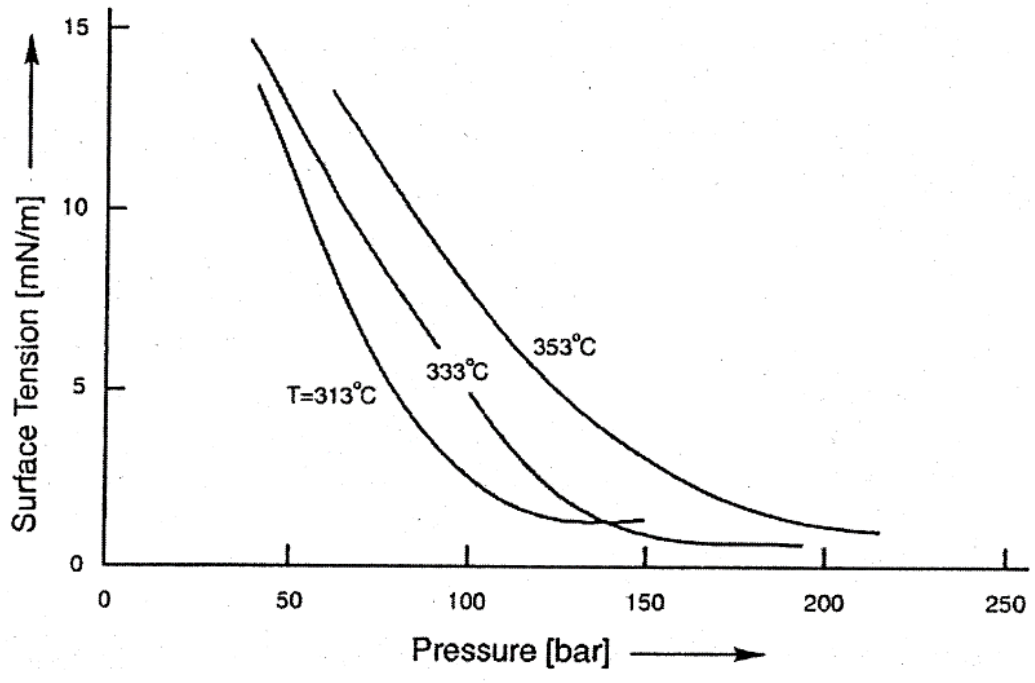

Figure 2-13. Surface intension for the system squalane-CO_2 (100 bar=10 MPa)[6]

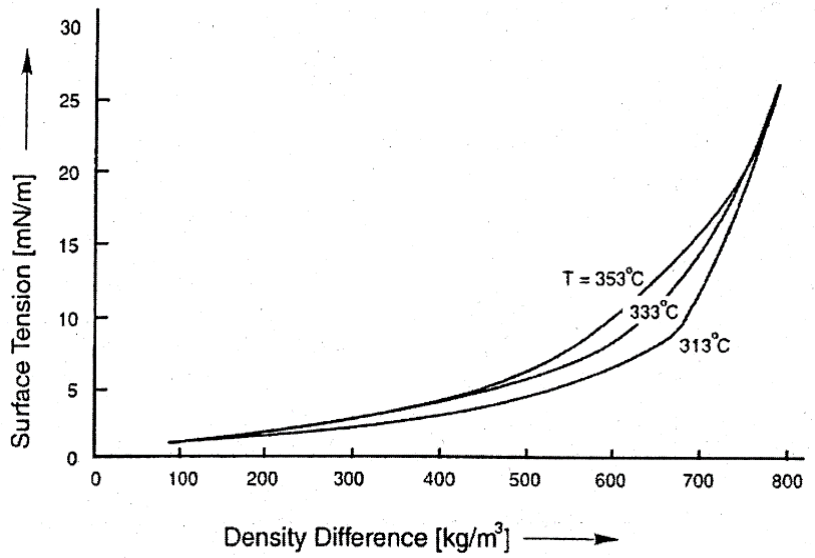

Figure 2-14. Surface intension for the system squalane-CO_2 with density difference between coexisting phases [6]

References

[1] M. McHugh, V. Kurukonis, Supercritical Fluid Extraction, 2nd ed., *Butterworth-Heinemann, Stoneham,* MA, USA (1994).

[2] S. Saito, Science and technology of supercritical fluid, *Sankyo Business* (1996)

[3] A. Akgermsean, G. Madras, Editors: E. Kiran, J.M.H.L. Sengers, Fundamentals of Solids Extraction by Supercritical Fluids, in Supercritical Fluids-Fundamentals for Application-, *Springer, NATO ASI Series E: Applied Sciences,* 273(1994)

[4] Detabace of Thermophysical Properties of Fluid Systems by National Institute of Standards and Technology(NIST) http://webbook.nist.gov/chemistry/fluid/

[5] M. Mukhopadhyay, Natural extracts using supercritical carbon dioxide, *CRC press LLC,* Florida, USA (2000)

[6] G. Brunner, Gas Extraction: An introduction to fundamentals of supercritical tluids and the application to separation processes, *Steinkopff Darmstadt, Springer,* New York, USA (1994)

[7] K. Nagahama, H. Notomi, H. Kato, New extraction technology - supercritical-liquid film, reverse micelle -, *Society of Chemical Engineers, Japan* (2002)

Chapter 3

Carotenoids extraction from natural product

3-1. Fundamentals of carotenoid

3-1-1. Carotenoid

Carotenoids are one of pigments which consist of eight isoprene units joined in a head to tail pattern and it has highly vivid color. The main function of carotenoids is to remove active oxygen generated by various bio-reactions in plants [1]. Carotenoids are widely used as high quality natural colorants in food, cosmetic, and nutraceutical industries [2]. Carotenoids are also used in dietary supplements, because they have a lot of functions such as inhibitory effects on several cancers of lung, breast and blood, in addition to the antioxidant activity [3-5]. Commercially available carotenoids are usually crystalline powders that are soluble in oils and organic solvent, and they have a low solubility against water [6-7]. Currently, in order to obtain the carotenoids from plants, organic solvent extraction is mainly used. Ethyl acetate and hexane are used as a solvent for the purpose. However, there are some problems of (i) oxidation and thermal denaturation of carotenoids, (ii) the impact on the human body, and (iii) residual solvents for environments. Carotenoid fine particles are effectively absorbed into human body, which is attested by concentration of carotenoid in serum and lymph. Thus the micronization of crystalline carotenoids is indispensable to enhance the bioavailability without excess accumulation [8]. The physicochemical properties of β-carotene and lycopene are summarized in **Table 3-1**.

Table 3-1. Physicochemical properties of β-carotene and lycopene [9]

	Formula	Molecular weight	Melting point (°C)
β-carotene	$C_{40}H_{56}$	536.87	172 − 173
Lycopene	$C_{40}H_{56}$	536.87	172 − 173

3-2. Extraction of functional substance from Gac fruit

3-2-1. Introduction

Momordica cochinchinensis known as "Gac fruit" is cultivated in tropically regional countries such as Vietnam. It is botanically classified to the *Cucurbitaceae* family, and has been used as natural red colorants for traditional cooking or traditional medicine in East and Southeast Asia. Gac fruit is known to contain much amounts of lycopene, β-carotene and fatty acids. In medical aspects, the seed membranes have been used for the relief of dry eyes. In addition, the price of Gac fruit is very cheap and its growth speed is high. Therefore, it can be regarded as a useful carotenoid source of nutrition. Aoki et al. reported that 380 μg of lycopene is included in 1g of the seed membrane of Gac fruit [10-11].

3-2-2. Objectives

The present study focuses mainly on the SC-CO_2 extraction of carotenoids from *Momordica cochinchinensis* in order to perform high recoveries by adjusting temperatures (50 – 90 °C) and pressures (20 – 40 MPa). The solubility of the two focused carotenoids, lycopene and β-carotene, was also evaluated from experimental results.

3-2-3. Experimental

3-2-3-1. Materials and Chemicals

Puree samples of *Momordica cochinchinensis* (Gac fruit) were supplied by Kamaya Co., Ltd, Japan. The moisture content of the sample was about 80 %. Sample was freeze-dried using EYELA FDU-1200, Japan. Standard lycopene, β-carotene, High-Performance

Liquid Chromatography (HPLC)-grade methanol and THF used for analysis were purchased from Wako Pure Chemical Industries, Ltd., Japan. CO_2 (99.9 %) was obtained from Uchimura Co., Japan.

3-2-3-2. Equipment and Procedures

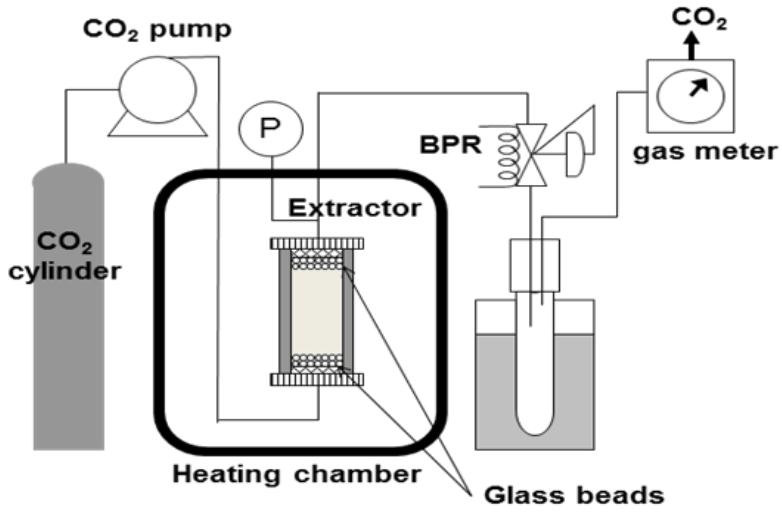

Figure 3-1. Schematic diagram of the SC-CO_2 extraction apparatus [18]

Extraction experiments were carried out using the experimental apparatus shown in Fig. 3-1. The apparatus consists of a high-pressure pump for CO_2 (Jasco PU-2080 100 MPa, Japan), a heating chamber (EYELA /NDO-401 Japan), a 10-mL extraction vessel (Thar Tech, Inc., USA), back-pressure regulator (Jasco BP-2080, Japan), a number of collection vials, and a wet gas meter (Sinagawa Co., Japan). In order to determine the effects of temperature and pressure on the yield of extracted carotenoids, operating conditions were set 50–90 ^{o}C and 20–40 MPa with a constant CO_2 flow rate of 3 mL/min. In all experiments, 3 g of dried Gac fruit was loaded into the extractor filled with glass

beads at the top and bottom, as shown in **Figure 3-1**. The cell was placed in a heating chamber maintained at an operating temperature set in the range. The extract in vials was collected at 15, 30, 60, 90, 120, 180 min, and stored at -20 ^{o}C in the dark until analysis. In order to investigate the extracted components obtained by the conventional method, 3 g of freeze-dried Gac fruit was extracted with 100 mL of chloroform using a Soxhlet apparatus for 15 h until the color of the condensed solvent at the top of the apparatus was clear, indicating that no carotenoids remain in the sample. Chloroform gave the highest yield of extracted lycopene when compared to other solvents used in the present study.

3-2-3-3. HPLC Analysis

Analysis of lycopene and β-carotene extracted by SC-CO_2 was carried out using high performance liquid chromatography (HPLC) equipped with UV/visible detector (UV-970, Jasco, Japan). Extract dissolved in chloroform was injected through a 20-μL loop and separated with an STR ODS-II column (5 μm; 4.6 × 250 mm; Shinwa Chemical Industries, Ltd., Japan) at 40 ^{o}C. The mobile phase was a binary solvent consisting of 1:9 (v/v) THF: methanol flowing at a rate of 1.5 mL/min. Lycopene and β-carotene were monitored at 477 nm. The signals of the detector were recorded in BORWIN chromatography software. Peak corresponding to lycopene and β-carotene was assigned by comparison of retention times and scanned spectra with those of standards. The weight of lycopene and β-carotene thus extracted was calculated by comparison of their peak areas with those of the standards, respectively.

3-2-3-4. Calculation of Recovery

Recovery rate of each carotenoid was calculated using this formula:

$$\text{Recovery}(\%) = \frac{lycopene\ or\ \beta - carotene\ extract(mg/g)}{Initial\ lycopene\ or\ \beta - carotene\ in\ the\ sample(mg/g)} \times 100\%$$

The contents of lycopene and β-carotene in the samples were determined from the results obtained by Soxhlet extraction (Chloroform). The amount of lycopene and β-carotene in the samples was 7.828 and 0.545 mg/g, respectively.

3-2-4. Results and Discussion

3-2-4-1. Effects of Temperature

The effects of temperature on the recoveries of lycopene and β-carotene were studied at a constant pressure of 40 MPa. **Figure 3-2** shows the result of extraction behavior at various temperatures. Figures 3-3 and 3-4 shows the recovery rate of lycopene and β-carotene with respect to temperatures, respectively. The recovery rate of both lycopene and β-carotene increased with temperature, because the solubility of the carotenoids in SC-CO_2 are proportional to temperature. The highest recovery rate of lycopene and β-carotene was both obtained at 90°C. However, in the case of lycopene, it is necessary to extend extraction time, because the recovery rate of lycopene was still low. The yield of total carotenoids also increased significantly with increasing temperature due to thermal

effects on cell wall disruption of the sample. With the disruption, an increase in the transport properties of CO_2 in the sample matrix is expected to increase the rate of extraction, thus resulting in a higher recovery rate. An increase in extraction temperature also resulted in an increase in solute vapor pressure. Under this condition, the density of SC-CO_2 at a constant pressure decreases as temperature increases, but the change in the density becomes smaller at elevated pressures. Additionally, other substances which accounts for about 70 % was expected to fatty acid because of gac fruit is consist by various fat such as palmitic acid (29.2 %), oleic acid (32.3 %) and linoleic acid (28.1 %) in a gac fruit seed membrane [10]. It might be the oil acts as an entrainer, there is a possibility that the oil is promoted carotenoid extraction.

3-2-4-2. Effects of Pressure

The effects of pressure on the recovery rate of lycopene and β-carotene were examined at a constant temperature of 90 ^{o}C. **Figure 3-5** shows the result of extraction behavior at various pressures. **Figures 3-6** and **3-7** also show the effects of pressure on the recovery rate of lycopene and β-carotene at a constant temperature of 90 ^{o}C, respectively. As shown in Figs. 3-6 and 3-7, the recovery rate of both lycopene and β-carotene drastically increased with (increasing) pressure. This is because an increase in pressure gives rise to an increase in both solvent density and solubility of lycopene and β-carotene in SC-CO_2.

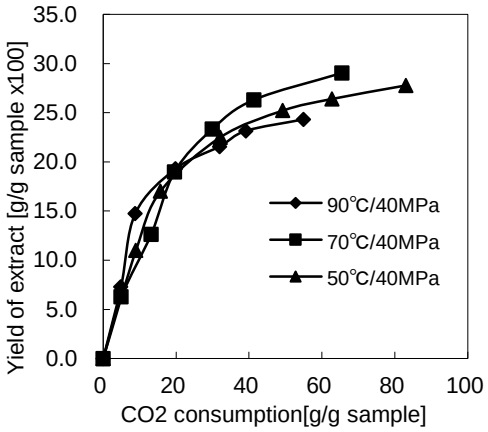

Figure 3-2. Yield of total extract at various temperatures

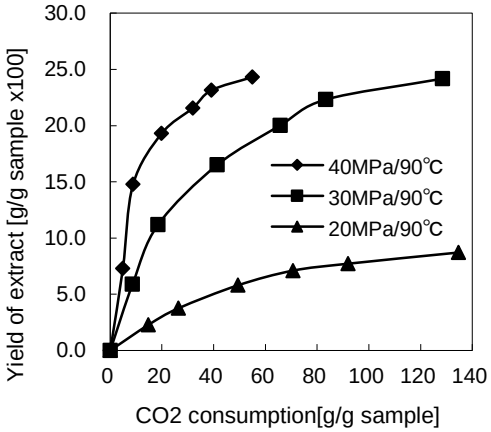

Figure 3-3. Yield of total extract at various pressures

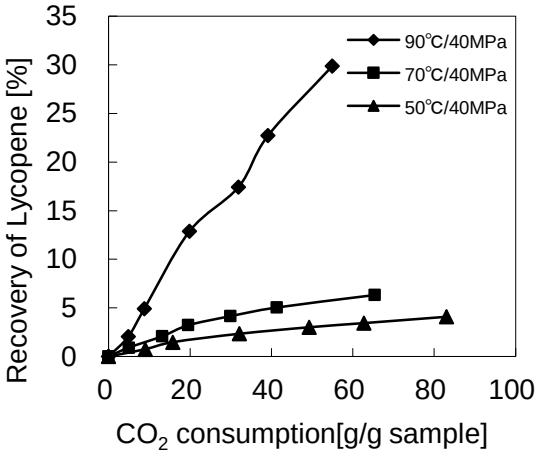

Figure 3-4. Recovery rate of lycopene at various temperatures

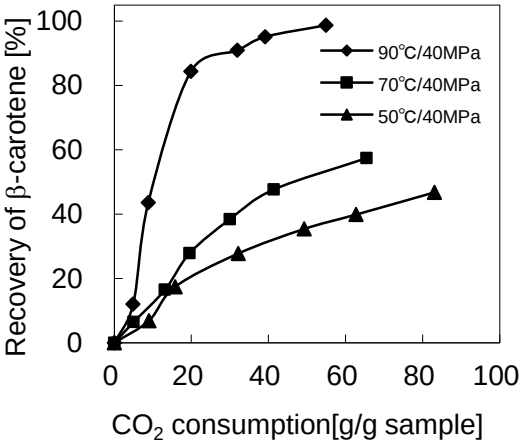

Figure 3-5. Recovery rate of β-carotene at various temperatures

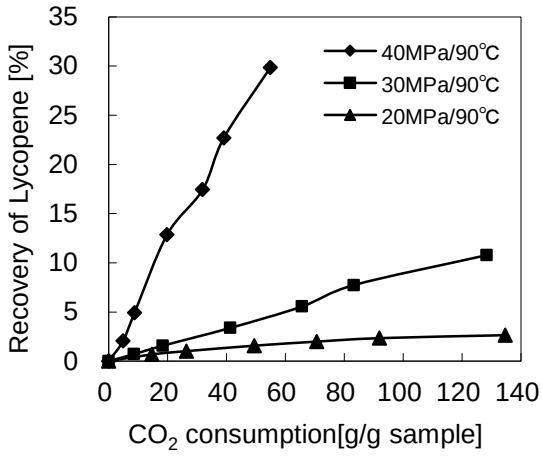

Figure 3-6. Recovery rate of lycopene at various pressures

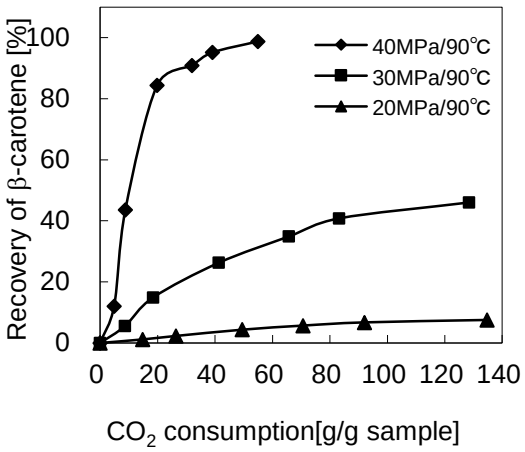

Figure 3-7. Recovery rate of β-carotene at various pressures

3-2-4-3. Solubility of Carotenoids in SC-CO_2

The solubility of both lycopene and β-carotene in SC-CO_2 was also studied at various temperatures and pressures. The results show a correlation between solubility *S* of the solute in the SC-phase and density ρ of the fluid. According to the equation proposed by Chrastil [12], the Chrastil model assumes that the solvation of the solute can be described as an equilibrium between a number of fluid molecules and solute through formation of a solvato complex, and the following equation has been proposed:

$$\ln S = k \ln \rho - \left(\frac{a}{T} + b \right) \qquad (1)$$

Where, *S* is the concentration of the solute in the supercritical phase (g/L), ρ is the density of CO_2 (g/L) at the absolute temperature (*T*), *k* corresponds to the fluid molecules in association with one molecule of solute to form the solvate complex, *a* and *b* are both constants, which take into account the total heat of the reaction and the molecular weight

of the species. The experimental values of solubility were obtained from the slope of the linear section of the extraction yield curve at low CO_2 consumption shown in **Figure 3-4** to **Figure3-7**.

Figures 3-8 and **Figure 3-9** show the solubility of lycopene and β-carotene in the SC-phase as a function of the solvent density at various temperatures, respectively. The constant values used for calculation in Chrastil model are listed in **Table 3-2**. To estimate the correlation of data between experimental and calculated values, the percentage of the average absolute deviation (AAD %) was calculated by considering all concentration values. The results showed that the Chrastil equation fairly represents the solubility behavior of both lycopene and β-carotene in SC-CO_2 with AAD % less than 10.

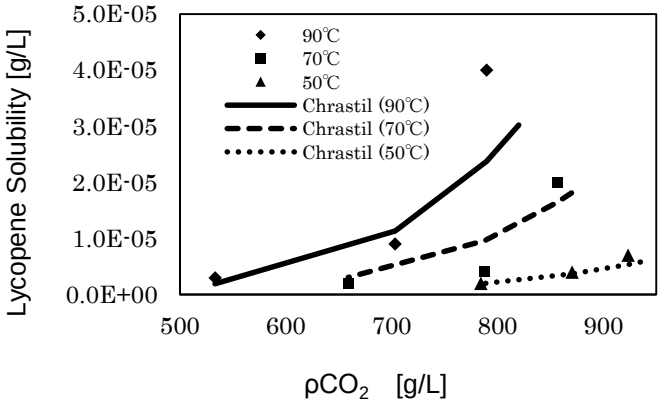

Figure 3-8. Solubility of lycopene

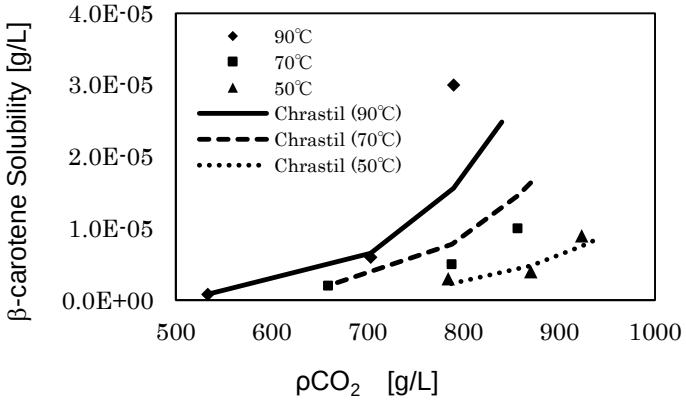

Figure 3-9. Solubility of β-carotene

Table 3-2 Values of Chrastil model constants

	k	*a*	*b*	AAD
Lycopene	6.378596	279.4622	50.09834	0.40～4.89 %
β-carotene	7.510778	214.4595	58.79294	0.13～5.89 %

3-2-5. Conclusions

Lycopene and β-carotene were extracted from Gac fruit using SC-CO_2 at various temperatures and pressures. Recovery rate of carotenoids increased with both temperature and pressure. The highest recovery rate of carotenoids was obtained to be at 90 ^{o}C and 40 MPa. Solubility of lycopene and β-carotene in SC-CO_2 was calculated respectively, using Chrastil equation. However, continuous process of carotenoid extraction and micronization has the following problems. SC-CO_2 is excellent for the extraction of oil because it is non-polar solvent. Therefore the extract contains oil in addition to carotenoids and it is difficult to produce fine particles. However, the oil acts as an entrainer, there is a possibility that the oil is promoted carotenoid extraction. The presence of oil is also important in this extraction.

3-3. Extraction of functional substance from Saffron

3-3-1. Introduction

Crocus sativus L (saffron) is perennial herb that belongs to Iridaceae. It is popular because of its delicate aroma (safranal), pigment (crocin) and bitterness flavor (picrocrocin). Crocin is one of the carotenoids, which is water-soluble. The saffron flower is composed of six purple petals, three golden yellow stamens and one red pistil. Spice saffron is obtained by drying the pistil which consists of three stigmas [13]. Saffron is cultivated in the area of Iran, Turkey and Greece, but now it is also successfully cultivated in European countries such as Spain, Italy, France, and Switzerland, as well as in Morocco, Egypt, Israel, Azerbaijan, Pakistan, India, New Zealand, Australia, China, and Japan [14]. To prevent deterioration of the spices saffron, it is important to introduce drying process immediately after harvesting and control the temperature and humidity perfectly during drying process [15]. Many saffron which are failed drying process are defined to be low grade by ISO3632, and these often have been discarded, and these have not been utilized to its full potential. Recently, the pigments of spice saffron are increasingly attracting attention because of their much functionality, such as prevention effect of Alzheimer's disease, colon cancer, neurodegenerative disorders accompanying memory impairment and so on [16]. Crocin is being hydrolysed so that four glucoses are dissociated from crocin, which change to crocetin. Yukihiro Shoda et al. were examined for the pharmacological activity of crocin and its degradation product. Strongest antioxidant activity of crocin is reduced in accordance with the dissociation of glucose [17]. (**Figure 3-10**)

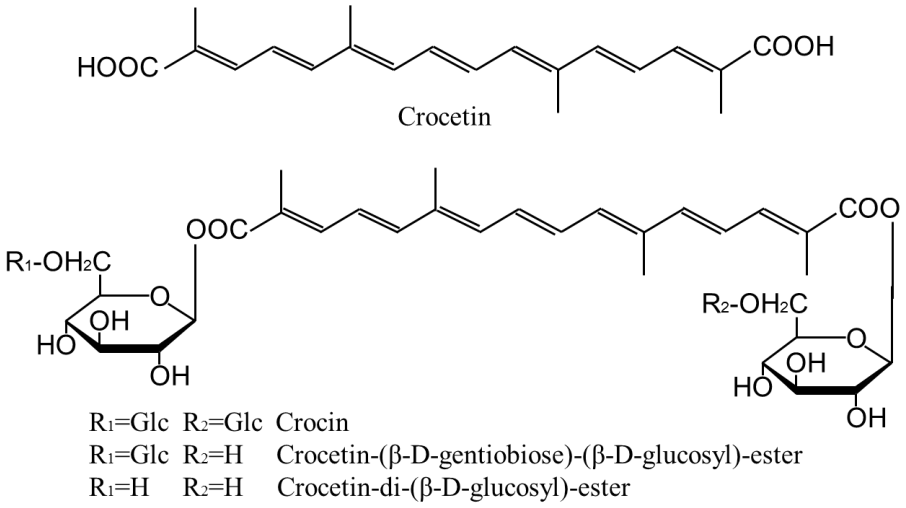

Figure 3-10. Structure of crocetin and its glycosides

The components of spice saffron such as picrocrocin, safranal, HTCC (2,6,6-trimethyl-4-hydroxy-1-carboxproducts), crocin, and crocetin have a high enzymatic and chemical reactivity and heat labile. Picrocrocin is sensitive to heat, namely, it is changed to safranal by hydrolyzation. On the other hand, HTCC is degraded by enzyme called β-glucosidase which exists widely in plants. In addition, HTCC is dehydrated by proton and is converted to safranal. Besides, crocin undergoes an oxidation process with light and oxygen, because it has a conjugated double bond. Furthermore, if there is more moisture, crocin undergoes an enzymatic hydrolysis by endogenous [17]. Therefore, it is assumed that the composition of the extract components strongly depends on the extracting method and extraction conditions.

Supercritical fluid is also used to extract fat-soluble components. SC-CO_2 is the most frequently used extraction solvent in supercritical extraction. SC-CO_2 is neither toxic, nor flammable, and exhibits a high selectivity as a result of low viscosity, high diffusivity, and liquid-like density and act-like hexane [18]. Siti Machmudah et al. succeeded in

extracting caffeine and chlorogenic acids from coffee beans with water and SC-CO_2. These studies basically focused on obtaining both water-soluble components and oil-soluble component by using both the entrainer and SC-CO_2 together in the extraction process [19].

3-3-2. Objectives

In this work, phytochemicals were extracted from spice saffron using SC-CO_2 extraction in order to clarify the effects of some extraction parameters such as temperature (from 40 to 80 ^oC) and pressure (from 20 to 40 MPa).

3-3-3. Experimental

3-3-3-1. Materials and Chemicals

Spice saffron was supplied by Sumimoto packaging consultant office, Japan. Samples were milled to size of 10 μm using IKA Co. MF10 basic, Japan. 4-nitroaniline as an internal standard and HPLC-grade methanol used for analysis were purchased from Wako Pure Chemical Industries, Ltd., Japan. CO_2 was obtained from Sogo Co., Japan.

3-3-3-2. Equipment and Procedures

Extraction experiments were carried out using the experimental apparatus shown in Fig. 3-11. The apparatus consists of a high-pressure pump for CO_2 (Jasco PU-2086 Plus, Japan), a heating chamber (EYELA /WFO-400W Japan), a 10 mL extraction vessel (Thar Tech, Inc., USA, 10 mL in volume), a back-pressure regulator (Jasco BP-2080, Japan), a number of collection vials, and a wet gas meter (Sinagawa Co., Japan). In order to determine the effect of temperature and pressure on the yield of extracted components,

extracts were extracted from saffron at temperatures between 40 and 80 ºC, pressures of 20 to 40 MPa and CO_2 flow rate of 3 mL/min. In each experiment, approximately 0.5 g of milled saffron was loaded into the extraction vessel and the remaining volume was filled with glass beads at the bottom and top of the cell. The cell was placed in the heating chamber to maintain the operating temperature. The extract was collected in a collection vessel at every 15, 30, 60, 120, 180, 240 min, and analyzed immediately after the extraction. In order to compare the extracted components with those obtained by the conventional method, 0.5 g of milled saffron was extracted with 100 mL of water or organic solvent using a magnetic stirrer (AS ONE REXIM RSH-IDR, Japan) for 60 min. The extract was collected in a collection vessel at every 10, 20, 30, 40, 50, 60 min.

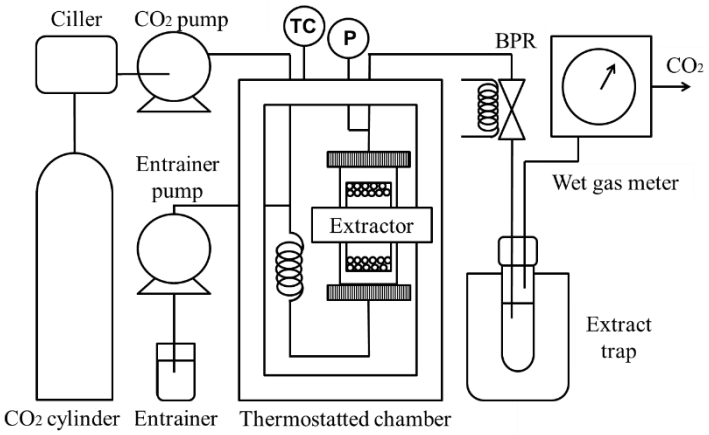

Figure 3-11 Schematic diagram of the SC-CO_2 extraction apparatus

3-3-3-3. HPLC Analysis

Analysis of extracts was carried out using high performance liquid chromatography (HPLC) equipped with intelligent UV/visible detector (SPD-M10A, SHIMADZU Ltd., Japan). Extract diluted with methanol was injected through 50 μL and separated with a Nova-Pak C18 column (4 μm; 3.9 × 150 mm; Waters, Japan) at 30 ºC. A liner gradient

elution of methanol (20-70 %) at 1 % methanol/min gradient speed and 1 mL/min flow rate was selected as the best analysis condition [15]. Picrocrocin and HTCC were monitored at 250 nm, safranal at 310 nm, croin at 440nm, while 4-nitroaniline as internal standard was monitored at all three wavelengths. The signals of the detector were recorded in SHIMADZU Ltd. Peaks corresponding to individual extracts were assigned by the comparison of retention time and capacity factor *k'* of components [15]. Since pure standards of all saffron components are difficult to be commercially available, quantitative determinations were made as the ratio of each compound integration area to the internal standard integration area (*A* Comp /*A* I.S.), obtained at the wavelength of the maximum absorbance.

3-3-4. Results and Discussion

The color of the initial extract by SC-CO_2 and water was vivid red, whereas it was a vivid yellow when SC-CO_2 and methanol was used. The extract gradually changed into colorless by increasing the consumption of solvent towards the end of the extraction process. The detected functional materials were picrocrocin and HTCC at 250 nm, safranal at 310 nm, and crocin and its degradation product at 440 nm. The functional materials of picrocrocin, safranal, and crocin were extracted successfully by SC-CO_2 with water as an entrainer. It is considered that it might be possible to extract not only water-soluble components (picrocrocin, HTCC, crocin) but also lipophilic components (safranal) by using the SC-CO_2.

The amount of extracted components at various temperature, pressure and extraction solvents were shown in **Figure 3.12 - 3.16**, **Figure 3.17 – 3.21,** and **Figure 3.22 – 3.26**, respectively. The amount of extracted components were staled as ratio of each component

integration area to the internal standard integration area.

3-3-4-1. Effects of Temperature

For all components, the amount of extracted components increased with increasing temperature of SC-CO_2 extraction with water as an entrainer. It can be explained that vapor pressure of water increased with increasing temperature that resulted in the increasing soluble extracted components, such as picrocrocin, HTCC, safranal, crocin and decomposed crocin. Since safranal is a non-polar components, the ratio if its integration area and internal standard was low. However, with the increasing of temperature, the vapor pressure of safranal might be increased as the temperature increased. For the comparison with water and methanol extraction, higher temperature of SC-CO_2 extraction with water as entrainer yielded higher amount of extracted components.

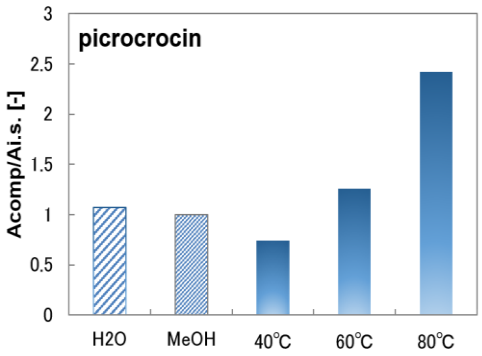

Figure 3-12 Amount of Picrocrocin at various temperatures

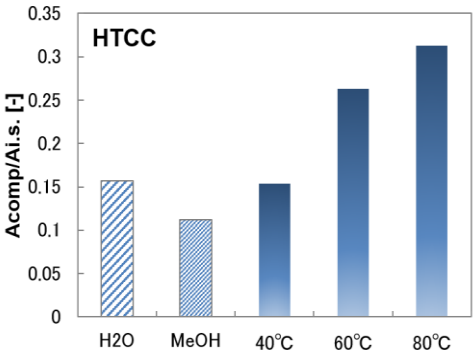

Figure 3-13 Amount of HTCC at various temperatures

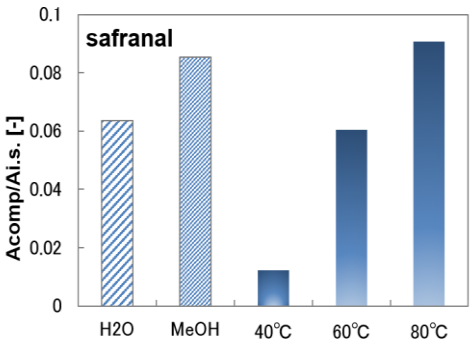

Figure 3-14 Amount of Safranal at various temperatures

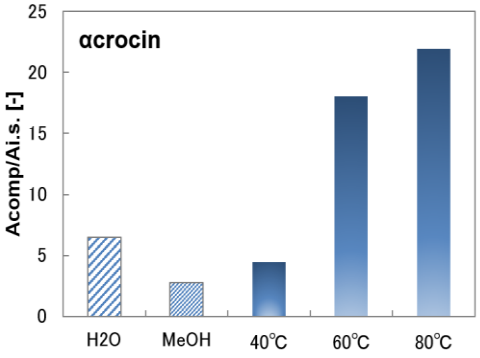

Figure 3-15 Amount of α-crocin at various temperatures

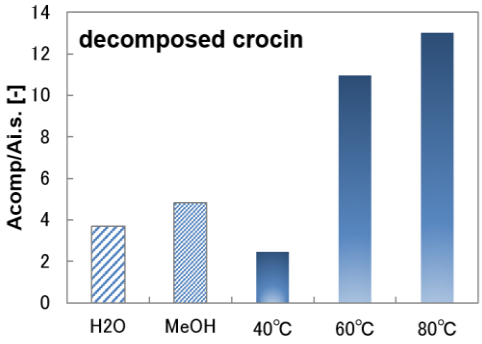

Figure 3-16 Amount of Decomposed crocin at various temperatures

3-3-4-2. Effects of Pressure

In general, the increase of pressure resulted in increasing all extracted components, due to the increasing for picrocrocin, α-crocin, and decomposed crocin, the highest amount of extracted components was obtained at 30 MPa. While for HTCC and safranal, the highest amount was obtained at 40 MPa. It might be due to the effect of water as entrainer in SC-CO_2 extraction. The higher the pressure, the denser CO_2 might higher the flow of water to extract the components.

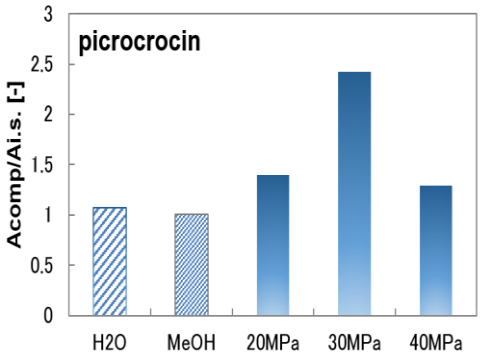

Figure 3-17 Amount of Picrocrocin at various pressures

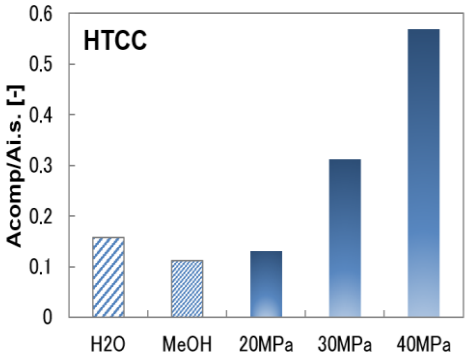

Figure 3-18 Amount of HTCC at various pressures

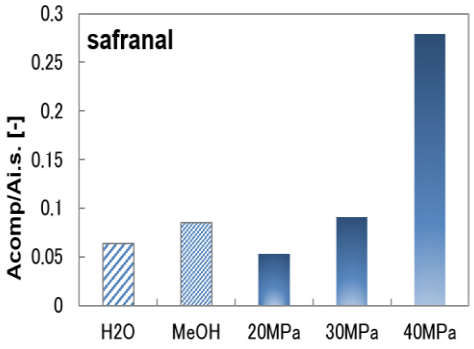

Figure 3-19 Amount of Safranal at various pressures

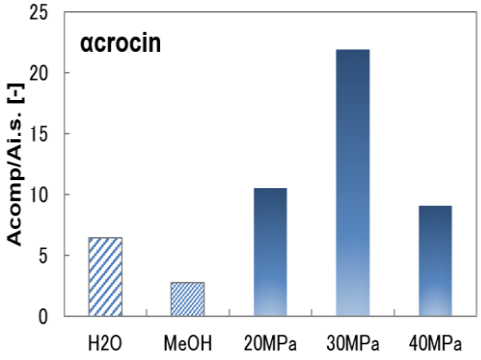

Figure3-20 Amount of α-crocin at various pressures

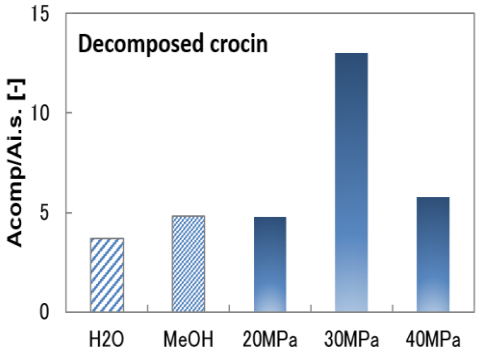

Figure3-21 Amount of Decomposed crocin at various pressures

3-3-4-3. Effects of Solvent

As shown in **Figure 3.22 – 3.26**, solvent played an important role to extract the components. By using water and methanol as a solvent, small amount of components could be extracted. By adding of water or methanol in SC-CO_2 extraction, the amount of extracted components increased dramatically. It was understand that the addition of entrainer causes the enhancement the components. However, for α-crocin and decomposed crocin, the addition of methanol caused negative effect on the extraction.

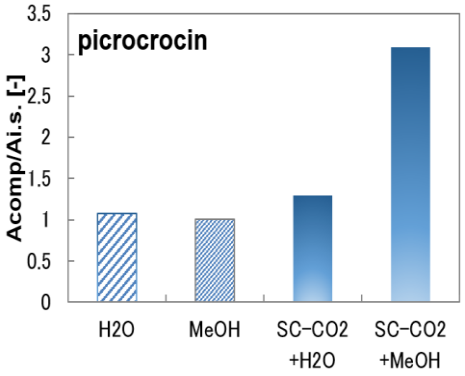

Figure 3-22 Amount of Picrocrocin at various extraction solvent and entrainer

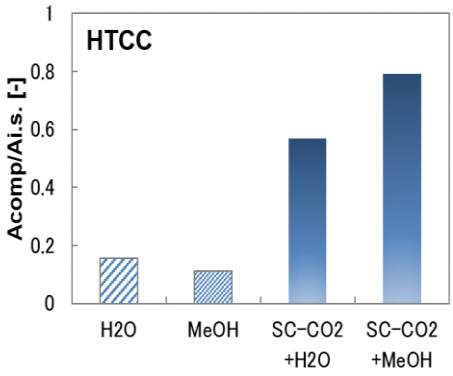

Figure3-23 Amount of HTCC at various extraction solvent and entrainer

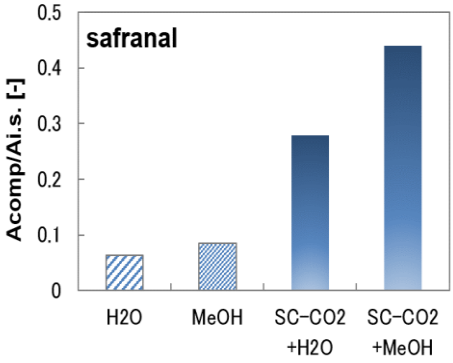

Figure3-24 Amount of Safranal at various extraction solvent and entrainer

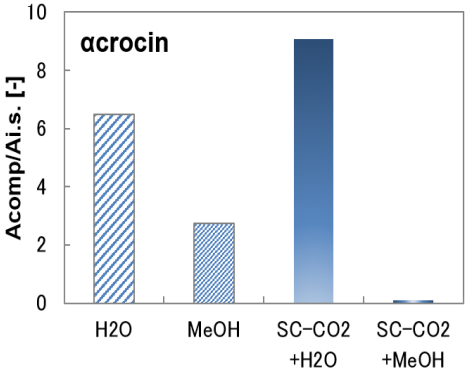

Figure 3-25 Amount of α-crocin at various extraction solvent and entrainer

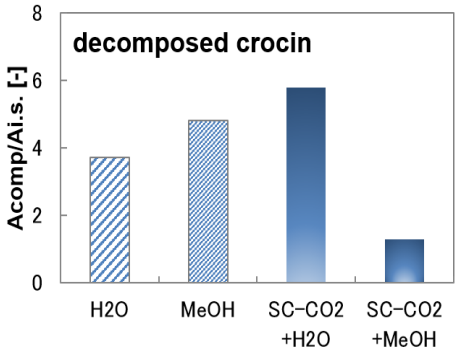

Figure 3-26 Amount of Decomposed crocin at various extraction solvent and entrainer

3-3-5. Conclusions

Functional components were successfully extracted by various extraction solvents such as water, organic solvent, SC-CO_2 with an entrainer such as water and methanol. However, component compositions of the extracts depend on the extraction method and experimental conditions such as temperature, pressure and entrainer.

References

[1] F. Mattea, Á. Martín, M.J. Cocero, Carotenoid processing with supercritical fluids, *J. Food Eng*., 93, 255-265 (2009)

[2] F. Miguel, A. Martín, T. Gamse, M.J. Cocero, Supercritical anti solvent precipitation of lycopene: Effect of the operating parameters, *J. Supercritical Fluids*, 36(3), 225-235 (2006)

[3] J. Dulińska, D. Gil, J. Zagajewski, J. Hartwich, M. Bodzioch, A. Dembińska-Kieć, T. Langmann, G. Schmitz, P. Laidler, Different effect of □-carotene on proliferation of prostate cancer cells, *BBA-Mol. Basis. Dis*., 1740(2), 189-201 (2005).

[4] J. Levy, E. Bosin, B. Feldman, Y. Giat, A. Miinster, M. Danilenko, Y. Sharoni, Lycopene is a more potent inhibitor of human cancer cell proliferation than either alpeha-carotene or beta-carotene, *Nutr Cancer*., 24(3), 257-266 (1995).

[5] H. Amir, M. Karas, J. Giat, M. Danilenko, R. Levy, T. Yermiahu, J. Levy, Y. Sharoni, Lycopene and 1,25-Dihydroxyvitamin D3 Cooperate in the Inhibition of Cell Cycle Progression and Induction of Differentiation in HL-60 Leukemic Cells, *Nutr Cancer*., 33(1), 105-112 (1999).

[6] A. Martín, F. Mattea, L. Gutiérrez, F. Miguel, M.J. Cocero, Co-precipitation of carotenoids and bio-polymers with the supercritical anti-solvent process, *J. Supercritical Fluids*, 41(1), 138-147 (2007).

[7] F. Mattea, Á. Martín, A.M. Gago, M.J. Cocero, Supercritical antisolvent precipitation from an emulsion: β-Carotene nanoparticle formation, *J. Supercritical Fluids*, 51(2), 238-247 (2009)

[8] H. Hayashi, M. Nakajima, K. Murota, N. Yamanaka, T. Inakuma, The miniaturization of β-carotene particle enhances the bioavailability. *Abstract of International Conference on Food Factors* (2011)

[9] M. Skerget, Z. Knez, Solubility of Binary Solid Mixture α-Carotene-Capsaicin in Dense CO_2. *J. Agric. Food Chem.,* 45, 2066-2069 (1997)

[10] B.K. Ishida, C. Turner, M.H. Chapman, T.A. Mckeon, Fruit Fatty Acid and Carotenoid Composition of Gac (Momordicacochinchinensis Spreng) *J. Agric. Food Chem.,* 52, 274-279 (2004)

[11] H. Aoki, M. Kieu, N. Kuze, K. Tomisaka, V. N. Chuyen, Fruit Fatty Acid and Carotenoid Composition of Gac (Momordicacochinchinensis Spreng), *Biosci. Biotech. Biochem.*, 66 (11), 2479-2482 (2002)

[12] J. Chrastil, *J. Phys. Chem.* 86 (15), 3016-3021 (1982)

[13] J. Serrano-Díaz, A.M. Sánchez, L. Maggi, M. Carmona, G.L. Alonso, Synergic effect of water-soluble components on the coloring strength of saffron spice, *J. Food Compos Anal*, 24, 873-879 (2011)

[14] H. Caballero-Ortega, R. Pereda-Miranda, F.I. Abdullaev, HPLC quantification of major active components from 11different saffron (Crocus sativus L.) sources, *Food Chemistry,* 100, 1126–1131 (2007)

[15] P. Lozano, M.R. Castellar, M.J. Simancas, J.L. Ibora, Quantitative high-performance liquid chromatographic method to analysis commercial saffron (*Crocus sativus L.*) procucts, *J. Chromatogr. A.* 830, 477-483 (1999)

[16] A.V Loskutov, C.W Beninger, G.L Hosfield, K.C Sink, Development of an improved procedure for extraction and quantitation of safranal in stigmas of Crocus sativus L. using high performance liquid chromatography, *Food Chemistry,* 69, 87–95 (2000)

[17] M. Shozan, Pharmacological activity of saffron, *Nagasaki International University review*, 9, 61-73 (2009)

[18] H. Nerome, S. Machmudah, A.T. Quitain, M. Sasaki, M. Goto, *J. Sci. Technol*., 49, 177-183 (2012)

[19] S. Machmudah, K. Kitada, M. Sasaki, M. Goto, J. Munemasa, M. Yamagata: *Ind Eng Chem Res.*, 50, 2227-2235 (2011)

Chapter 4

Particle formation of carotenoid using SC-CO_2

Chapter 4.1 Particle formation of β-carotene

4-1-1. Introduction

Industrial carotenoids are usually crystalline powders that are soluble in oils and organic solvents, and they have a low water-solubility [1-2]. β-Carotene is one of the most common carotenoid pigments used in the industries. Micronized β-carotene particles are effective for human nutrition, since micronization increases the β-carotene concentration in the serum and lymph. The micronization of carotenoid particles may enhance the bio-availability without causing excessive their accumulation in the body [3].

Fine particle formation using supercritical carbon dioxide (SC-CO_2) has recently been attracted attention. Since CO_2 has a low critical temperature, it may be suitable for heat-sensitive materials. In addition, SC-CO_2 can be easily separated from the produced particles along with the organic solvent, because SC-CO_2 becomes gas phase again at ambient temperature and pressure. The supercritical anti-solvent (SAS) process is one of the micronization methods applied to make fine particles from various materials such as pharmaceutical and cosmetic materials and pigments [4-9]. In a typical SAS process, both a solution containing compounds to be processed and an organic solvent are fed via a nozzle into a precipitator to produce particles filled with SC-CO_2. Supersaturation was caused by mixing the solution with SC-CO_2 in the precipitator, leading to crystal nucleation and growth. Several factors affect the particle size and morphology, for examples, operating temperature, pressure, CO_2 and solution flow rate, the kind of organic solvents, and the nozzle type and its inner diameter [10-17].

The solution-enhanced dispersion by supercritical fluids (SEDS) process is one of the modified SAS processes. In this process, the solution and SC-CO_2 are sprayed into a

precipitator by a coaxial nozzle [18-22]

4-1-2. Objectives

In this work, fine particle production of β-carotene with some organic solvents that are approved as food additives has been investigated for application to food products. The most appropriate solvent was selected from *n*-hexane, ethyl acetate, dichloromethane (DCM), and DMF. *n*-Hexane and ethyl acetate are allow to used for food processing. DMF and DCM are not approved anywhere in the world for use in food or supplement products. However these are widely used for micronization process for pharmaceutical industries. therefore DCM and DMF were used as comparison in this session.The effects of operating pressure and temperature of the process on the size and shape of the particles thus obtained were examined. The SEDS process was carried out in a semi-continuous cell at 8–12 MPa and 40–60 °C. The morphology of the particles generated was observed by field emission-scanning electron microscopy (FE-SEM).

4-1-3. Experiment

4-1-3-1. Materials and chemicals

β-Carotene (purity > 80%), which was crushed mechanically, was purchased from Wako Pure Chemical Industries, Ltd., Japan. DCM (purity > 99%), DMF (purity > 99.5%), *n*-hexane (purity > 95%), and ethyl acetate (purity 99.3%) were obtained from Kanto Chemical Co., Inc., Japan. CO_2 (purity > 99.5%) was supplied by Sogo Co., Japan.

4-1-3-2. Equipment, methods, and procedures

The SEDS process was carried out in a semi-continuous precipitation vessel. **Figure 4.1-1** shows a schematic diagram of the SEDS apparatus. The apparatus consists of a CO_2 chiller (Cooling Unit CLU-33, Iwaki Asahi Techno Glass, Tokyo, Japan), HPLC pumps for CO_2 and solution (PU-980 Intelligent HPLC pump, JASCO Co., Tokyo, Japan), a heating chamber (Incubator EI-700B, AS ONE Co, Osaka, Japan), a precipitation vessel (SUS316 cell, inner diameter: 3 cm, length: 17 cm, volume: 120 cm^3, maximum design pressure: 30 MPa), a coaxial nozzle (**Figure 4.1-2**, nozzle inner diameters: 2.4 and 0.8 mm, inner diameter of the nozzle outlet: 0.4 mm, custom-made by Taiatsu Techno Co., Tokyo, Japan), a wet gas meter for CO_2 flow rate (Sinagawa Co., Tokyo, Japan), a membrane filter for collecting particles (100 nm PTFE membrane filter, Advantec, Tokyo, Japan) placed inside a Swagelok filter housing, and a back-pressure regulator (AKICO Co., Tokyo, Japan).

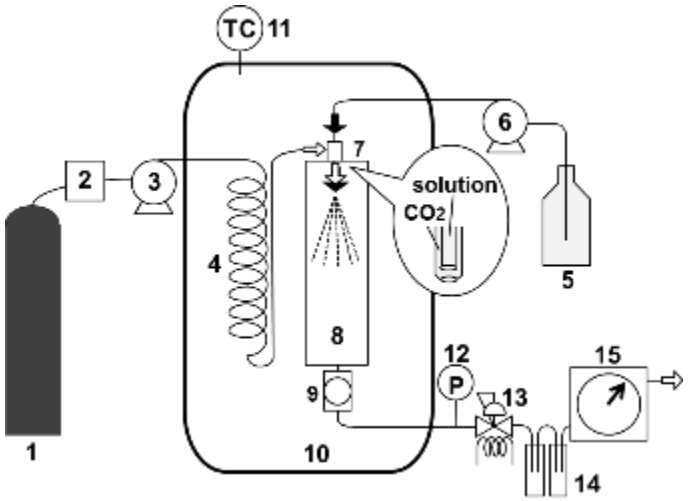

Figure 4.1-1. Schematic diagram of the SEDS process. (1) CO_2 cylinder, (2) chiller, (3) CO_2 pump, (4) CO_2 pre-heater, (5) carotenoid solution, (6) feed pump, (7) coaxial nozzle, (8) precipitator, (9) membrane filter placed in Swagelok filter, (10) heating chamber, (11) temperature controller, (12) pressure gauge, (13) back-pressure regulator, (14) trap, and (15) wet gas meter

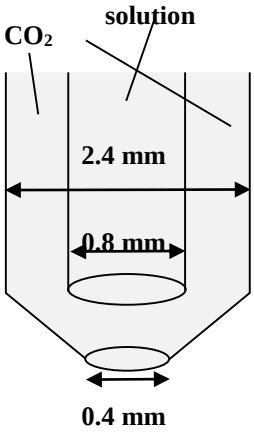

Figure 4.1-2. Schematic diagram of the coaxial nozzle

Experiments on the SEDS process were carried out as follows: liquefied CO_2 was introduced into the system using an HPLC pump (-5 °C and operating pressure) at a constant flow rate. The CO_2 was heated in the preheater, placed in heating chamber, to change it to the supercritical state. When the temperature and pressure in the system

reached the desired operating conditions, β-carotene dissolved in the organic solvent was pumped using an HPLC pump (at the operating temperature and pressure) at the desired flow rate. SC-CO_2 and the β-carotene solution were mixed and introduced into the precipitator via the coaxial nozzle. β-Carotene was precipitated by supersaturation by using the anti-solvent effect. After stopping the solution feed pump, the particles and the system line were washed with SC-CO_2 to help remove the organic solvent from the particles. Finally, particles were collected from the membrane filter after depressurization. The experiments were carried out at operating pressures 8–12 MPa and operating temperatures 40–60 °C. The concentration of β-carotene in the organic solvent was 1.5 mg/mL. The flow rates of the solution and supercritical CO_2 were 0.25 and 20 mL/min (at the pump conditions), respectively. **Table 4.1-1** shows the detailed experimental conditions.

Table 4.1-1. Experimental conditions (Concentration of 1.5 kg/m^3, liquefied CO_2 flow rate of 20 mL/min, solution flow rate of 0.25 mL/min)

Sample No.	Solvent	Pressure (MPa)	Temperature (°C)
1	*n*-Hexane	12	40
2	Ethyl acetate	12	40
3	DCM	12	40
4	DMF	12	40
5	Ethyl acetate	8	40
6	Ethyl acetate	10	40
7	Ethyl acetate	12	50
8	Ethyl acetate	12	60

DCM; Dichloromethane, DMF; *n*,*n*-Dimethylformamide

4-1-3-2. Analysis and characterization

The shape and surface characteristics of the pristine materials and the SEDS-processed particles were observed using a FE-SEM (S-5200, Hitachi, Tokyo, Japan). The samples were sputter-coated with gold in a high-vacuum evaporator and examined using FE-SEM at 30 kV. The particle sizes were measured using Image J software which was developed by the National Institutes of Health.

4-1-4. Results and Discussion

4-1-4-1. Selection of solvent

Table 4.1-2. Physicochemical properties of organic solvents

	Formula	Molecular weight (g/mol)	Melting point (°**C**)	Boiling point (°**C**)
n-Hexane	C_6H_{14}	86.18	-95	69
Ethyl acetate	$C_4H_8O_2$	88.11	-83.6	77
DCM	CH_2Cl_2	84.93	-96.7	39.8
DMF	C_3H_7NO	73.09	-61	153

DCM: Dichloromethane, DMF: *n*,*n*-Dimethylformamide.

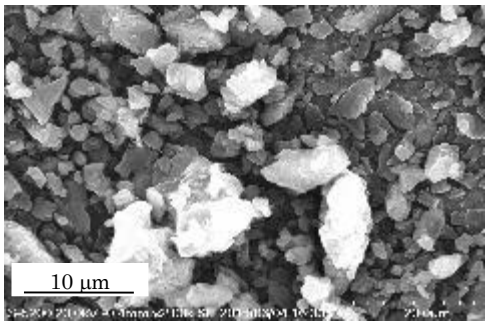

Figure 4.1-3 SEM image of the raw material for the β-carotene crystal

The suitability of the solvent in the SEDS process was tested at 12 MPa and 40 °C for solvents DCM, DMF, *n*-hexane, and ethyl acetate. **Table 4.1-2** shows the physicochemical properties of these organic solvents (chemical database by NCMS and Showa Chemical Co., Ltd.). The experiments showed that particles were obtained for all conditions; however, their size and morphology were different, depending on the solvent. **Figure 4.1-3** shows the SEM image of the raw material for β-carotene, which was crushed mechanically.

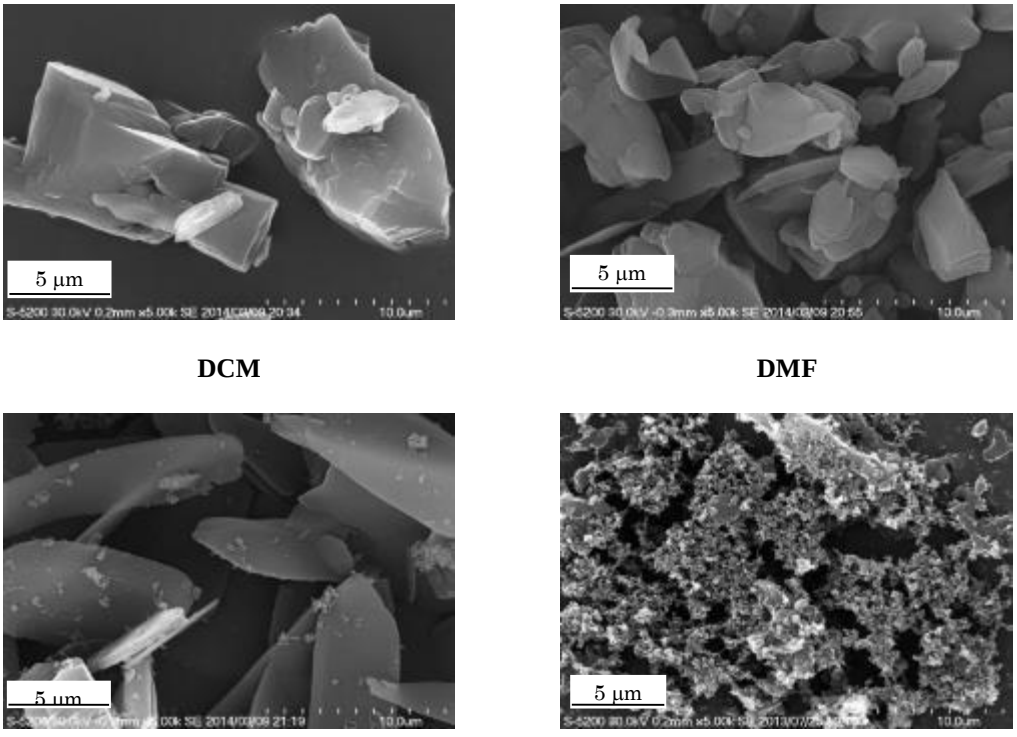

DCM **DMF**

***n*-hexane** **ethyl acetate**

Figure 4.1-4. SEM image of β-carotene particles treated with various solvents (as shown) under the following conditions: temperature, 40 °C; pressure, 12 MPa; CO_2 flow rate, 20 mL/min; solution flow rate, 0.25 mL/min; and concentration, 1.5 kg/m^3

Figure 4.1-4 shows the SEM image of the particles produced by SEDS. The particle

size of the raw material for β-carotene was 2–15 μm. In the case of processing with DCM and DMF, irregular micro-particles were formed. On the other hand, plate-like micro-particles were generated by using *n*-hexane as the solvent. Irregular nanoparticles were precipitated by ethyl acetate. The critical point of the binary system can be found from the phase equilibrium curve. **Figure 4.1-5** shows the phase compositions for the systems of CO_2 and DMF, DCM, *n*-hexane, and ethyl acetate, respectively, at 40 or 45 °C [23-24]. The maximum value of the four curves indicates a critical point of the mixture of organic solvent and CO_2. The critical point of the CO_2+DMF system is at 9 MPa, while for all the other solvents it is near 8 MPa. As seen in **Figure 4.1-5**, for the 4-MPa condition, the compositions of the CO_2 and organic solvent systems were different for each type of solvent. The most soluble organic solvent was ethyl acetate, followed in the decreasing order by hexane, DCM, and DMF. The solubility is an important parameter in this process. The particle size is reduced by increasing the supersaturation levels. The supersaturation depends on the difference of β-carotene solubility between before and after the contact of the organic solvent with SC-CO_2. The characteristics of subcritical CO_2, such as density, viscosity, diffusivity, and surface tension are quite different in the SC-CO_2 region [27].

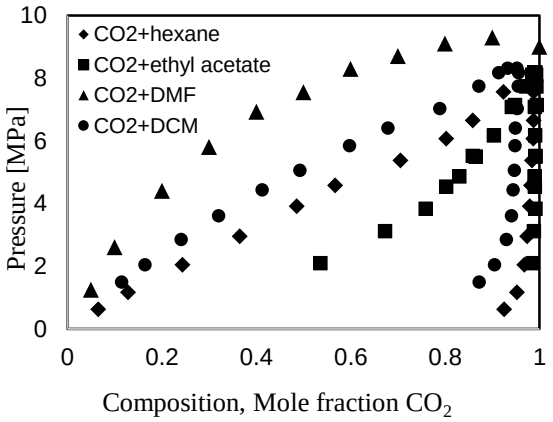

Figure 4.1-5 Phase composition for the system of CO_2 with *N*,*N*-dimethylformamide (DMF) (40 °C), dichloromethane (DCM) (45 °C), *n*-hexane (40 °C), and ethyl acetate (40 °C), using reported experimental data [23-24]

The reason why the size and shape of the particles changed, depending on the kind of organic solvent used, is considered next. The effects of the SAS system on the solubility of the three-component system comprising β-carotene, CO_2, and organic solvent should be evaluated. However, because there is no data available on this three-component system and the calculation process would be highly complicated, this system has been discussed by using solubility parameters. **Table 4.1-3** shows the Hansen solubility parameters of β-carotene and organic solvents [28-29]. Additionally, Hansen solubility parameters of CO_2 at various temperature and pressure conditions were calculated by King; for the 40 °C and 12 MPa condition, the total solubility parameter of CO_2 was about 10 [30]. Hansen solubility parameters are used to predict the solubility of a substance based on the following concept: two substances are easily soluble with each other when the molecules of the respective substances exhibit similar interactions. Hansen solubility parameters consist of three parameters, δ_d, δ_p, and δ_h, which denote the dispersion, polar, and hydrogen bonding interactions, respectively. When the parameters

of two components are located near each other in the Hansen space, it means that the two molecules will easily dissolve into each other.

Table 4.1-3 Hansen solubility parameters of β-carotene and organic solvents

	Solubility parameter ($MPa^{1/2}$)			
	δ_d	δ_p	δ_h	δ_t
β-Carotene (25 °C)	17.1	2.39	5.54	18.0
n-Hexane (RT)	14.9	0	0	14.9
Ethyl acetate (RT)	15.8	5.3	7.2	18.1
DCM (RT)	18.2	6.3	6.1	20.2
DMF (RT)	17.4	13.7	11.3	24.9

δ_d: Dispersion solubility parameter, δ_p: Polar solubility parameter, δ_h: Hydrogen bonding solubility parameter, δ_t **:** Total solubility parameter, RT**:** Room temperature, DCM: dichloromethane, DMF: *n*,*n*-dimethylformamide

The total Hansen solubility parameter can be calculated using Eq. (2).

$$\delta_t^2 = (\delta_d)^2 + (\delta_p)^2 + (\delta_h)^2 \qquad (2)$$

Where, δ_t is the total solubility parameter, δ_d is the dispersion solubility parameter, δ_p is the polar solubility parameter, and δ_h is the hydrogen bonding solubility parameter [28].

Typically, prediction of whether the target substance is soluble in the solvent is carried out in the following manner. When the target substance and a solvent interaction radius (R_0) is given, the distance between the HSP and the HSP solvent of the target substance (R_a) is calculated by the following Eq. (3).

$$(R_a)^2 = 4(\delta_{d2}-\delta_{d1})^2+(\delta_{p2}-\delta_{p1})^2+(\delta_{h2}-\delta_{h1})^2 \qquad (3)$$

Relative energy difference (RED) is defined by R_0 and R_a as follows.

$$RED = R_a / R_0 \qquad (4)$$

RED <1 the molecules are alike and will dissolve

RED = 1 the system will partially dissolve

RED> 1 the system will not dissolve

However, it has not been possible to find the R0 data of carotenoid and organic solvent. Therefore, the solubility was evaluated by the total solubility parameter. The total solubility parameter of ethyl acetate is closest to that of β-carotene. Therefore, β-carotene may be more soluble in ethyl acetate than with the other organic solvents. After mixing the solution with SC-CO_2 and spraying this mixture into the precipitator, the solubility of β-carotene in these organic solvent decreases rapidly. In the case of the ethyl acetate system, the particle size became smaller, causing the solubility to decrease; as a result, supersaturation increased suddenly compared with the other solvents.

The morphology of the β-carotene particles was also quite different, depending on the organic solvent, probably because polymorphic crystals are affected by the solvent in which they were dissolved [31].

4-1-4-2. Effects of pressure and temperature

The effects of pressure and temperature on the morphology and size of the treated

particles were studied at constant concentrations of β-carotene in the ethyl acetate solution. The effect of pressure was considered in the pressure range 8–12 MPa and at a constant temperature of 40 °C. The particle sizes decrease with increasing pressure, as shown in **Figure 4.1-6**. This trend has also been observed in a previous work [32]. When the process was carried out at a lower pressure, the particles tended to be larger and plate-like. However, as the pressure increased, irregularly shaped nanoparticles were obtained. The smallest particles (diameter of around 135 nm) were formed at 10-12 MPa, 40 °C. This decrease in the particle size with increasing pressure can be explained by the rate of SC-CO_2 diffusion into the organic solvent droplets that is dependent on the operation pressure [27]. The solubility of the solvent in SC-CO_2 increases at higher pressures [33-34]. Moreover, the droplet size will also decrease with an increase in the SC-CO_2 density, and reduces the interfacial tension between SC-CO_2 and the solvent at higher pressures. This leads to SC-CO_2 diffusing into the solvent immediately when the pressure increases. The partial molar volume and cohesive energy density of the organic solvent will decrease due to an increase in the diffusive driving force. Therefore, the higher supersaturation of the carotenoid in the solvent is caused by a higher mass transfer rate and a higher solubility of the solvent in SC-CO_2. Therefore, the solvent power of the organic solvent for the solute decreases rapidly, causing the particle to become smaller [27].

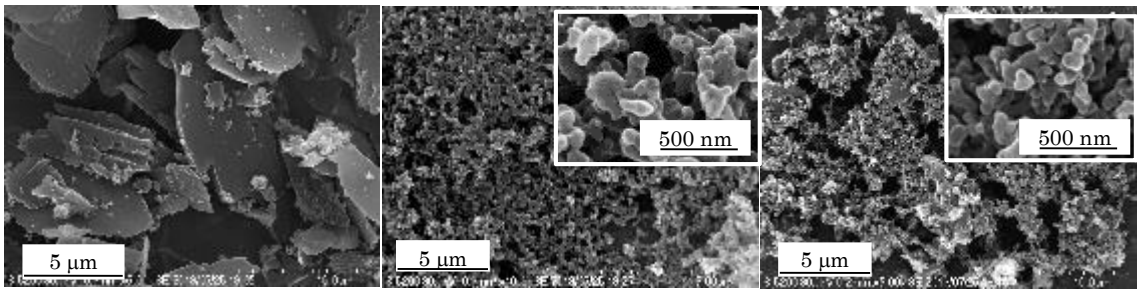

8 MPa **10 MPa** **12 MPa**

Figure 4.1-6 SEM image of treated particles precipitated from an ethyl acetate solution of β-carotene (1.5 kg/m^3) under the following conditions: temperature, 40 °C; CO_2 flow rate, 20 mL/min; solution flow rate, 0.5 mL/min; and various pressures (as shown)

The experiments were also carried out at various temperatures: 40, 50, and 60 °C, at a pressure of 12 MPa. Particle size increased with increasing temperature (**Figure 4.1-7)**. The smallest particles, with a diameter of around 135 nm, were formed at 40 °C and 12 MPa. Higher temperatures reduced the CO_2 density, forming larger droplets. Therefore, a lower CO_2 density leads to a higher solvent power for the solute, and it causes a lower mass transfer rate and lower supersaturation of solute in the organic solvent [27]. This explains why the particles sizes were reduced at lower temperatures.

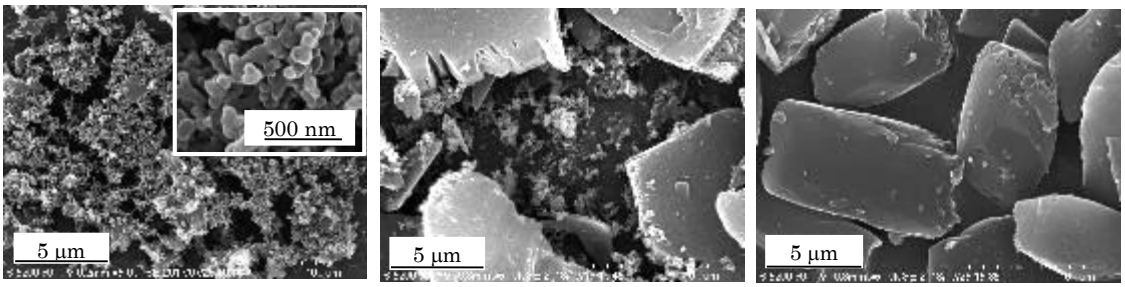

40 °C **50 °C** **60 °C**

Figure 4.1-7 SEM image of treated particles precipitated from an ethyl acetate solution of β-carotene (1.5 kg/m^3) under the following conditions: pressure, 12 MPa; CO_2 flow rate, 20 mL/min; solution flow rate, 0.5 mL/min; and various temperatures (as shown)

Therefore, the smallest particles of β-carotene were formed at above the critical pressure (10–12 MPa) and at the lower end of the critical temperature (40 °C), because the ethyl acetate solution immediately became supersaturated under these conditions [4, 24, 35].

4-1-5. Conclusions

Nano-particles of β-carotene were successfully produced by the SEDS process. The effects of parameters such as the kind of organic solvent, operating pressure, and temperature on the particle morphology and size were investigated. Irregularly formed micro-particles (5 to 20 μm) were precipitated when processing with DCM and DMF. Plate-like micro-particles (10 to 20 μm) were generated by using *n*-hexane as the solvent. Irregularly formed nanoparticles (135 nm) were precipitate by using ethyl acetate. The reduction of β-carotene particle size from 10 μm to 135 nm by increasing pressure was observed. And particles size of β-carotene were changed from 135 nm to 10 μm by increasing temperature. Optimum conditions for fine particle production (135 nm mean size) were found in this work to be 12 MPa and 40 °C and using ethyl acetate.

References

[1] A. Martín, F. Mattea, L. Gutiérrez, F. Miguel, M.J. Cocero, Co-precipitation of carotenoids and bio-polymers with the supercritical anti-solvent process, *J. Supercritical Fluids*, 41(1), 138-147 (2007)

[2] F. Mattea, Á. Martín, M. J. Cocero, Carotenoid processing with supercritical fluids, *J. Food Eng*., 93, 255-265 (2009)

[3] H. Hayashi, M. Nakajima, K. Murota, N. Yamanaka, T. Inakuma, The miniaturization of β-carotene particle enhances the bioavailability. *Abstract of International Conference on Food Factors* (2011)

[4] P. Boonnoun, H. Nerome, S. Machmudah, M. Goto, A. Shotipruk, Supercritical anti-solvent micronization of chromatography purified marigold lutein using hexane and ethyl acetate solvent mixture, *J. Supercritical Fluids*, 80, 15-22 (2013)

[5] Y.C. Cho, J.H. Cheng, S.L. Hsu, S.E. Hong, T.M. Lee, C.M.J. Chang, Supercriticalcarbon dioxide anti-solvent precipitation of anti-oxidative zeaxanthin highlyrecovered by elution chromatography from Nannochloropsis oculata, *Sep. Purif. Technol*., 78, 274-280 (2011)

[6] I. D. Marco, E. Reverchon, Supercritical antisolvent micronization of cyclodex-trins, *Powder Technol*., 183, 239–246 (2008)

[7] E. Reverchon, I. D. Marco, Supercritical antisolvent micronization of cefoni-cid: thermodynamic interpretation of results, *J. Supercritical Fluids*, 31, 207–215 (2004)

[8] E. Reverchon, I. D. Marco, Supercritical antisolvent precipitation ofcephalosporins, *Powder Technol*., 164, 139–146 (2006)

[9] Y. Wang, Y. Wang, J. Yang, R. Pfeffer, R. Dave, B. Michniak, The application of asupercritical antisolvent process for sustained drug delivery, *Powder Technol*., 164, 94–102 (2006)

[10] P. Boonnoun, H. Nerome, S. Machmudah, M. Goto, A. Shotipruk, Supercritical anti-solvent micronization of marigold-derived lutein dissolved in dichloromethane and ethanol, *J. Supercritical Fluids*, 77, 103-109 (2013)

[11] S.D. Yeo, M.S. Kim, J.C. Lee, Recrystallization of sulfathiazole and chlorpropamide using the supercritical fluid antisolvent process, *J. Supercritical Fluids*, 25, 143–154 (2003)

[12] M.S. Kim, S. Lee, J.S. Park, J.S. Woo, S.J. Hwang, Micronization of cilostazol using supercritical antisolvent (SAS) process: effect of process parameters, *Powder Technol*., 177, 64–70 (2007)

[13] M. Bahrami, S. Ranjbarian, Production of micro- and nano-composite particles by supercritical carbon dioxide, *J. Supercritical Fluids*, 40, 263–283 (2007)

[14] G. Caputo, E. Reverchon, Use of urea as habit modifier in the supercritical antisolvent micronization of sulfathiazole, *Ind. Eng. Chem*., 46(12), 4265–4272 (2007)

[15] E. Reverchon, R. Adami, G. Caputo, I. D. Marco, Spherical microparticles production by supercritical antisolvent precipitation: Interpretation of results, *J. Supercritical Fluids*, 47, 70–84 (2008)

[16] K. Byrappa, S. Ohara, T. Adschiri, Nanoparticles synthesis using supercritical fluid technology-towards biomedical applications, *Adv. Drug. Deliver. Rev.*, 60, 299–327 (2008)

[17] E. Badens, O. Boutin, G. Charbit, Laminar jet dispersion and jet atomization in pressurized carbon dioxide, *J. Supercritical Fluids*. 36(1), 81–90 (2005)

[18] Y. Z. Zhang, X. M. Liao, G. F. Yin, P. Yuan, Z. B. Huang, J. W. Gu, Y. D. Yao, X. C. Chen, Preparation of water soluble drugs-loaded microparticles using modified solution enhanced dispersion by supercritical CO_2, *Powder Technol.*, 221, 343-350 (2012)

[19] A. Tabernero, E.M. Martín del Valle, M.A. Galán, Precipitation of tretinoin and acetaminophen with solution enhanced dispersion by supercritical fluids (SEDS). Role of phase equilibria to optimize particle diameter, *Powder Technol.*, 217, 177-188 (2012)

[20] Y. Kang, G. Yin, P. Ouyang, Z. Huang, Y. Yao, X. Liao, A. Chen, X. Pu, Preparation of PLLA/PLGA microparticles using solution enhanced dispersion by supercritical fluids (SEDS), *J. Colloid. Interf. Sci*., 322, 87-94 (2008)

[21] S.J. Park, S.D. Yeo, Recrystallization of caffeine using gas antisolvent process, *J. Supercritical Fluids*, 47, 85–92 (2008)

[22] A.Z. Chen, L. Li, S B. Wang, C. Zhao, Y.G. Liu, G.Y. Wang, Z. Zhao, Nanonization of methotrexate by solution-enhanced dispersion by supercritical CO_2, *J. Supercritical Fluids*, 67, 7-13 (2012)

[23] K. Ohgaki, T. Katayama, Isothermal vapor-liquid equilibrium data for binary systems containing carbon dioxide at high pressures: methanol-carbon dioxide, *n*-hexane-carbon dioxide, and benzene-carbon dioxide systems, *J. Chem. Eng. Data*, 21(1), 53–55 (1976)

[24] Z. Wagner, J. Pavlíček, Vapour-liquid equilibrium in the carbon dioxide-ethyl acetate system at high pressure, *Fluid Phase Equilibr*., 97, 119–126 (1994)

[25] M. Temtem, T. Casimiro, A. Aguiar-Ricardo, Solvent power and depressurization rate effects in the formation of polysulfone membranes with CO_2-assisted phase inversion method, *J. Membrane Sci*., 283, 244–252 (2006)

[26] I. Tsivintzelis, D. Missopolinou, K. Kalogiannis, C. Panayiotou, Phase compositions and saturated densities for the binary systems of carbon dioxide with ethanol and dichloromethane, *Fluid Phase Equilibr*., 224, 89–96 (2004)

[27] H.Y. Jin, M. Hemingway, F. Xia, S.N. Li, Y.P. Zhao, Production of β-Carotene Nanoparticles by the Solution Enhanced Dispersion with Enhanced Mass Transfer by Ultrasound in Supercritical CO_2 (SEDS-EM), *Ind. Eng. Chem. Res.,* 50(23), 13475–13484 (2011)

[28] C. M. Hansen, Hansen solubility parameters A user's handbook, 2nd ed. *CRC press* (2007)

[29] J. Smith, E. Charter, K. Srinivas, J. W. (Eds.) King, Functional Food Product Development, first ed. Chapter3, Supercritical carbon dioxide and subcritical water: Complementary agents in the processing of functional foods, *Wiley-Blackwell*. 40-78 (2010)

[30] J. W. King, Supercritical fluid extraction at high pressures: theoretical considerations and practical applications, *Proceedings of ⅢIberoamerican conference on supercritical fluids* (2013)

[31] M. Matsuoka, Society of Chemical Engineers, Japan, ed., Crystallization engineering, *Baifukan* (2002)

[32] H. Nerome, S. Machmudah, Wahyudiono, R. Fukuzato, T. Higashiura, Y.S. Youn, Y.W. Lee, M. Goto, Nanoparticle formation of lycopene/ β-cyclodextrin inclusion complex using supercritical antisolvent precipitation, *J. Supercritical Fluids*, 83, 97-103 (2013)

[33] E. Reverchon, Supercritical Antisolvent Precipitation of Microand Nano-particles, *J. Supercritical Fluids*, 15, 1-21 (1999)

[34] E. Reverchon, G. Della Porta, M.G. Falivene, Process Parameters and Morphology in Amoxicillin Micro and Submicro Particles Generation by Supercritical Antisolvent Precipitation, *J. Supercritical Fluids,* 17, 239 (2000)

[35] F. Miguel, A. Martín, F. Mattea, M. J. Cocero, Precipitation of lutein and co-precipitation of lutein and poly-lactic acid with the supercritical anti-solventprocess, *Chemical Engineering and Processing*, 47, 1594–1602 (2008)

Chapter 4.2

Nanoparticle formation of carotenoid and cyclodextrin inclusion complex

4-2-1. Introduction

There are more than 600 different types, but only around 20 of are present in the human body. β-carotene, lycopene, lutein and zeaxanthin are most important carotenoid. [1-2]. Because of their chemical structures, they behave as natural anti-oxidants [3], particularly lycopene showing the highest anti-oxidant activity. Carotenoids generally exist in the part of the plant body where oxygen is generated. Commercial carotenoids are usually in the form of crystalline powders that are soluble in oils and organic solvents, but poorly soluble in water [4].

Cyclodextrins (CDs) are a toroidal molecule whose the most important structural characteristic is a doughnut-shaped hydrophobic cavity in which various guest molecules such as drugs may be encased or form clathrates. These phenomena have been much attention in the pharmaceutical field, because of its potential utility to improve the aqueous solubility, dissolution and release rates, bioavailability, and chemical/physical stabilities of various drug molecules, along with pharmacokinetic modification [5]. The physicochemical properties of β-CD are summarized in **Table 4.2-1**.

Table 4.2-1. Physicochemical properties of lycopene and β-CD[5]

	Molecular formula	Molar mass (g/mol)	Melting point (°**C**)
β-CD	$C_{42}H_{70}O_{35}$	1134.98	290-300

4-2-2. Objectives

Since the use of SEDS method for fabrication of lycopene and β-CD inclusion particles has not been reported yet, the present work applied this method to form nanoparticles containing a complex of lycopene and β-CD. The effects of pressure, temperature, CO_2 flow rate, and solution flow rate on the size and shape of the particles thus obtained were examined. Differential scanning calorimetry (DSC) was used to confirm the formation of the complex.

4-2-3. Materials and Methods

4-2-3-1. Material and chemicals

Crystalline lycopene (purity > 80%) and β-CD (> 80 %) were purchased from Wako and Sigma-Aldrich Japan, respectively. *n,n*-Dimethylformamide (DMF) (> 99. 5%), dimethylsulfoxide (DMSO) (> 99.9 %) and dichloromethane (DCM) (> 99 %), tetrahydrofuran (THF) (> 99.9 %) were provided by Wako, Japan. CO_2 (> 99.5 %) was supplied by Uchimura Co., Japan.

4-2-3-2. Equipment, methods and procedures

The SEDS process was carried out in a semi-continuous micronization vessel. **Figure 4.2-1** shows a schematic diagram of the SEDS apparatus. The apparatus consists of a CO_2 Chiller (Cooling Unit CLU-33, Iwaki Asahi Techno Glass, Japan), a pump for CO_2 (LC-8A preparative liquid chromatography solvent delivery pump, Shimadzu,

Japan), a pump for the solution (PU-980 Intelligent HPLC pump, JASCO, Japan), a heating chamber (AKICO, Japan), a precipitation vessel (SUS316 cell, inner diameter: 3 cm, length: 17 cm, volume: 120 cm^3, maximum pressure: 30 MPa), a coaxial nozzle (for CO_2 and solution tube: 1/8 and 1/16 inch tubes, nozzle inner diameter: 2.4 and 0.8 mm, respectively, custom-made), a wet gas meter (Sinagawa Co., Japan), a membrane filter (100 nm PTFE membrane filter, Advantec) placed in Swagelok filter and a back pressure regulator (AKICO, Japan).

A typical experimental procedure was as follows: supercritical CO_2 was added to the micronization vessel until the desired pressure and temperature conditions were reached, and these were maintained. The carotenoid solution was then injected at a suitable flow rate until a certain amount of the solution had been processed. Supercritical CO_2 was allowed to flow continuously for 1 h to eliminate the residual organic solvents from the particles. Finally, the particles were collected from the membrane filter after depressurization. The experiments were carried out at pressures in the range 10–14 MPa and at temperatures in the range 40–50°C. The concentration of lycopene and β-CD in DMF solution was 0.35 mg/mL and 0.74 mg/mL, respectively. The flow rate of the solution and supercritical CO_2 was varied in the range 15–25 mL/min at the pump and in the range 0.25–0.75 mL/min, respectively. **Table 4.2-2** summarizes the detailed experimental conditions.

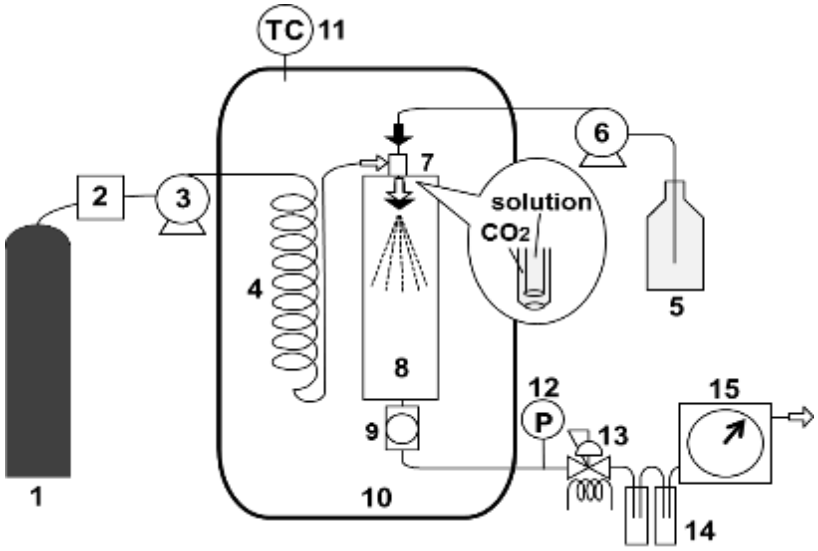

Figure 4.2-1. Schematic diagram of the SEDS process. (1) CO_2 cylinder, (2) chiller, (3) CO_2 pump, (4) CO_2 pre heater, (5) carotenoid solution, (6) feed pump, (7) coaxial nozzle, (8) precipitation vessel, (9) membrane filter placed in Swagelok filter, (10) heating chamber, (11) Temperature control, (12) pressure gauge, (13) back pressure regulator, (14) trap, and (15) wet gas meter

Table 4.2-2. Experimental conditions

Sample	Lycopene / β-CD
Solvent	*n*,*n*-Dimethylformamide (DMF) Dimethylsulfoxide (DMSO) Dichloromethane (DCM)
Temperature and Pressure	40 °C : 10, 12, 14 MPa 45 °C : 10, 12, 14 MPa 50 °C : 10, 12, 14 MPa
CO_2 flow and Solution flow rate -5 °C and operating pressure	(CO_2)15 ml/min: (Solution)0.25, 0.5, 0.75 ml/min (CO_2)20 ml/min: (Solution)0.25, 0.5, 0.75 ml/min (CO_2)25 ml/min: (Solution)0.25, 0.5, 0.75 ml/min
CO_2 flow rate	0.25, 0.5, 0.75 ml/min
Concentration	Lycopene : β-CD =0.35 : 0.74 mg/ml

4-2-3-3. Analysis and characterization

The morphology characteristics of the raw materials and the SEDS-processed particles were observed by scanning electron microscopy (SEM, JSM-6390 LV JEOL, Japan) and field emission-scanning electron microscopy (FE-SEM, SU-8000, Hitachi, Japan). The samples were sputter-coated with gold in a high-vacuum evaporator and the samples were examined using SEM and FE-SEM at 15 kV. Particle sizes and size distributions were measured using Image J software for at least 100 particles collected at each experiment.

4-2-3-4. Differential scanning calorimetric analysis

The thermal behavior of the resulting particles was investigated by differential scanning calorimetry (DSC-Q1000, TA Instruments, UK). When guest molecules are incorporated into the CD cavity, their melting, boiling or sublimation points are usually shifted or disappear within the temperature range where CD decomposes [4]. DSC measurements were conducted for 1 mg samples placed in an aluminum pan and covered with an aluminum disk using a crimping press. The temperature was increased continuously from 50 °C to 350 °C with a rate of 20 °C/min.

4-2-4. Results and Discussion

4-2-4-1. Particle formation by SEDS

To observe the morphology of each substance used for the SEDS process, lycopene

(in DCM solution) and β-CD (in DMSO solution) were treated separately. Lycopene and β-CD are completely soluble in DCM and DMSO, respectively. However, lycopene and β-CD cannot be dissolved in DMSO and DCM, respectively. Thus DMF would be used as a solvent for inclusion formation of lycopene and β-CD, since both compounds can be dissolved completely. **Figure 4.2-2** shows SEM images of lycopene and β-CD particles before and after SEDS process. For pristine lycopene and β-CD (**Figure 4.2-2(A)** and **(C)**, respectively), the original particles were prismatic particles with a mean size of 88 μm and 55 μm, respectively. As shown in **Figure 4.2-2(B)** and **(D)**, the treated lycopene and β-CD particles showed flake-shaped particles with a mean width of 1 μm and spherical particles with a mean diameter of 100 nm, respectively.

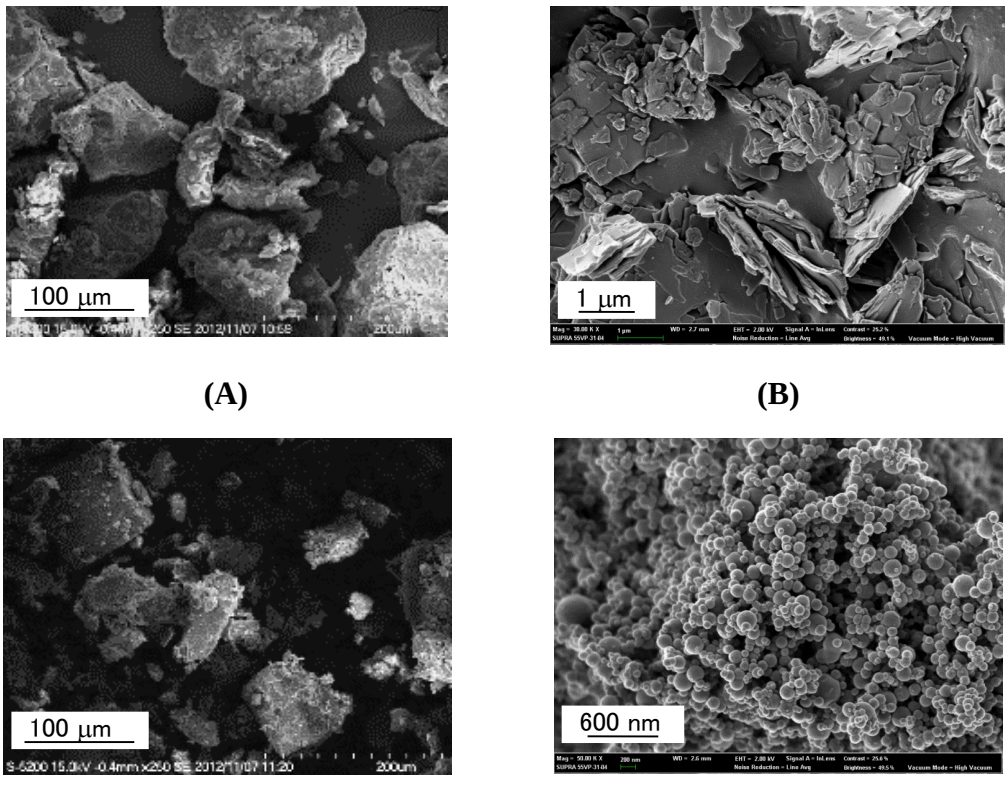

(A) **(B)**

(C) **(D)**

Figure 4.2-2. SEM images of raw materials and particles obtained by SEDS. (A) Lycopene; (B) SEDS-processed lycopene using DCM as a solvent (12 MPa , 45 °C); (C) β-CD; (D) SEDS-processed *β*-CD using DMSO as a solvent (12 MPa, 45 °C)

4-2-4-2. Particle formation of lycopene/β-CD complex by SEDS

4-2-4-2-1. Solvent selection

DCM have been used as a good solvent of carotenoids. Additionally, DMSO, THF and DMF has been used as good solvent of CD. Therefore carotenoid and CD were mixed with those organic solvent. However, carotenoids and CD were dissolved only by DMF.

4-2-4-2-2. Effects of pressure and temperature

The effects of pressure and temperature on the morphology of the treated particles were studied at a constant concentration of both lycopene and β-CD (0.35 and 0.74 mg/mL, respectively) in DMF solution. Particles with various morphologies from spheroid to agglomeration were generated by the SEDS process at various pressures and temperatures, as shown in **Figure 4.2-3(A)** to **(I)**. When the process was carried out at a low temperature and pressure, the particles tended to be larger and agglomerated. However, as the temperature and pressure increased, the particles became smaller and more spherical **(I)**. This indicates that a high temperature and pressure enhanced the anti-solvent properties of CO_2, resulting in the production of smaller particles. **Figure 4.2-4** shows the particle size distributions of the treated complex particles presented in **Figure 4.2-3**. When a low temperature was used, the particle sizes were distributed over a wide range, with a larger mean particle size of 121 nm compared to other temperatures. The formation of large particles at low temperature can be explained by reference to an incipient agglomeration process in which the formation of linking bridges leads to the production of larger particles.

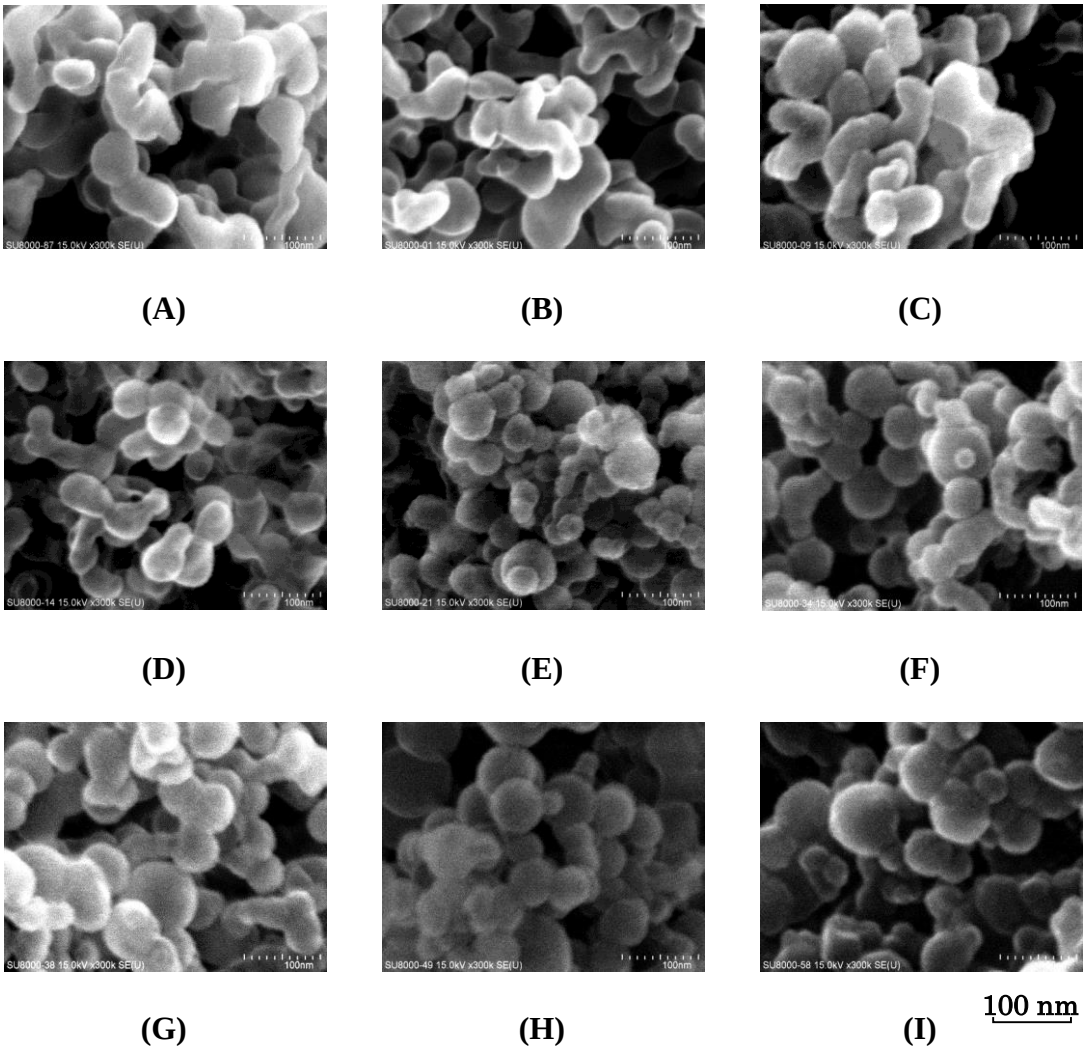

Figure 4.2-3. FE-SEM images (300,000× magnification) of treated complex particles precipitated from a DMF solution of lycopene/β-CD (0.35:0.74 mg/mL) at CO_2 flow rate of 20 mL/min, solution flow rate of 0.25 mL/min and various pressures and temperatures. (A) 10 MPa, 40 °C; (B) 10 MPa, 45 °C; (C)10 MPa, 50 °C; (D) 12 MPa, 40 °C; (E) 12 MPa, 45 °C; (F) 12 MPa, 50 °C; (G) 14 MPa, 40 °C; (H) 14 MPa, 45 °C; (I) 14 MPa, 50 °C

At high temperature and pressure, the particle size distribution was very sharp, with a smaller mean particle size of 41 nm. For instance, at a pressure of 14 MPa, the decrease in particle size with increasing temperature was obvious, resulting in a minimum particle size of 41 nm at 50 °C. The effects of temperature and pressure on the size of the treated

particles were confirmed based on the mean particle sizes and particle size distributions for all conditions.

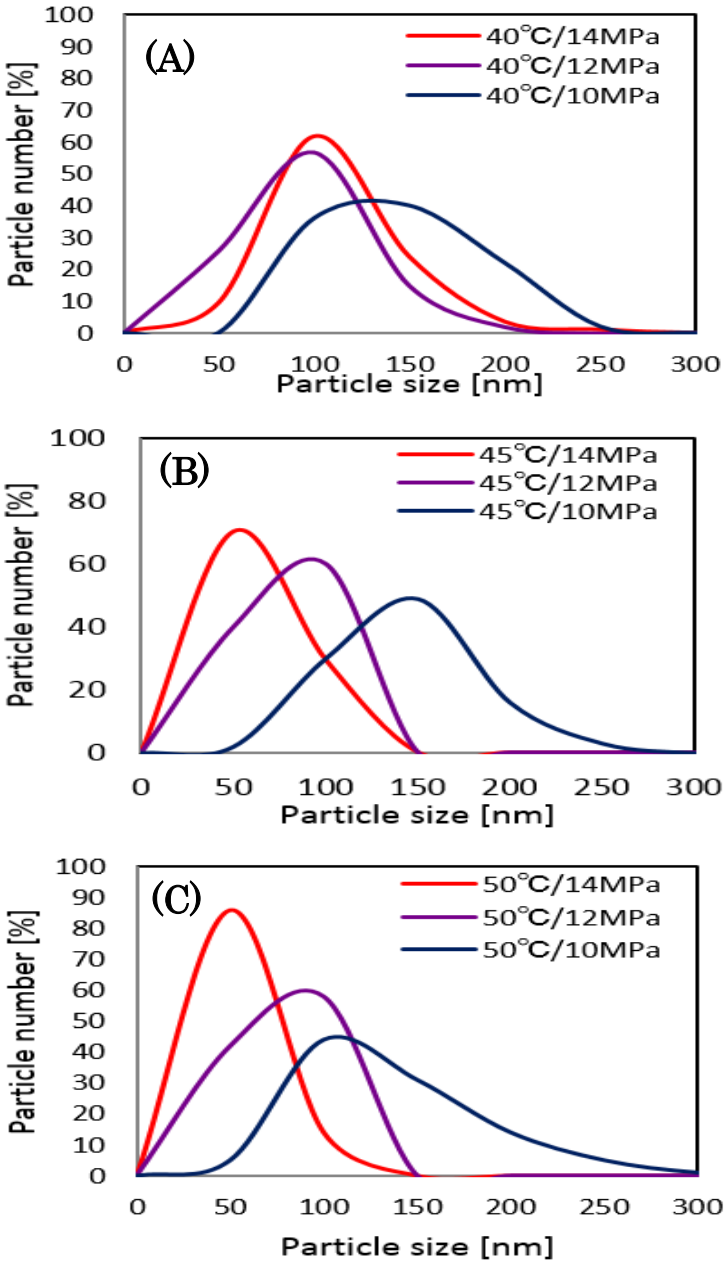

Figure 4.2-4. Particle size distributions of micronized particles precipitated from a DMF solution of lycopene/β-CD (0.35:0.74 mg/mL) at CO_2 flow rate of 20 mL/min, solution flow rate of 0.25 mL/min and various temperatures. (A) 40 °C, (B) 45 °C, (C) 50 °C

At constant pressure, the vapor pressure of DMF increases with increasing temperature, which results in increasing solubility in SC-CO_2. Moreover, at high pressure, the density of SC-CO_2 increases, also resulting in higher solubility of DMF. Therefore, separation of the carotenoid occurred immediately, with the production of fine particles.

As pointed out by Reverchon and De Marco [6], the position of the process operating point with respect to the critical point of the mixture CO_2–organic solvent can have a strong influence on the results. **Figure 4.2-5** depicted the phase compositions for the system of CO_2 and DMF at 40, 45 and 50^oC) that were calculated using the Peng-Robinson equation of state (PR-EOS) with quadratic mixing rules [8]. PR-EOS is a kind of state equation of real gas that has been proposed in 1976 by Ding-Yu Peng and Donald B. Robinson which is often used in the calculation at high pressure conditions [7].

The critical properties and interaction parameters between CO_2 and DMF used in the calculations were taken from Temtem et al. [9] and Byun et al. [10], respectively, as listed in **Table 4.2-3** and **Table 4.2-4.** At 50 °C the highest solubility of DMF in SC-CO_2 is presented, followed by the solubility at 45 and 40 °C. In the case of phase equilibrium at 40 and 50 °C, and pressure less than 8 and 10 MPa, the equilibrium mixture of DMF and CO_2 lies in the two-phases region and the material precipitates from the liquid-rich phase. Additionally, the organic solvent remains in the product at near the maximum value conditions due to the phase instability. Furthermore, it resulted in particle agglomeration occurred upon wetting. At 14 MPa, fine spherical particles were obtained. It is conceivable that the operating points were above the critical point of CO_2 and solvent mixture, at which CO_2 and the solvent are completely mixed; moreover, precipitation occurred from the supercritical phase and fine nanoparticles were generated

instantaneously. Accordingly, the precipitated particles represent the transition in morphology from agglomeration to nanoparticles [6, 9, 11–19].

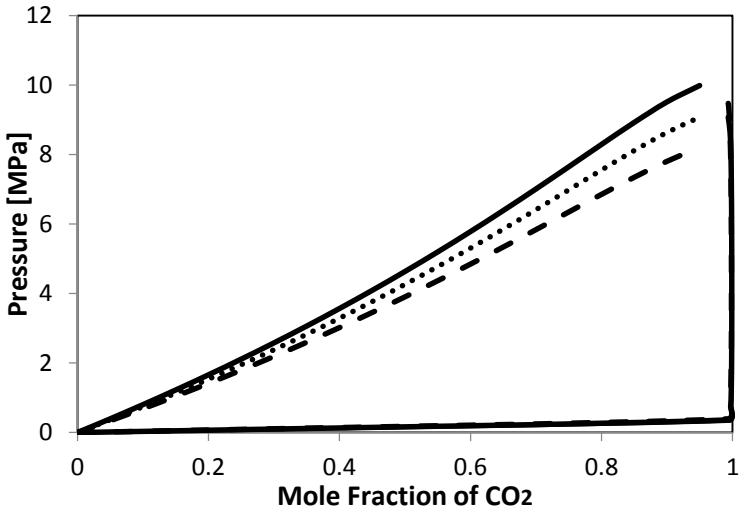

Figure 4.2-5. Phase composition for the system CO_2 and *n,n*-dimethylformamide at various temperatures (full line: 50 °C, dotted line: 45 °C, dashed line: 40 °C) calculated by using Peng–Robinson equation of state [7, 8]

Table 4.2-3. Values of the critical temperatures (T_c), critical pressures (P_c), and acentric factors (ω) used in the PR-EOS [9, 10]

Solvent	T_c (°C)	P_c (MPa)	ω
Carbon dioxide	**31.05**	**7.38**	**0.225**
DMF	**376.45**	**5.50**	**0.367**

Table 4.2-4. Binary interaction parameters between CO_2 and DMF used in PR-EOS [9]

	k_{ij}	l_{ij}
Carbon dioxide + DMF	**0.0170**	**-0.0430**

***Adjusted for PR-EOS**

4-2-4-2-3. Effect of solution and CO_2 flow rates

The effects of the flow rates of the solution and CO_2 on the morphology of the treated particles

were studied at a constant initial concentration of lycopene and β-CD in DMF solution at a pressure of 14 MPa and a temperature of 50 °C. Under these conditions, particles with morphologies from spheroid to agglomeration were produced as shown in **Figure 4.2-6**. **Figure 4.2-7** shows the particle size distributions of the treated lycopene/β-CD particles. At high solution flow rate and low CO_2 flow rate, rough agglutinated particles with a mean diameter of 116 nm were formed (**G**), while at low solution flow rate, smaller particles with a mean diameter of 38 nm were precipitated (**C**). Generally, three regimes of liquid-phase dispersion depend on flow rate: (i) the dripping regime, in which droplets are formed at the outlet of a nozzle; (ii) the laminar regime, in which the solvent flows smoothly and continuously before a break-up zone, in which uniform-sized droplets are formed; (iii) and the turbulent regime, in which the jet surface becomes irregular and the resulting non-uniform droplets are formed as stretched or small broken droplets [14, 17]. When the solution flow rate is high, mixing between the jet and the surroundings is better due to stronger turbulence. This leads to greater supersaturation in the jet, in which shows the supersaturation inside the jet for two different solution flow rates. Therefore, smaller particles are obtained at higher solution flow rates. However, the effect of this parameter is relatively small compared to that of the parameters affecting phase equilibrium. Accordingly, the solvent flow rate does not have a significant effect on the yield. Higher CO_2 flow rate may improve mixing due to increased turbulence, resulting in greater supersaturation at the edge of the jet. Nevertheless, the main influence of the CO_2 flow rate on the process is that it determines the composition of the bulk fluid that results in complete mixing between CO_2 and the solvent. If the flow rate of CO_2 is increased, the bulk fluid contains a smaller amount of organic solvent; as a result, the solubility of the solid in this fluid is smaller, and therefore smaller particles are obtained [18-21]. 7 to 80 μm lycopene particles were obtained by various operating conditions taking from F. Miguel et al. [2]. Therefore nanoparticles were difficult to produce from only lycopene. β-CD was helping to produce nanoparticles of lycopene.

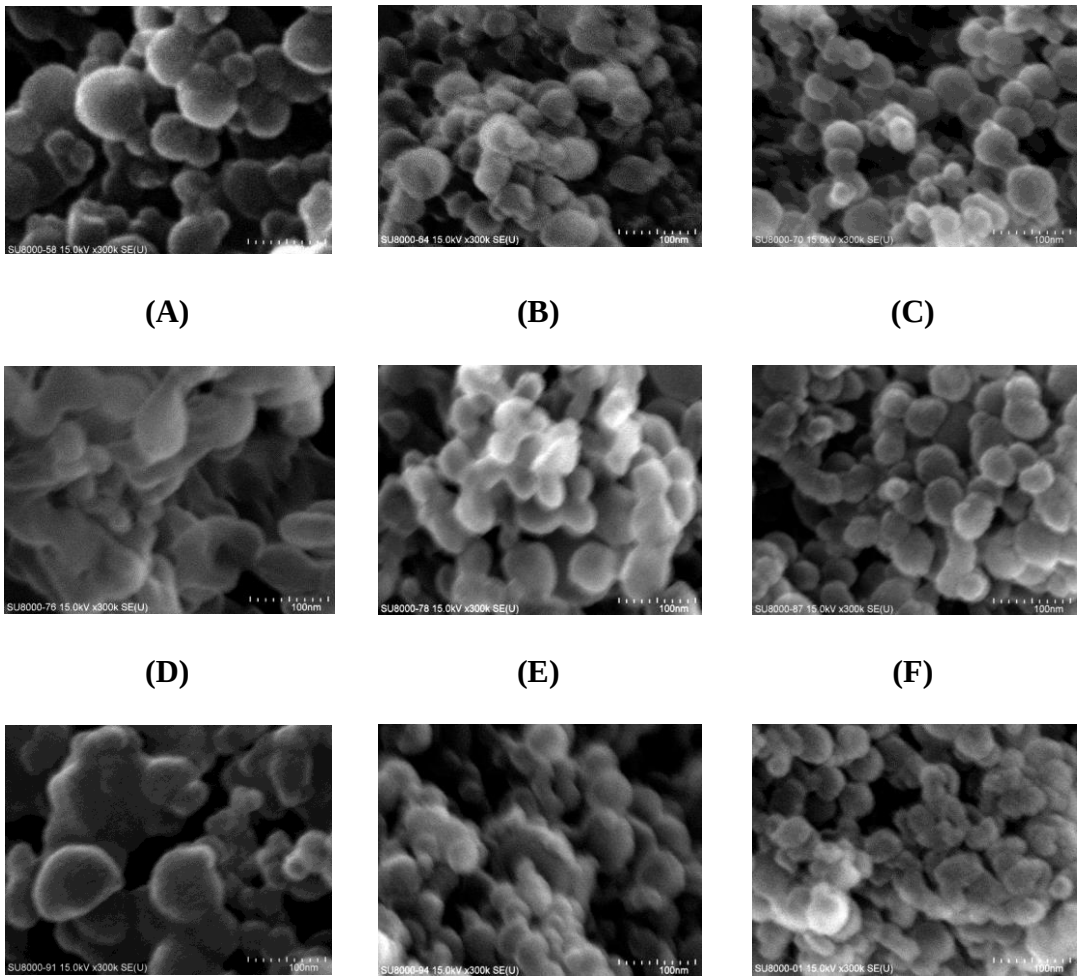

Figure 4.2-6. FE-SEM image (300,000× magnification) of treated complex particles precipitated from a DMF solution of lycopene β-CD (0.35:0.74 mg/mL) at 50 °C, 14 MPa and various solution/CO_2 flow rates. (A) 0.25/15 mL/min; (B) 0.25/20 mL/min; (C) 0.25/25 mL/min; (D) 0.5/15 mL/min; (E) 0.5/20 mL/min; (F) 0.5/25 mL/min; (G) 0.75/15 mL/min; (H) 0.75/20 mL/min; (I) 0.75/25 mL/min

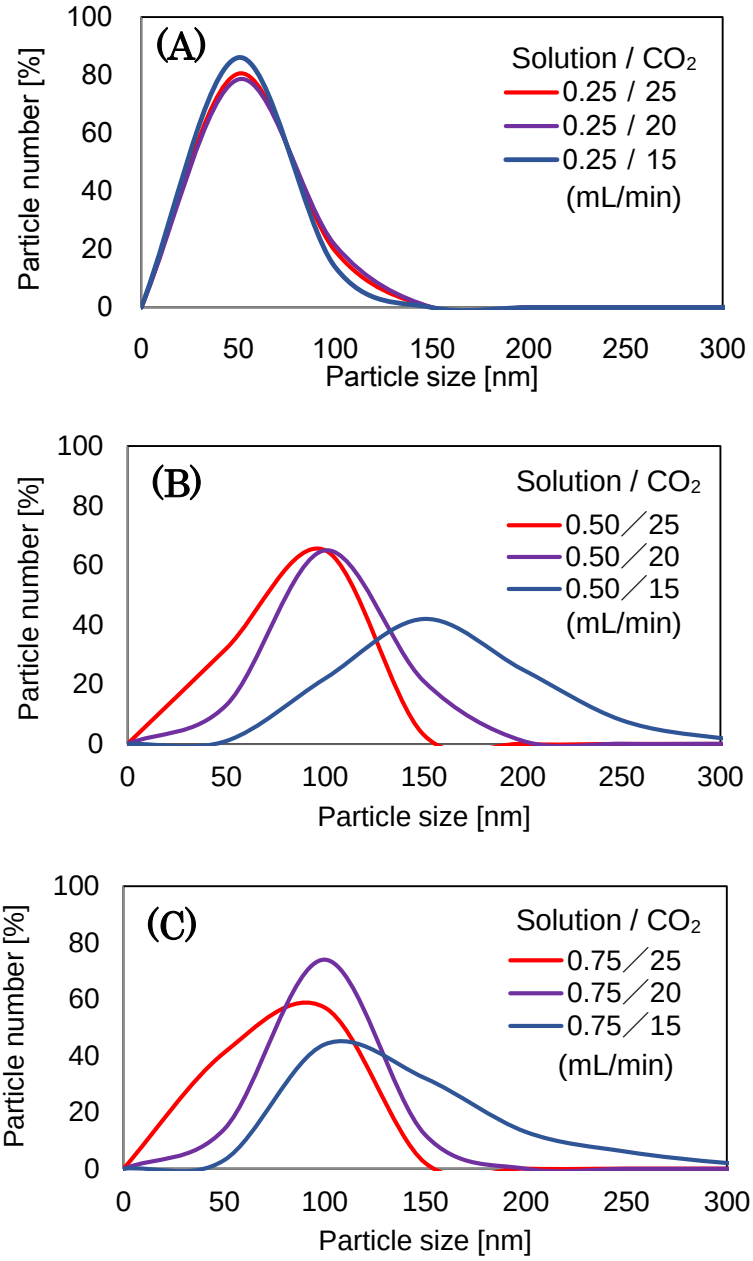

Figure 4.2-7. Particle size distribution of micronized particles precipitated from a DMF solution of lycopene/β-CD (0.35:0.74 mg/mL) at 50 °C, 14 MPa and various solution flow rates. (A) 0.25 mL/min, (B) 0.5 mL/min, (C) 0.75 mL/min

4-2-4-2-4. Analysis of inclusion complex

To confirm the formation of an inclusion complex between lycopene and β-CD, DSC was used to examine the melting point. **Figure 4.2-8** shows DSC chromatograms of the raw materials, lycopene and β-CD, the physical mixture, and particles of the complex after SEDS treatment. A sharp peak for uncomplexed lycopene was detected at 180 °C (line A), while a broad peak for uncomplexed β-CD was found at 100–150 °C (line B). Typically, the characteristic peak of a carotenoid disappears or shifts when an inclusion compound is formed [22, 23]. Although peaks for both lycopene and β-CD appeared in the physical mixture (line C), in the chromatogram of the particles formed by SEDS in DMF solution, the lycopene peak seemed to disappear (line D). This result indicated that an inclusion compound had been successfully formed using the SEDS process.

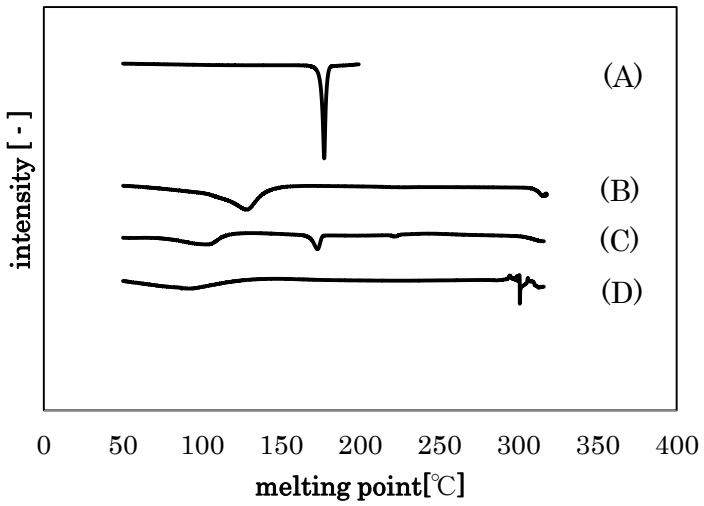

Figure 4.2-8. DSC chromatograms of raw material and treated particles. (A) Lycopene; (B) β-CD; (C) physical mixture; (D) Lycopene/β-CD complex obtained by SEDS process

The thermal degradation of medicine is significantly inhibited by inclusion with CD and their derivatives. CD can be convert fat soluble components to powdered forms of the inclusion complexes which have low heat conductivity compared with oils or fat soluble components. For instance, crystalline E-type prostaglandins are thermally degraded to oily products such as A-type prostaglandins at higher temperatures. However, in the case of inclusion complexes, small amounts of oily products is formed [24]. Therefore thermal stability of the target substances is markedly improved by complexation with CD.

4-2-5. Conclusion

Particles of an inclusion complex were obtained by precipitation using the SEDS process, with DMF as a solvent. Particles of the lycopene/β-CD complex with morphologies from spherical to agglomerated were generated at various temperatures, pressures, solution flow rates and CO_2 flow rates. The smallest particle size of 38 nm was obtained at high temperature and high pressure with a low solution flow rate.

References

[1] E. Franceschi, A.M. Cesaro, M. Feiten, S.R. S. Ferreira, C. Dariva, M.H. Kunita, A.F. Rubira, E.C. Muniz, M.L. Corazza, J.V. Oliveira, Precipitation of β-carotene and PHBV and co-precipitation from SEDS technique using supercritical CO_2, *J. Supercritical Fluids,* 47, 259–269 (2008)

[2] F. Miguel, A. Martín, F. Mattea, T. Gamse, M.J. Cocero, Supercritical anti solvent precipitation of lycopene: Effect of the operating parameters, *J. Supercritical Fluids,* 36, 225–235 (2006)

[3] F. Mattea, A. Martín, M.J. Cocero, Co-precipitation of β-carotene and polyethylene glycol with compressed CO_2 as an antisolvent: Effect of temperature and concentration, *Ind. Eng. Chem. Res*., 47, 3900–3906 (2008)

[4] A. Martín, F. Mattea, L. Gutiérrez, F. Miguel, M.J. Cocero, Co-precipitation of carotenoids and bio-polymers with the supercritical anti-solvent process, *J. Supercritical Fluids*, 41, 138–147 (2007)

[5] H. M. C. Marques, J. Hadgraft, I.W. Kellaway, Studies of cyclodextrin inclusion complexes. I. The salbutamol-cyclodextrin complex as studied by phase solubility and DSC, *Int. J. Pharm*., 63, 259–266 (1990)

[6] E. Reverchon, I. D. Marco, Supercritical antisolvent micronization of Cefonicid: thermodynamic interpretation of results, *J. Supercritical Fluids*, 31, 207–215 (2004)

[7] D.Y. Peng, D.B. Robinson, A new two-constant equation of state, *Ind. Eng. Chem. Fund*, 15, 59–64 (1976)

[8] F. Zahran, C. Pando, A. Cabañas, J.A.R. Renuncio, Measurements and modeling of high-pressure excess molar enthalpies and isothermal vapor–liquid equilibria of the carbon dioxide + N,N-dimethylformamide system, *J. Supercritical Fluids*, 55, 566–572 (2010)

[9] M. Temtem, T. Casimiro, A. Aguiar-Ricardo, Solvent power and depressurization rate effects in the formation of polysulfone membranes with CO_2-assisted phase inversion method, *J. Membrane Sci*., 283, 244–252 (2006)

[10] H. S. Byun, N. H. Kim, C. Kwak, Measurements and modeling of high-pressure phase behavior of binary CO_2–amides systems, *Fluid Phase Equilibr*., 208, 53–68 (2003)

[11] A. Braeuer, R. Adami, S. Dowy, M. Rossmann, A. Leipertz, Observation of liquid solution volume expansion during particle precipitation in the supercritical CO_2 antisolvent process, *J. Supercritical Fluids*, 56, 121-124 (2011)

[12] A. Gokhale, B. Khusid, R.N. Dave, R. Pfeffer, Effect of solvent strength and operating pressure on the formation of submicrometer polymer particles in supercritical microjets, *J. Supercritical Fluids*, 43, 341-356 (2007)

[13] B. Y. Shekunov, J. Baldyga, P. York.: Particle formation by mixing with supercritical antisolvent at high Reynolds numbers, *Chem. Eng. Sci*., 56, 2421-2433 (2001)

[14] E. Badens, O. Boutin, G. Charbit, Laminar jet dispersion and jet atomization in pressurized carbon dioxide, *J. Supercritical Fluids*, 36, 81-90 (2005)

[15] I.D. Marco, E. Reverchon, Supercritical antisolvent micronization of cyclodextrins, *Powder Technol*. 183, 239–246 (2008)

[16] E. Reverchon, I. D. Marco, E. Torino, Nanoparticles production by supercritical antisolvent precipitation: A general interpretation, *J. Supercritical Fluids,* 43, 126–138 (2007)

[17] E. Reverchon, I. D. Marco, R. Adami, G. Caputo, Expanded micro-particles by supercritical antisolvent precipitation: Interpretation of results, *J. Supercritical Fluids*, 44, 98–108 (2008)

[18] I. D. Marco, E. Reverchon, Influence of pressure, temperature and concentration on the mechanisms of particle precipitation in supercritical antisolvent Micronization, *J. Supercritical Fluids,* 58, 295–302 (2011)

[19] E. Reverchon, G. D. Porta, M. G. Falivene, Process parameters and morphology in amoxicillin micro and submicro particles generation by supercritical antisolvent precipitation, *J. Supercritical Fluids,* 17, 239–248 (2000)

[20] A.Z. Chen, L. Li, S.B. Wang, C. Zhao, Y.G. Liu, G.Y. Wang, Z. Zhao, Nanonization of methotrexate by solution-enhanced dispersion by supercritical CO_2, *J. Supercritical Fluids*, 67, 7–13 (2012)

[21] A. Martín, M.J. Cocero, Numerical modeling of jet hydrodynamics, mass transfer, and crystallization kinetics in the supercritical antisolvent (SAS) process, *J. Supercritical Fluids,* 32, 203–219 (2004)

[22] J. He, W. Li, Preparation of borneol–methyl-b-cyclodextrin inclusion complex by supercritical carbon dioxide processing, *J. Incl. Phenom. Macro*., 65, 249–256 (2009)

[23] P.P. Shah, R.C. Mashru, Formulation and evaluation of taste masked oral reconstitutable suspension of primaquine phosphate, *AAPS Pharm. Scitech*., 9, 1025–1030 (2008)

[24] H. Dodziuk, Cyclodextrins and Their Complexes: Chemistry, Analytical Methods, Applications, *Wiley-VCH*, (2006)

Chapter 4.3

Effects of Precipitation vessel type on particle formation of carotenoid

4-3-1. Introduction

Several types of presipitator have been used in SAS and SEDS processes, and the most common presipitator is a vessel type. In the work of Miguel et al. [1], 7-80 μm particles of carotenoid were obtained using 2 L volume vessel under various operating conditions. Boonnounet et al. reported that 0.8-3.4 μm particles of carotenoid were obtained using a vessel type precipitator. The precipitator had an inner diameter of 30 mmϕ a length of 170 mm long with a volume of 120 mL and various operation conditions were examined [2, 3]. In **chapter 4.2**, water-soluble nanoparticles of carotenoid/cyclodextrin complex were produced for application to medicines by SEDS process using a vessel-type precipitator. The properties of precipitator were inner diameter; 30 mm, lenght; 300 mm, volume; about 200 mL. In this work, we obtained nanoparticles with a mean size of 40 nm [4]. Moreover, a concentric tube-type precipitator was investegated by Boutin et al. in the micronization of L-poly lactic acid. Precipitator inner diameter were 3.85 or 8.50 mm, lenght were 54.5 or 62 cm. And particles of 0.5-3 μm were obtained by various condition with these presipitator[5]. In this work, β-carotene and ethyl acetate were used as raw material and organic solvent, respectively of micronization using tube type precipitator. **Table 4.3-1** shows the physico-chemical properties of β-carotene and ethyl acetate [6, 7].

Table 4.3-1. Physicochemical properties of β-carotene[6]

	Formula	Molecular weight	Melting point (°C)
β–carotenoe	$C_{40}H_{56}$ 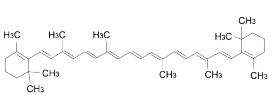	536.87	172–173

4-3-2. Objectives

In this work, tube type precipitator was investigated in order to produce more finer particles. To ensure a sufficient separation space of the solvent from the particles, the cell was designed with a length of about 5 m. β-Carotene and ethyl acetate were used as raw material and organic solvent, respectively of micronization. Effect of precipitator type on the particle mophorogy and size were considered at various CO_2 flow rate and solution flowrate conditions. β-Carotene was dissolved in ethyl acetate and concentration of solution was constant of 1.5 mg/mL. The SEDS process was carried out in a semi-continuous tube type precipitator at pressures of 14 MPa, temperatures of 40 °C, CO_2 flow rate of 0.31, 0.62, 1.26 kg/h, and solution flow rate of 0.25, 0.5, 1.0 mL/min. Morphology and size of generated particles were observed by field emission-scanning electron microscope (FE-SEM).

4-3-3. Materials and Methods

4-3-3-1. Material and chemicals

β-Carotene (purity > 80%) which was crushed mechanically was purchased from Wako pure chemical industries, Ltd., Japan. Ethyl acetate (99.3 %) are obtained by Kanto Chemical Co., Inc, Japan. Carbon dioxide (> 99.5 %) was supplied by Sogo Co., Japan.

4-3-3-2. Equipment, methods and procedures

The SEDS process was carried out in a semi-continuous tube type precipitator. **Figure 4.3-1** shows a schematic diagram of the SEDS apparatus. The apparatus consists of a CO_2 chiller (Cooling Unit CLU-33, Iwaki Asahi Techno Glass, Tokyo, Japan), a pump for CO_2 and solution (PU-980 Intelligent HPLC pump, JASCO Co., Tokyo, Japan), a heating chamber (Incubator EI-700B, AS ONE Co, Osaka, Japan), a precipitation vessel (SUS316 tube, outside diameter:3.17, inside diameter: 2.17 mm, length: 5.4 m, volume: 20 mL), a coaxial nozzle as shown in **Figure 4.3-2** (nozzle inside diameter 2.17 and 0.8

mm, respectively), a membrane filter for collecting particles (100 nm PTFE membrane filter, Advantec, Tokyo, Japan) was placed in between the inside of the Swagelok filter, and a back-pressure regulator (AKICO Co., Tokyo, Japan), a wet gas meter for CO_2 flow rate (Sinagawa Co., Tokyo, Japan).

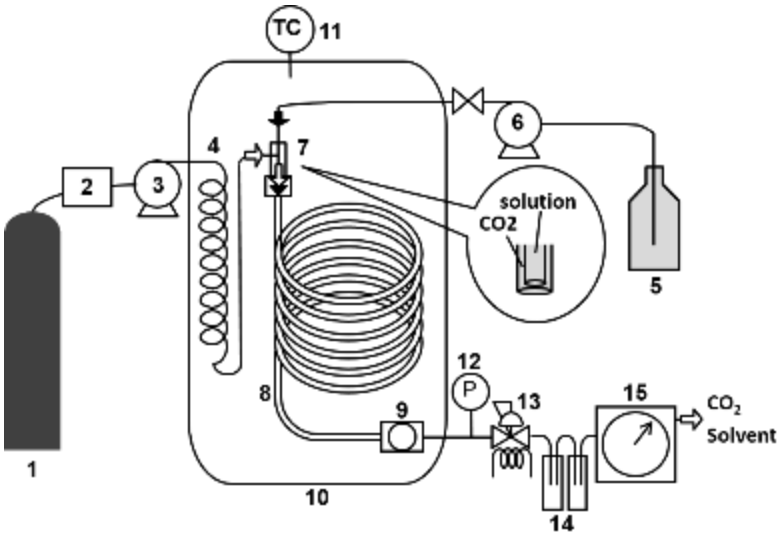

Figure 4.3-1. Schematic diagram of the SEDS process. (1)CO_2 cylinder, (2)Chiller, (3)CO_2 pump, (4)Pre heater, (5)Carotenoid solution, (6)Feed pump, (7)Coaxial nozzle, (8)Tube type precipitator, (9)Membrane Filter, (10)Heating chamber, (11)Temperature controller, (12)Pressure gauge, (13)Back-pressure regulator, (14)Trap, and (15)wet gas meter

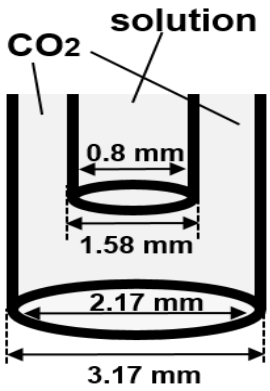

Figure 4.3-2. Schematic diagram of the coaxial nozzle

Experiments of SEDS process were carried out as follows: liquefied CO_2 was introduced into the system using HPLC pump (-5 °C and operating pressure) at constant

flow rate. The CO_2 was heated in the pre heater placed in heating chamber to change to supercritical state. Temperature and pressure in the system were reached to operating conditions, β-carotene which is solved in the organic solvent was pumped by HPLC pump (operating temperature and pressure) at desired flow rate. SC-CO_2 and β-carotene solution were mixed and introduced into the precipitator from the coaxial nozzle. β-Carotene precipitated by supersaturation with anti-solvent effect. After stopped solution feed pump, particles and the system line were washed by SC-CO_2. It helped to remove organic solvent from the particles. Finally particles were collected from the membrane filter after the depressurization. The experiment was carried out at pressure of 14 MPa and temperatures of 40 °C. The concentration of β-carotene in organic solvent were 1.5 mg/mL. The flow rates of the supercritical CO_2 were 0.31, 0.62, 1.26 kg/h, and solution were 0.25, 0.5, 1.0 mL/min at pump condition, respectively. **Table 4.3-3** shows the detailed experimental conditions.

Table 4.3-3. Experimental conditions of CO_2 flow rate and solution flow rate

Sample No.	CO_2 flow rate (kg/h)	Solution flow rate (mL/min)
1	1.26	0.25
2	0.62	0.25
3	0.31	0.25
4	1.26	0.50
5	1.26	1.00

4-3-3-3. Analysis and characterization

The shape and surface characteristics of the raw materials and the treated particles were observed by a field emission-scanning electron microscopy (FE-SEM S-5200, Hitachi, Tokyo, Japan). The samples were sputter-coated with gold in a high-vacuum evaporator and the samples were examined using SEM at 30 kV. Particle sizes and size distributions were measured using Image J software which was developed by the National Institutes of Health.

4-3-4. Results and Discussion

4-3-4-1. Effect of SC-CO_2 and solution flow rate

Figures 4.3-3 shows the SEM image of raw material of β-carotene which was crushed mechanically. The particle size was in the range 2-15 μm.

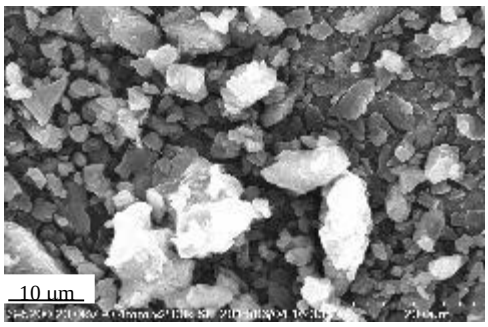

Figure 4.3-3. SEM image of raw material of β-carotene crystal

A suitable flow rate of CO_2 in the SEDS process at a constant initial concentration of β-carotene in ethyl acetate and pressure of 14 MPa and temperature of 40 ^oC were investigated. As a result of experiment, the particles were obtained under all conditions, however the size and morphology of the particles depended on the flow rate of CO_2. **Figures 4.3-4** shows the SEM image of particles produced by SEDS at a constant solution flow rate and at CO_2 flow rate of 0.31, 0.62, 1.26 kg/h. At CO_2 flow rate of 1.26 kg/h, spherical nanoparticles with a mean size of 220 nm were obtained. On the other hand, irregular plate-like particles and few spherical particles were precipitated by decreasing flow rate (0.31, 0.62 kg/h) **(Figure 4.3-4)**.

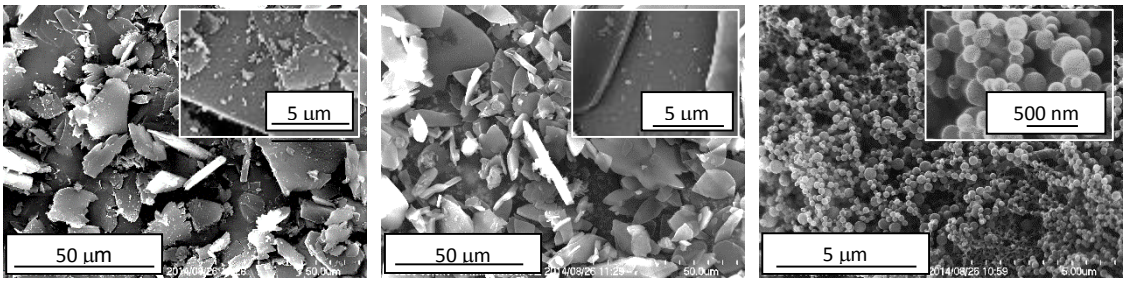

0.31 kg/h **0.62 kg/h** **1.26 kg/h**

Figure 4.3-4. SEM image of treated particles at 40 ^oC, 14 MPa, solution flow rate of 0.25 mL/min and various CO_2 flow rate (0.31, 0.62, 1.26 kg/h).

Additionally, at a higher flow rate of solution, particle size was larger than that obtained at a lower one. Mophorogy of particles were changed from spherical to plate-like irregular particles by increasing the solution frow rate **(Figure 4.3-5)**.

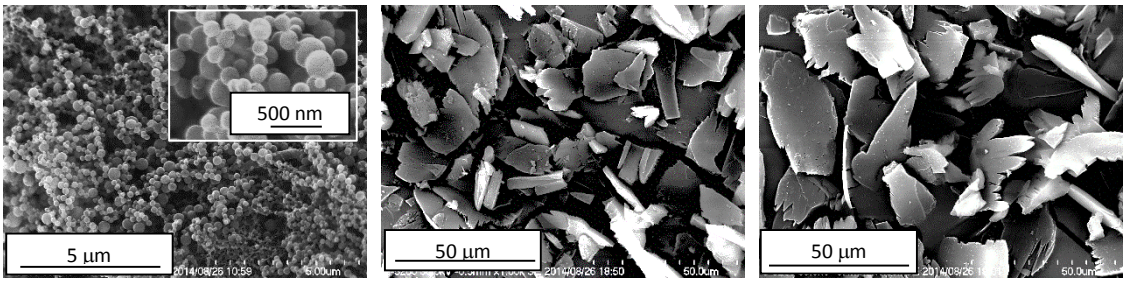

0.25 mL/min **0.5 mL/min** **1.0 mL/min**

Figure 4.3-5. SEM image of treated particles at 40 ºC, 14 MPa, CO_2 flow rate of 1.26 kg/h and various solution flow rate. (0.25, 0.5, 1.0 mL/min)

Table 4.3-4. Summary of experimental results

Sample No.	CO_2 flow rate (kg/h)	Solution flow rate (mL/min)	Mean particle size	Mophorogy
1	1.26	0.25	220 nm	Spherical
2	0.62	0.25	14.05 μm	Irregular plate-like
3	0.31	0.25	16.38 μm	Irregular plate-like
4	1.26	0.5	19.05 μm	Irregular plate-like
5	1.26	1.0	22.59 μm	Irregular plate-like

Usually, three regimes of liquid-phase dispersion affected by flow rate. In the dripping regime, droplets are formed at the outlet of a nozzle. In the laminar regime, the solution droplet of uniform-sized flows smooth and continuously until break-up zone. In the turbulent regime, the droplet go to the break-up zone. On the jet surface becomes irregular and non-uniform droplets such as stretched or small broken droplets are formed [8, 9]. When the higher solution flow rate, mixing of the jet in the space is promoted and it causes stronger turbulence. This achieved greater supersaturation in the jet, in which shows the supersaturation inside the jet for two different solution flow rates. Accordingly, finer particles are collected at higher solution flow rates. However, the effect of this

parameter is smaller than that of affecting phase equilibrium. On the other hand, higher flow rate of CO_2 may improve mixing according to increased turbulence, resulting in higher supersaturation at the edge of the jet. If the flow rate of CO_2 is increased, the bulk fluid contains a smaller amount of organic solvent and causes higher supersaturation level. Therefore finer particles are obtained by higher CO_2 flow rate and lower solution flow rate conditions. [10-13].

In the previous work, nanoparticle of carotenoid/cyclodextrin complex were produced by SEDS process using vessel type precipitator. The properties of precipitator were inner diameter; 30 mm, lenght; 300 mm, volume; about 200 mL. In the case of 40 °C, 14 MPa and CO_2 flow rate of 1.26 kg/h, linear velocity is 2.3 m/h [4].

On the other hand, the cell used in this study, at the same temperature, pressure and CO_2 flow rate conditions, the linear velocity is 111.5 m/h.

4-3-5. Conclusions

The micro to nano particles were obtained by SEDS process usign tube type precipitator. Effects of CO_2 flow rate and solution flow rate were considered at a constant temperature (40 ℃), pressure (14 MPa), and concentration (1.5 mg/mL) dissolved in ethyl acetate. Effects of CO_2 flow rate was examined at 0.31, 0.62, 1.26 kg/h under a constant solution flow rate of 0.25 mL/min. Effects of solution flow rate was examined at 0.25, 0.5, 0.1 mL/min under a constant CO_2 flow rate of 1.26 kg/h. Spherical nanoparticles (220 nm) were obtaind at a higher CO_2 flow rate and a lower solution flow rate (1.26 kg/h, 0.25 mL/min). On the other hand, plate-like irregular micro particles were formed under the other conditions. A higher CO_2 flow rate was suitable for nanoparticle formation in this process. This may be because the mixing of solution and SC-CO_2 is improved by increasing turbulence.

References

[1] F. Miguel, Á. Martín, M.J. Cocero, Supercritical anti solvent precipitation of lycopene: Effect of the operating parameters, *J. Supercritical Fluids*. 36(3), 225-235 (2006)

[2] P. Boonnoun, H. Nerome, S. Machmudah, M. Goto, A. Shotipruk, Supercritical anti-solvent micronization of chromatography purified marigold lutein using hexane and ethyl acetate solvent mixture. *J. Supercritical Fluids*, 80, 15-22 (2013)

[3] P. Boonnoun, H. Nerome, S. Machmudah, M. Goto, A. Shotipruk, Supercritical anti-solvent micronization of marigold-derived lutein dissolved in dichloromethane and ethanol. *J. Supercritical Fluids*, 77, 103-109 (2013)

[4] H. Nerome, S. Machmudah, Wahyudiono, R. Fukuzato, T. Higashiura, Y.S. Youn, Y.W. Lee, M. Goto, Nanoparticle formation of lycopene/ β–cyclodextrin inclusion complex using supercritical antisolvent precipitation, *J. Supercritical Fluids*, 83, 97-103 (2013)

[5] O. Boutin, C. Maruejouls, G. Charbit, A new system for particle formation using the principle of the SAS process: The Concentric Tube Antisolvent Reactor (CTAR), *J. Supercritical Fluids*, 40, 443–451 (2007)

[6] M. Skerget, Z. Knez, Solubility of Binary Solid Mixture α-Carotene-Capsaicin in Dense CO_2, *J. Agric. Food Chem*., 45, 2066-2069 (1997)

[7] Properties of organic solvents were searched from "National Center for Manufacturing Sciences" (NCMS) http://www.ncms.org/, http://solvdb.ncms.org/SOLV01.htm

[8] E. Badens, O. Boutin, G. Charbit, Laminar jet dispersion and jet atomization in pressurized carbon dioxide, *J. Supercritical Fluids*, 36(1), 81–90 (2005)

[9] E. Reverchon, I.D. Marco, R. Adami, G. Caputo, Expanded micro-particles bysupercritical antisolvent precipitation: interpretation of results, *J. Supercritical Fluids*, 44, 98–108 (2008)

[10] A.Z. Chen, L. Li, S.B. Wang, C. Zhao, Y.G. Liu, G.Y. Wang, Z. Zhao, Nanonization of methotrexate by solution-enhanced dispersion by supercritical CO_2, *J. Supercritical Fluids*, 67, 7-13 (2012)

[11] I.D. Marco, E. Reverchon, Influence of pressure, temperature and concentration on the mechanisms of particle precipitation in supercritical antisolventMicronization, *J. Supercritical Fluids*, 58, 295–302 (2011)

[12] E. Reverchon, G. Della Porta, M.G. Falivene, Process Parameters and Morphology in Amoxicillin Micro and Submicro Particles Generation by Supercritical Antisolvent Precipitation, *J. Supercrit. Fluids*, 17, 239-248 (2000)

[13] A. Martín, M.J. Cocero, Numerical modeling of jet hydrodynamics, mass transfer, and crystallization kinetics in the supercritical antisolvent (SAS) process, *J. Supercritical Fluids*, 32, 203–219 (2004)

Chapter 5

Summary and Conclusions

5-1. Summary of the present works

Supercritical carbondioxide (SC-CO_2) has been used as a solvent for extraction of pigment and functional substance from natural products. Additionally SC-CO_2 has been also used as an anti-solvent for micro to nano particle formation of the pigment, functional substance and medicine. This process has been widely used in food, pharmaceutical and cosmetic industries.

In this work, extraction and particle formation of functional substances were studied. In Chapter 3, the effect of extraction conditions on the yield and recovery of extracted functional substances were investigated. In addition, various optimum conditions such as extraction temperature, pressure, and solvent of SC-CO_2 extraction were determined.

Additionally, in Chapter 4, particle formation of the functional pigment at various experimental conditions were also studied. Optimum conditions such as operating temperature, pressure, solution flow rate and CO_2 flow rate for obtaining the carotenoid nanoparticles were determined.

5-1-1. Extraction of functional substances from Gac fruit

Momordica cochinchinensis, most commonly known as gac fruit, can be found mostly in tropical regions such as Southeast Asian countries. Recently, the fruit has been marketing outside of Asia in the form of juice dietary supplements because of its high phytonutrient content including carotenoids such as lycopene and β-carotene. In this work, extraction of these carotenoids from gac fruit using supercritical CO_2 was investigated at various conditions. Extraction was conducted in counter-current extraction column at various temperatures (50 - 90 ^oC) and pressures (20 - 40 MPa). The amounts of lycopene and β-carotene in the extracts were analyzed using HPLC at a wavelength of 477 nm. The

highest recoveries were obtained at 90 ^{o}C and 40 MPa. The contents of these two main carotenoids in the extracts also varied with the extraction conditions.

5-1-2. Extraction of functional substances from Saffron

Crocus sativus L (saffron) is perennial herb that belongs to Iridaceae and is cultivated in Spain, Iran, and China. Pigments included in *C. sativus* L are widely used for dyeing and coloring food. Recently, attention has been focused on *C. sativus* L pigments because they have high prevention effect for Alzheimer's disease and inhibitory effect for colon cancer. However, the low grade *C. sativus* L defined by ISO 3632 has not been utilized to its full potential. In addition, ingredients in *C. sativus* L such as picrocrocin, safranal, HTCC (2,6,6-trimethyl-4-hydroxy-1-carboxyproducts), crocin, and crocetin have high enzymatic and chemical reactivity and heat labile. Therefore, mild extraction for these components has been required. In this study, we examined various extraction solvents such as supercritical carbon dioxide (SC-CO_2), organic solvent, and water for the recovery of phytochemicals. The SC-CO_2 and entrainer (water and methanol) were fed by a high pressure pump with flow rates of 3 mL/min and 0.5 mL/min, respectively. The extraction experiments were carried out at 30 MPa pressure and different temperatures (40-90 ^{o}C) for the determination of phytochemicals, the extract was analyzed by high performance liquid chromatography coupled with a UV/Vis detector at 250, 310, and 440 nm. The extracted phytochemicals were qualitatively identified in terms of capacity factor *k'*. The functional materials of picrocrocin, safranal, and crocin were extracted successfully by SC-CO_2 and entrainer. It is considered that it might be possible to extract not only water-soluble components (picrocrocin, HTCC, crocin) but also lipophilic components (safranal) by using the SC-CO_2.

5-1-3. Nanoparticle formation of β-carotene

Production of micro- to nano-sized particles of β-carotene was investigated using the solution-enhanced dispersion by supercritical fluids (SEDS) process. β-Carotene was dissolved in dichloromethane (DCM), *n*,*n*-dimethylformamide (DM3), *n*-hexane, or ethyl acetate, and supercritical carbon dioxide was used as an anti-solvent. The effects of the organic solvent, operating pressure, and temperature were examined. The morphologies of the particles produced by the SEDS process were observed by field emission-scanning electron microscopy (FE-SEM) and particle sizes were determined by image analysis. Irregularly formed particles (5–15 μm) were produced by DCM and DMF. Plate-like particles were produced by *n*-hexane (10 μm), and irregular nanoparticles were produced by ethyl acetate. For experiments carried out using ethyl acetate at pressures 8–12 MPa and temperatures 40–60 °C, the smallest mean particle size, about 135 nm, was found under the conditions 10–12 MPa and 40 °C.

5-1-4. Nanoparticle formation of Lycopene and cyclodextrin inclusion complex

With a view to promoting dispersion of lycopene in water, the precipitation of an inclusion complex of lycopene and β-cyclodextrin was investigated using the solution-enhanced dispersion by supercritical fluids (SEDS) process. The inclusion complex, which was prepared in *n*,*n*-dimethylformamide (DMF), was dissolved in the same solvent and then micronized by SEDS, using carbon dioxide (CO_2) as a supercritical antisolvent. The effects of the initial concentrations of lycopene and β-cyclodexitrin, the CO_2 flow rate, the solution flow rate, and the pressure and temperature at which the process was conducted were examined. The morphologies of the resulting particles were observed by

scanning electron microscopy (SEM) and field emission-scanning electron microscopy (FE-SEM). Small spherical particles were obtained at all operating conditions. At high pressure, high temperature, high CO_2 flow rate and low solution flow rate, particles with an average particle size of about 40 nm were obtained.

5-1-5. Effect of precipitation vessel type on particle formation of carotenoid

Micro to nano particle production of β-carotene was investigated using the solution-enhanced dispersion by supercritical fluids (SEDS) process. β-Carotene was dissolved in ethyl acetate, and supercritical carbon dioxide was used as an anti-solvent. The effects of the operating CO_2 flow rate (0.31-1.26 kg/h) and solution flow rate (0.25-1.0 mL/min) were examined. The morphologies of the particles produced by SEDS process were observed by field emission-scanning electron microscopy (FE-SEM) and particle sizes were determined by image analysis. Irregular form particles (14.05-22.59 μm) were produced at lower CO_2 flow rate and higher solution flow rate. Spherical nano-particles were produced at the highest CO_2 flow rate and the lowest solution flow rate (1.26 kg/h, 0.25 mL/min). Mean particle size of 220 nm was obtained on the conditions. Drastic change on the particle size was observed in the between the solution flow rate of 0.5 and 0.25mL/min. In the future we would like to discuss it in quantitative.

5-2. Final Comments

SC-CO_2 have been widely used in the food, pharmaceutical and cosmetic processing because of it has various merits such as low viscosity, high density, high diffusivity, no toxicity, easy to separate from sample. Major objectives are extraction and particle formation. In the extraction process, SC-CO_2 is used for extraction such as oil, fat-soluble functional ingredient and dyes. Additionally, micronization process is classified into depending on difference of the solubility of the target component to the SC-CO_2. One is the method using SC-CO_2 as a good solvent, and the other one is using it as anti-solvent. In this study, conducted basic research for achieving the continuous process of extraction and micronization of carotenoids using SC-CO_2.

In the extraction session, functional substances were successfully extracted from gac fruit and spice saffron. Lycopene and β-carotene were extracted from gac fruit, picrocrocin, safranal, α-crocin and decomposed crocin were obtained from spice saffron.

In the micronization session, β-carotene, lycopene and cyclodextrin complex nanoparticles were obtained successfully by supercritical anti-solvent process. Various optimum parameters such as organic solvent effect, temperature, pressure, flow rate and vessel type were determined.

Acknowledgement

I would like to express my sincere gratitude to my supervisor, *Professor Motonobu Goto* (Graduate School of Engineering, Nagoya University) and *Dr Hideki Kanda* (Graduate School of Engineering, Nagoya University) for providing me this precious study opportunity as a Ph.D student in their laboratory.

I especially would like to express my deepest appreciation to my supervisor, *Dr. Wahyudiono* (Graduate School of Engineering, Nagoya University) and *Dr Siti Machmudah* (Institut Teknologi Sepuluh Nopember, Indonesia) for their considerable encouragement and invaluable discussion that make my research of great achievement and my study life unforgettable since when I was undergraduate.

I am grateful to *Dr. Ryuich Fukuzato* (SCF Techno-Link, Inc., guest professor of Kumamoto University). He gave me a lot of precious advices and elaborated guidance.

And I also would like to thank *Professor Youn-Woo Lee* (School of Chemical and Biological Engineering, Seoul National University), *Dr. Yong-Suk Youn* (School of Chemical and Biological Engineering, Seoul National University), *Prof. Lee's family* and *his students*. I received a courteous support on experiment and also life support in Korea from them when I visited to his laboratory.

I also acknowledge *Ms. Yuko Kurita* for her administrative support throughout this study. Special thanks are for *Professor Tadafumi Adschiri* (Tohoku University), *Dr. Mitsuru Sasaki* (Graduate School of Science and Technology, Kumamoto University), *Dr. Armando T. Quitain* (Graduate School of Science and Technology, Kumamoto University), and *all members of the Goto laboratory* for their friendly cooperation and assistance.

I am very grateful to *Kagome Co., Ltd*. for their valuable cooperation in my experiments. And this work was also supported by *Grant-in-Aid for JSPS Fellows.*

Finally I would like to appreciate to *family* for their understanding, support, encouragement and sacrifice throughout my study.

Hazuki Nerome